



US Department  
of Transportation  
**Federal Railroad  
Administration**

# **Correlation of Concrete Tie Track Performance in Revenue Service and at the Facility for Accelerated Service Testing**

---

Office of Research and  
Development  
Washington, DC 20590

Volume I A Detailed Summary

---

DOT/FRA/ORD-84/02.1

August 1984  
Final Report

This document is available to the  
U.S. public through the National  
Technical Information Service,  
Springfield, Virginia 22161



|   |  |  |   |   |           |
|---|--|--|---|---|-----------|
| 1. Report No.<br>FRA/ORD-84/02.1  |  | 2. Government Accession No.                          |   | 3. Recipient's Catalog No.  |           |
| 4. Title and Subtitle<br>Correlation of Concrete Tie Track Performance in Revenue Service and at the Facility for Accelerated Service Testing   |  |  |   | 5. Report Date<br>August 1984   |           |
|   |  |  |   | 6. Performing Organization Code<br>BCL (Battelle)                               |           |
| 7. Author(s) H. D. Harrison* E. T. Selig**<br>F. E. Dean* H. E. Stewart**   |  |  |   | 8. Performing Organization Report No.   |           |
| 9. Performing Organization Name and Address<br>*Battelle Columbus Laboratories 505 King Avenue Columbus, OH 43201<br>**University of Massachusetts Amherst, MA 01003  |  |  |   | 10. Work Unit No. (TRAIS)   |           |
|   |  |  |   | 11. Contract or Grant No.<br>DOT-FR-8164  |           |
| 12. Sponsoring Agency Name and Address<br>Federal Railroad Administration<br>400 Seventh Street, SW<br>Washington, D.C. 20590   |  |  |   | 13. Type of Report and Period Covered<br>Final Report<br>March 1979 - July 1982 |           |
|   |  |  |   | 14. Sponsoring Agency Code<br>RRD-10  |           |
| 15. Supplementary Notes   |  |  |   |   |           |
| 16. Abstract<br><p>This report is the first of three volumes which describe a comparative study of concrete tie track in U.S. revenue service and at the Facility for Accelerated Service Testing (FAST). The work was undertaken to develop an understanding of the degree to which FAST represents the "real world" of revenue service. The loading environment, structural characteristics and long-term performance of concrete tie track at FAST were compared with corresponding data from four concrete tie track segments in revenue service.</p> <p>The major conclusions of the study include:</p> <p>a. Impact loads of high magnitude relative to nominal wheel loads occur because of small percentages of freight and passenger traffic in revenue service. These impact loads are caused by wheel tread irregularities and produce bending cracks at the rail seats of concrete ties. Without detection and removal of the worst wheel tread conditions or attenuation of the impact loads, the service lives of the concrete ties may be significantly shortened.</p> <p>b. While FAST has the highest mean loads of any site examined, crack-producing impact loads do not occur at FAST because of the extremely good (untypical) FAST consist wheel maintenance program.</p> <p>c. Track surfacing maintenance (raising and tamping) loosens the ballast structure, reduces the uniformity of support and contributes to large variations in relative track settlement. Uniformity of initial track support conditions is a key to good track performance.</p> |  |  |   |   |           |
| 17. Key Words<br>Concrete Ties, Track Loading, Track Performance, FAST, Track Structures, Permanent Deformation   |  |  | 18. Distribution Statement<br>Document is available to the U.S. public through the National Technical Information Service, Springfield, VA 22161. |   |           |
| 19. Security Classif. (of this report)<br>UNCLASSIFIED  |  | 20. Security Classif. (of this page)<br>UNCLASSIFIED |   | 21. No. of Pages<br>148   | 22. Price |

METRIC EQUIVALENTS OF ENGLISH UNITS USED IN THIS REPORT

Multiply the English Unit by To obtain the Metric Unit

Basic Units:

|                    |      |                |                 |      |
|--------------------|------|----------------|-----------------|------|
| Foot               | (ft) | 0.3048         | Meter           | (m)  |
| Inch               | (in) | 25.4           | Millimeter      | (mm) |
| Pound (force)      | (lb) | 4.4482         | Newton          | (N)  |
| Degrees Fahrenheit | (°F) | $5/9 (F - 32)$ | Degrees Celsius | (C)  |

Combined Units

|               |                |        |                   |              |
|---------------|----------------|--------|-------------------|--------------|
| Kip = 1000 lb | (kip)          | 0.3048 | Kilonewton        | (kN)         |
| Foot-Pound    | (ft-lb)        | 1.3358 | Joule = Watt-Sec. | (J)          |
| Pound/Inch    | (lb/in)        | 1.751  | Newton/millimeter | (N/mm)       |
| Strain        | ( $\mu$ in/in) | 1      | Strain            | ( $\mu$ m/m) |

## PREFACE

This report is a summary of the research performed under contract DOT-FR-8164 by Battelle's Columbus Laboratories (BCL) and its subcontractor, the University of Massachusetts (UMass), and was sponsored by the U. S. Department of Transportation, Federal Railroad Administration. The program manager for this study was Howard G. Moody of the Federal Railroad Administration.

Harold D. Harrison, Senior Research Scientist of BCL, managed the prime contract and the subcontracts with UMass and the four participating railroads and was the principal investigator for the research performed at BCL. The BCL team of researchers included Robert H. Prause, Manager of the Applied Dynamics and Acoustics Section, and Francis E. Dean who were both heavily involved in the initial planning of the program. James M. Tuten was responsible for all data processing and analysis with help from W. Tony So and Michael D. Kurre. Technical support was provided by Matthew S. Zelinski, Kenneth Schueller, Gary Conkel, and Donald Skaggs. Administrative support was provided by Constance Leavens and Audrey Knapp.

The University of Massachusetts research was conducted under the direction of Ernest T. Selig, Professor of Civil Engineering, and Principal Investigator. Donald R. McMahon served as Research Engineer. Graduate students also participated in the UMass research. In particular, Harry E. Stewart, a co-author, focused on the prediction methodology, presented in Volume II. Additional technical support was provided by Ronald F. Bukoski, Deh C. Ho, Gillian M. Norman, Donna M. Feng, Thomas J. Giller, Ching L. Kuo, Michael C. McVay, and Robert S. Grout. Administrative support was provided by Kristin J. Currier and Thomas E. Sikora.

Four railroads were subcontracted to support the field testing at their respective test sites. The technical liaison was provided by the following railroad personnel on behalf of their chief engineers: Mr. Steve Heath and Mr. John Baker of the Atchison, Topeka and Santa Fe Railway (ATSF), Mr. Dan Jerman of Amtrak, Mr. Bruce Dunseth of the Chessie System, and Mr. Robert Catlett of the Norfolk and Western Railway (N&W).

Data acquired from the Facility for Accelerated Service Testing (FAST) were provided through the efforts of Larry Daniels and Jack Heiss.



TABLE OF CONTENTS

|   | <u>Page</u> |
|---|-------------|
| 1.0 SUMMARY . . . . .   | 11          |
| 2.0 INTRODUCTION . . . . .  | 13          |
| 3.0 SITE DESCRIPTIONS . . . . .   | 15          |
| 3.1 The Facility for Accelerated Service Testing (FAST) Site<br>at Pueblo, Colorado . . . . . | 15          |
| 3.2 AT&SF Site Near Streator, Illinois . . . . .  | 16          |
| 3.2.1 Location . . . . .  | 16          |
| 3.2.2 Physical Layout . . . . .   | 16          |
| 3.3 Chessie System Site Near Richmond, Virginia . . . . .                                     | 21          |
| 3.4 Amtrak Northeast Corridor Site Near Aberdeen, Maryland . . . . .                          | 25          |
| 3.4.1 Location . . . . .  | 25          |
| 3.4.2 Physical Layout . . . . .   | 25          |
| 3.5 The Norfolk and Western Site Near Roanoke, Virginia . . . . .                             | 25          |
| 4.0 CORRELATION MEASUREMENT PLAN . . . . .  | 31          |
| 4.1 Summary of Measurements . . . . .   | 31          |
| 4.2 Measurement Locations . . . . .   | 35          |
| 5.0 DYNAMIC MEASUREMENTS . . . . .  | 36          |
| 5.1 Traffic Loads . . . . .   | 36          |
| 5.1.1 FAST Loads . . . . .  | 44          |
| 5.1.2 Streator Loads . . . . .  | 44          |
| 5.1.3 Richmond Loads . . . . .  | 45          |
| 5.1.4 Aberdeen Loads . . . . .  | 45          |
| 5.1.5 Roanoke Loads . . . . .   | 45          |
| 5.1.6 Load Summaries . . . . .  | 46          |
| 5.1.7 Speed Effects . . . . .   | 46          |
| 5.1.8 Effects of Vehicle Weight . . . . .   | 50          |
| 5.2 Rail Seat Bending . . . . .   | 51          |
| 5.3 Tie Center Bending . . . . .  | 56          |
| 5.4 Ancillary Dynamic Measurements . . . . .  | 56          |
| 5.4.1 Tie Bending Modes . . . . .   | 56          |
| 5.4.2 Rail and Tie Accelerations . . . . .  | 59          |
| 6.0 TRACK SYSTEM CHARACTERISTICS AND PERFORMANCE . . . . .                                    | 62          |
| 6.1 Track Stiffness/Modulus . . . . .   | 62          |
| 6.2 Track Settlement/Roughness . . . . .  | 69          |
| 7.0 BALLAST AND SUBGRADE CHARACTERISTICS . . . . .  | 79          |
| 7.1 Ballast Descriptions . . . . .  | 79          |
| 7.2 Physical State Tests . . . . .  | 84          |
| 7.2.1 Ballast Density Tests . . . . .   | 86          |
| 7.2.2 Plate Load Tests . . . . .  | 90          |
| 7.2.3 Lateral Tie Push Tests . . . . .  | 93          |
| 7.3 Subgrade Description . . . . .  | 93          |
| 7.3.1 Standard Penetration Tests . . . . .  | 93          |
| 7.3.2 Cone Penetration Tests . . . . .  | 96          |
| 7.3.3 Water Content and Atterberg Limits . . . . .  | 96          |

TABLE OF CONTENTS (Continued)

|   | <u>Page</u> |
|---|-------------|
| 7.4 Moisture Instrumentation and Weather Data . . . . .                         | 99          |
| 7.5 Laboratory Stress-Strain and Strength Testing . . . . .                     | 102         |
| 8.0 COMPONENT PERFORMANCE . . . . .   | 105         |
| 8.1 Rail Seat Flexural Cracks . . . . .   | 105         |
| 8.2 Top-of-Tie Inspections and Fastener Performance . . . . .                   | 108         |
| 9.0 CORRELATIONS . . . . .  | 115         |
| 9.1 Tie Loads vs. Tie Cracking . . . . .  | 115         |
| 9.2 Predicted vs. Measured Track Vertical Load-Deflection<br>Response . . . . . | 120         |
| 9.3 Correlation of Track Modulus With Ballast Depth . . . . .                   | 125         |
| 9.4 Predicted vs. Measured Track Settlement . . . . .                           | 125         |
| 9.5 Track Roughness vs. Absolute Settlement . . . . .                           | 140         |
| 10.0 CONCLUSIONS . . . . .  | 145         |
| 10.1 Wheel Loads vs. Tie Cracking . . . . .                                     | 145         |
| 10.2 Ballast/Subgrade Support and Track Settlement/<br>Roughness . . . . .      | 145         |
| 10.3 Wood vs. Concrete Tie Track . . . . .                                      | 146         |
| REFERENCES . . . . .  | 147         |

LIST OF TABLES

|   |     |
|---|-----|
| Table 1. Summary of Measurements and Data Reductions . . . . .                                | 32  |
| Table 2. Dynamic Wheel/Rail Load Statistics Summary . . . . .                                 | 48  |
| Table 3. Vertical Track Stiffness and Modulus . . . . .                                       | 68  |
| Table 4. Effect of Disturbance of Ballast Support on Track<br>Stiffness and Modulus . . . . . | 70  |
| Table 5. Summary of Ballast Index Test Results From Field Sites . . . . .                     | 86  |
| Table 6. Summary of Cracked Ties . . . . .  | 107 |
| Table 7. Summary of the Tie Surface and Fastener Inspection at<br>Streator, 11/2/79 . . . . . | 109 |
| Table 8. Summary of Tie Surface and Fastener Inspection at<br>Streator, 4/22/81 . . . . .     | 110 |
| Table 9. Summary of Tie Surface and Fastener Inspections at<br>Richmond, 12/18/79 . . . . .   | 112 |
| Table 10. Summary of Tie Surface and Fastener Inspections at<br>Aberdeen . . . . .            | 113 |
| Table 11. Results and Computations for Concrete Tie Cracks . . . . .                          | 119 |



## LIST OF ILLUSTRATIONS

|  | <u>Page</u> |
|--|-------------|
| Figure 1. Reconstruction of Fast Section 22 at 425 MGT . . . . .   | 17          |
| Figure 2. Layout of Streator Test Sites . . . . .  | 18          |
| Figure 3. Cross-Sections of Track at Streator Site . . . . .   | 19          |
| Figure 4. AT&SF Concrete Tie Test Site, Streator (Leeds), Ill., With<br>Westbound Geometry Car . . . . .               | 20          |
| Figure 5. Plan View of Chessie/Richmond Test Area . . . . .  | 22          |
| Figure 6. Chessie Concrete Tie Test Track, Richmond (Lorraine), VA.,<br>(3 Degree Curve) . . . . .                     | 23          |
| Figure 7. Cross-Section of Curve at Richmond Test Site<br>(Section A-A')(Ref. 3) . . . . .                             | 24          |
| Figure 8. Location of Northeast Corridor Test Site at<br>Aberdeen, MD . . . . .  | 26          |
| Figure 9. View of Aberdeen Test Site Looking Northeast . . . . .   | 28          |
| Figure 10. Layout of Concrete Tie Test Section at Roanoke, VA . . . . .  | 29          |
| Figure 11. N&W Concrete Tie Test Site, Near Roanoke, Va, Looking<br>West . . . . .                                     | 30          |
| Figure 12. Rail and Tie Instrumentation for Dynamic Measurements . . . . .   | 37          |
| Figure 13. Typical Layout of Dynamic Measurements in a Test Section . . . . .  | 38          |
| Figure 14. Static and Dynamic Wheel Loads at FAST, Section 22 . . . . .  | 39          |
| Figure 15. Static and Dynamic Wheel Loads at Streator (Santa Fe). . . . .  | 40          |
| Figure 16. Static and Dynamic Wheel Loads at Richmond (Chessie) . . . . .  | 41          |
| Figure 17. Combined Passenger and Freight Static and Dynamic Wheel<br>Loads at Aberdeen (Amtrak and Conrail) . . . . . | 42          |
| Figure 18. Static and Dynamic Wheel Loads at Roanoke (N&W). . . . .  | 43          |
| Figure 19. Summary Plot of Dynamic Wheel Loads at all Sites . . . . .  | 47          |
| Figure 20. Distribution of Train Speeds at Each Site . . . . .   | 49          |
| Figure 21. Summary of Tie Bending at All Sites . . . . .   | 52          |
| Figure 22. Statistical Rail Seat Bending Response at Streator-<br>Concrete . . . . .                                   | 54          |
| Figure 23. Statistical Rail Seat Bending Response at Roanoke . . . . .   | 55          |
| Figure 24. Summary of Tie Center Bending Response at All Sites . . . . .   | 57          |
| Figure 25. Tie Center Bending Response at Roanoke - Each Tie . . . . .   | 58          |
| Figure 26. Samples of First Three Bending Modes for CC-244-C<br>Concrete Tie . . . . .                                 | 60          |
| Figure 27. Transfer Function of Rail/Tie Acceleration for Three<br>Different Tie Pads . . . . .                        | 61          |

LIST OF ILLUSTRATIONS (Continued)

|  | <u>Page</u> |
|--|-------------|
| Figure 28. Summary of Track Stiffness at All Sites . . . . .                                     | 63          |
| Figure 29. Track Vertical Response to Point Load Application<br>at Streator-Wood . . . . .       | 65          |
| Figure 30. Track Vertical Response to a Point Load Application<br>at Streator-Concrete . . . . . | 66          |
| Figure 31. Track Vertical Response to a Point Load Application<br>at Richmond . . . . .          | 67          |
| Figure 32. Concrete Tie Track Settlement at FAST . . . . .                                       | 72          |
| Figure 33. Concrete Tie Track Settlement at Streator . . . . .                                   | 73          |
| Figure 34. Concrete Tie Track Settlement at Richmond . . . . .                                   | 74          |
| Figure 35. Concrete Tie Track Settlement at Aberdeen . . . . .                                   | 75          |
| Figure 36. Summary of Mean Track Settlement . . . . .  | 76          |
| Figure 37. Track Geometry at Streator (Leeds) Wood and Concrete<br>Tie Test Sites . . . . .      | 78          |
| Figure 38. Ballast Profile for Streator Wood Tie Section . . . . .                               | 80          |
| Figure 39. Ballast Profile for Streator Concrete Tie Section . . . . .                           | 81          |
| Figure 40. Ballast Profile for Richmond Concrete Tie Section . . . . .                           | 82          |
| Figure 41. Ballast Profile for Aberdeen Concrete Tie Section . . . . .                           | 83          |
| Figure 42. Composite Gradation Curves for Under-Tie Ballasts<br>From Revenue Sites. . . . .      | 85          |
| Figure 43. Ballast Densities--Under Tie at Rail Seat . . . . .                                   | 88          |
| Figure 44. Ballast Densities--Crib Near Rail Seat . . . . .                                      | 89          |
| Figure 45. Plate Bearing Index--Under Tie at Rail Seat . . . . .                                 | 91          |
| Figure 46. Plate Bearing Index--Under Center of Tie . . . . .                                    | 92          |
| Figure 47. Lateral Tie Push Resistance . . . . .   | 94          |
| Figure 48. Standard Penetration Resistance Versus Depth for<br>Field Sites . . . . .             | 95          |
| Figure 49. Cone Resistance Versus Depth for Field Sites . . . . .                                | 97          |
| Figure 50. Water Content and Atterberg Limits Versus Depth for<br>Field Sites . . . . .          | 98          |
| Figure 51. Moisture Content and Rainfall Data From Streator . . . . .                            | 100         |
| Figure 52. Moisture Content and Rainfall Data From Aberdeen and<br>Richmond . . . . .            | 101         |
| Figure 53. Ballast Box Test Apparatus . . . . .  | 103         |
| Figure 54. Concrete Tie Transverse Rail Seat Cracks . . . . .                                    | 105         |

LIST OF ILLUSTRATIONS (Continued)

|  | <u>Page</u> |
|--|-------------|
| Figure 55. Results of Final Inspections for Concrete Tie Cracks. . . . .                                     | 116         |
| Figure 56. Number of Axles Producing Rail Seat Moments Above<br>Cracking Strength at Aberdeen . . . . .      | 118         |
| Figure 57. Concept for Estimation of Tonnage at Which All Ties<br>Will be Cracked . . . . .                  | 121         |
| Figure 58. Ballast and Subgrade Properties Used for Analytical<br>Predictions . . . . .                      | 122         |
| Figure 59. Measured Versus Predicted Differential Rail Deflections<br>for 6- to 30-Kip Load Range . . . . .  | 123         |
| Figure 60. Measured and Predicted Track Moduli for Revenue Field<br>Sites, 6- to 30-Kip Load Range . . . . . | 126         |
| Figure 61. Ballast Depth Versus Track Modulus for Revenue Field<br>Sites . . . . .                           | 127         |
| Figure 62. Normalized First Cycle Strains as a Function of<br>Stress Ratios . . . . .                        | 129         |
| Figure 63. Measurements and Predictions of Track Settlement for<br>Streator Wood Tie Section . . . . .       | 131         |
| Figure 64. Measurements and Predictions of Track Settlement for<br>Streator Concrete Tie Section . . . . .   | 132         |
| Figure 65. Measurements and Predictions of Track Settlement for<br>Richmond . . . . .                        | 134         |
| Figure 66. Measurements and Predictions of Track Settlement for<br>Aberdeen . . . . .                        | 135         |
| Figure 67. Measurements and Predictions of Track Settlement for<br>FAST Section 22 After Rebuild . . . . .   | 136         |
| Figure 68. Logrithmic Settlement of Section 22, FAST, After<br>Maintenance . . . . .                         | 139         |
| Figure 69. Logrithmic Settlement at Aberdeen - Ballast Strain<br>Coil Data . . . . .                         | 141         |
| Figure 70. Track Roughness (RMS) for 60-Foot MCO Values . . . . .  | 142         |
| Figure 71. Track Roughness for 95th Percentile Deviation . . . . .   | 144         |



## 1.0 SUMMARY

The Facility for Accelerated Service Testing (FAST) was created to make comparative evaluations of track systems and components and of mechanical systems and components over their service life cycles. These evaluations are made under accelerated loading by measuring the rates of degradation and failure of the systems and components. Some of these results may be influenced by the specific environment in which they occur (such as the climate), while others may be influenced by the accelerated testing process. The accelerated test is not appropriate if, in the process of increasing the load or changing the rate of loading, something is left out (such as impact loading) or if the increase in loads creates other failure modes not seen in revenue service. The purpose of the correlation study was to determine whether the FAST results truly represent, in an accelerated manner, revenue service.

The area of study chosen was concrete tie track, because there was not a great deal of empirical information available about concrete tie performance for North American conditions. After evaluating over sixty potential locations, four distinctly different revenue service sites were selected because they met a variety of requirements established for this program. In general, the test sites contained prestressed monoblock concrete ties of equivalent length and strength to those being tested at FAST (designed to the current AREA recommended specifications). The fastener clips and pads were generally similar to those at FAST. The ballast and subgrade types and conditions were different at each site as were the climate, the traffic density and mix, and the track construction. This tended to improve the correlation analysis by providing a broader spectrum of service conditions to compare with the FAST results.

To understand the relationships between FAST and revenue service conditions, extensive data were collected and analyzed. These data were broken down into three basic groups:

- a. Primary performance measures: track geometry and track component degradation
- b. Governing structural characteristics: vertical and lateral track stiffness, transfer functions of the pads, subgrade moisture content, subgrade elastic and plastic limits, ballast degradation and general ballast condition
- c. Loading and load response: wheel rail loads, tie strains, and ballast strains.

The program was structured to compare data from the revenue service sites and similar data from FAST and to determine the applicability of FAST tests to revenue service conditions.

The major conclusions from this study are:

- a. There are significant differences in traffic loading at FAST and the revenue service sites which affect the performance of concrete ties. Impact loads of high magnitude relative to nominal wheel loads occur due to small percentages of freight and passenger traffic at most revenue sites. These impact loads are caused by wheel tread irregularities and produce bending cracks at the rail seats of concrete ties. While FAST has the highest mean axle loads of any site examined, crack-producing impact loads do not occur at FAST because of the extremely good (atypical) FAST-consist wheel maintenance program. The net result is few concrete tie cracks at FAST. The importance of this finding is in discovering the potential damage and the shortened revenue life of concrete ties (and the possibility of damage to other components such as rail, wheels, and bearings) because of a few defective wheel treads that are found in nearly all revenue traffic.
- b. Track surfacing maintenance (raising and tamping) loosens the ballast structure, reduces the uniformity of support and contributes to large variations in relative track settlement. Average track modulus does not change much after surfacing but the variability in modulus increases considerably. The mechanical resistance of ballast to deformation is principally dependent on the state of ballast compaction, rather than on ballast material properties. These findings, similar for FAST and revenue sites, indicate that FAST is generally representative, except for a bilinear settlement rate (possibly caused by freeze/thaw) observed at some of the revenue service sites.
- c. Uniformity of initial track support conditions is a key to good track performance. Newly constructed wood tie track at FAST showed nearly identical performance to adjacent, newly constructed concrete tie track, relative to track settlement and roughness. In contrast, older mainline track having a typical mix of wood ties of varied age and length, built on an old ballast bed was not as uniform as an adjacent newly constructed concrete tie section with a new, deeper ballast section.

## 2.0 INTRODUCTION

This report is the first of three volumes that describe a comparative study of concrete tie track in U.S. revenue service and at the Facility for Accelerated Service Testing (FAST). Called the Concrete Tie and Fastener Performance and Correlation Analysis, the work was undertaken to develop an understanding of the degree to which FAST represents the "real world" of revenue service. A measurement and analysis plan for the study is presented in [1].\*

This volume summarizes the results of the correlation study using data from Volumes II and III. Volume II describes an analytical and experimental investigation of long-term track deformation behavior and includes (a) the development of the MULTA/GEOTRACK model of track deformation under repeated loads, and (b) the methods used in a geotechnical evaluation of the ballast and subgrade properties through laboratory tests [2]. Volume III describes the field work and compiles the initial analyses of data from seven track segments, which include four concrete tie segments in revenue service, one wood tie control segment in revenue service, and a segment of concrete ties and wood ties at FAST [3].

The correlation is important to the economic justification for the use of concrete ties in U.S. revenue service. Part of the justification is based upon the assumption that they will last much longer than wood ties, and that requirements for certain types of maintenance will be reduced. While concrete ties have shown promise in reducing some of the chronic problems of wood tie track (gauge widening, spike killing), they have also encountered other problems, such as the development of bending cracks and the dislocation and failure of fasteners.

One of the major activities at FAST has consisted of the collection and evaluation of long-term performance data on concrete tie track. Since FAST operations began in September 1976, tonnage has been accumulated at an average rate of about seven times the nominal revenue service rate of 20 million gross tons per year. Portions of the track were constructed with a large variety of concrete ties and fasteners.

However, the FAST environment differs in several important respects from many revenue service environments. The climate near Pueblo is relatively mild and dry in comparison with the extremely cold climates of the plains states and the wet-cold climates of the midwestern and northeastern states. The track subgrade is sandy and stable. Train speeds do not exceed 45 mph. Perhaps the most important, the track and train are maintained daily. While the average axle load is high at 33 tons, wheel flats are not allowed to develop to the point of producing serious impact loads.

These differences in operating environments have resulted in many dissimilar performance results between FAST and revenue service test segments. While all the concrete ties in the revenue service test segments examined

---

\* Brackets indicate references listed in back of report.

in this study have developed rail seat bending cracks, none was found at FAST. On the other hand, the 5-degree curves at FAST have experienced rates of tie movement and fastener clip fallout and fracture which have not been approached, on a per-MGT basis, at any revenue service site.

Thus, the FAST concrete tie experiment is limited in its applicability to many of the major problems that affect the economic feasibility of concrete tie track in U.S. revenue service. This program was designed to define both the performance differences among the FAST and revenue service operations and the causes for these differences. This information can then be applied to the design of FAST experiments that accurately reproduce the revenue service environment.



### 3.0 SITE DESCRIPTIONS

When planning for this study began in 1979, there were over 60 concrete tie installations in North American revenue service tracks [4]. These ranged in size from 10 to over 300,000 ties. The designs of ties and fasteners, tie spacing, preparation of ballast and subgrade, and loading conditions of these installations varied widely. Since the first concrete ties were installed in 1960, bending strength requirements were increased in stages which culminated in recommendations of the American Railway Engineering Association (AREA) first published in 1973 (AREA Bulletin 644) and with minor changes in 1975 (AREA Bulletin 655). These developments are discussed in Reference [4]. Also during this development period, tie spacings were reduced from as much as 30 inches to the current 24-26 inches.

Because many of the early installations had experienced structural failures of ties and fasteners, it was decided to limit the correlation study to sections built to 1975 strength requirements and to a relatively small range of tie spacing (24-26 inches). It was also desirable to select locations with moderate to heavy tonnage, cold or wet-cold climates, and accessibility to the test site. These criteria limited the study to the following revenue service locations:

- (a) the Atchison, Topeka and Santa Fe (AT&SF) site near Streator, Illinois
- (b) the Chessie System site near Richmond, Virginia
- (c) the Amtrak Northeast Corridor (NEC) original installation near Aberdeen, Maryland
- (d) the Norfolk & Western (N&W) site near Roanoke, Virginia.

A segment of track just east of the concrete test site at Streator was selected as a wood tie control section. Section 22 at FAST was selected for study because it provided concrete and wood tie segments which duplicated the Northeast Corridor track construction. Supporting data from the 5-degree curve of the concrete tie Section 17 at FAST are also included.

#### 3.1 The Facility for Accelerated Service Testing (FAST) Site at Pueblo, Colorado

The FAST track is located at the Transportation Test Center, about 25 miles northeast of Pueblo, Colorado. The track is divided into 22 subsections which provide many combinations of track construction and tie/fastener components. The test train of 60 -76 cars is operated 5 nights a week at a maximum speed of 45 mph. The speed generally ranges from 40 - 50 mph, with 2-inch underbalance in the curves. The exception to this is found in counter-clockwise operation over the 5-degree curve and 2-percent upgrade of Section 17, where the consist speed can drop to 25 mph.

In July 1979, train operations were suspended to rebuild several sections of the track loop. Section 22 was allocated to provide accelerated data on the Northeast Corridor construction which was then in progress. The old ballast was removed and replaced with NEC traprock to a depth of 15 inches. The 300-tie test segments shown in Figure 1 reproduced the NEC tie/fastener construction for wood and concrete ties. These sections were separated with transition zones, also shown in the figure.

Eight new segments of concrete ties and fasteners were added to two original segments in the 5-degree curve of Section 17. Three segments of new AREA 3 ballast were combined with one segment of cleaned existing ballast and one segment of NEC traprock.

### 3.2 AT&SF Site Near Streator, Illinois

#### 3.2.1 Location

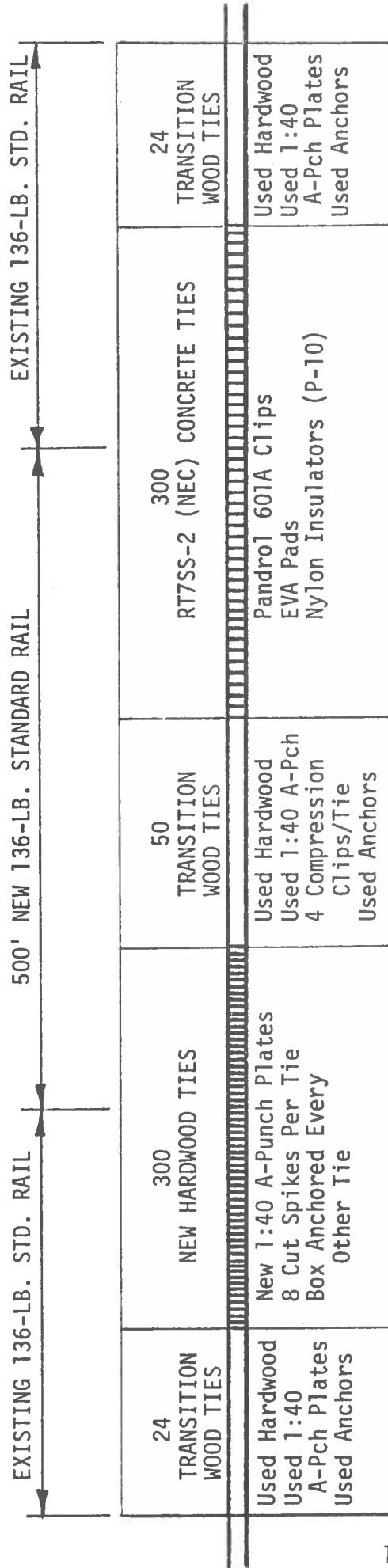
The track site near Streator, Illinois, is located in north-central Illinois, approximately midway between Chicago and Peoria. The test section at Leeds, which was once the location of a water stop and station platform is in the farming area, southwest of Streator. Both wood and concrete tie test sections were evaluated at this site.

#### 3.2.2 Physical Layout

A plan view sketch of the test section in relation to surrounding topographical features is shown in Figure 2. Cross sections at the wood and concrete tie test sites appear in Figure 3. Figure 4 is a photo of the site.

In the concrete tie test section, there are two types of ties: Gerwick RT-7S and Conforce Costain CC244C, in equal numbers. Pandrol spring clip fasteners are installed on all 200 of the Costain-type ties. There are three different types of fasteners on the RT-7S ties, one of which is the Pandrol fastener. To maintain as much uniformity as possible in the tie/fastener types examined at the various test sites, all dynamic measurements on concrete ties were confined to the CC244C ties, when available. (Aberdeen and FAST tracks were built with only the newer RT-7SS-2.)

The wood tie test section is located approximately 1500 ft east of the Leeds Road grade crossing and approximately 500 ft east of milepost 102. Both the wood and concrete sections are located on the north track of the Santa Fe's Chicago to Topeka double-track mainline. While the concrete tie test site is essentially at grade, the wood tie test site is located in a fill section. The timetable speed over the site is 60 mph for freight trains and 80 mph for passenger trains and TOFC/COFC trains (truck-trailer piggyback).



NOTE: EXISTING BALLAST REMOVED AND REPLACED WITH NEC TRAPROCK.

FIGURE 1. RECONSTRUCTION OF FAST SECTION 22 AT 425 MGT

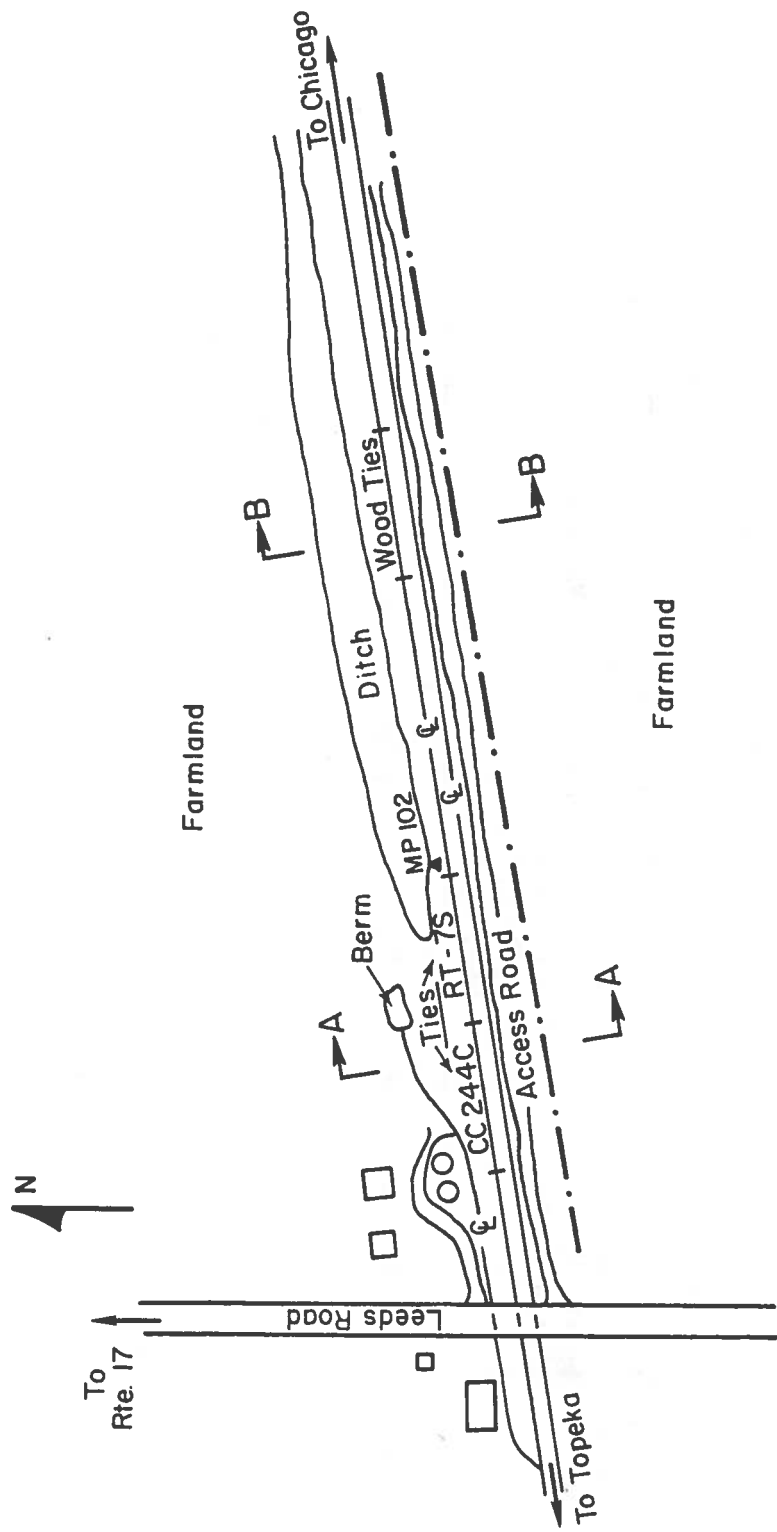
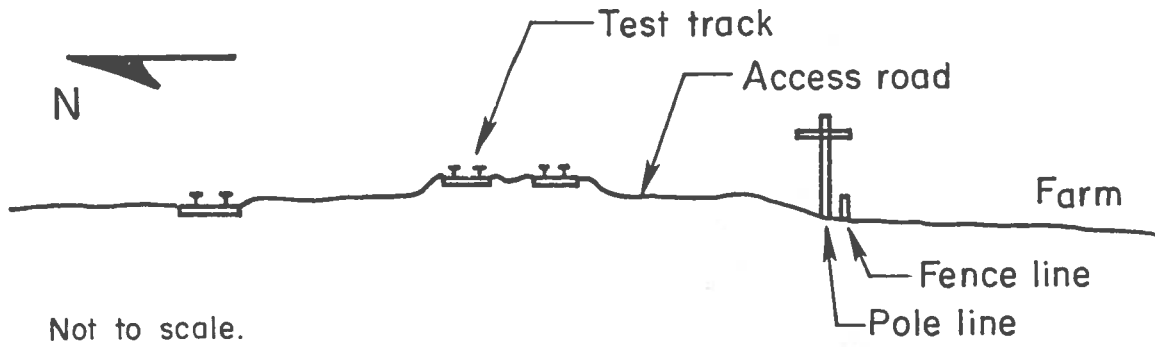
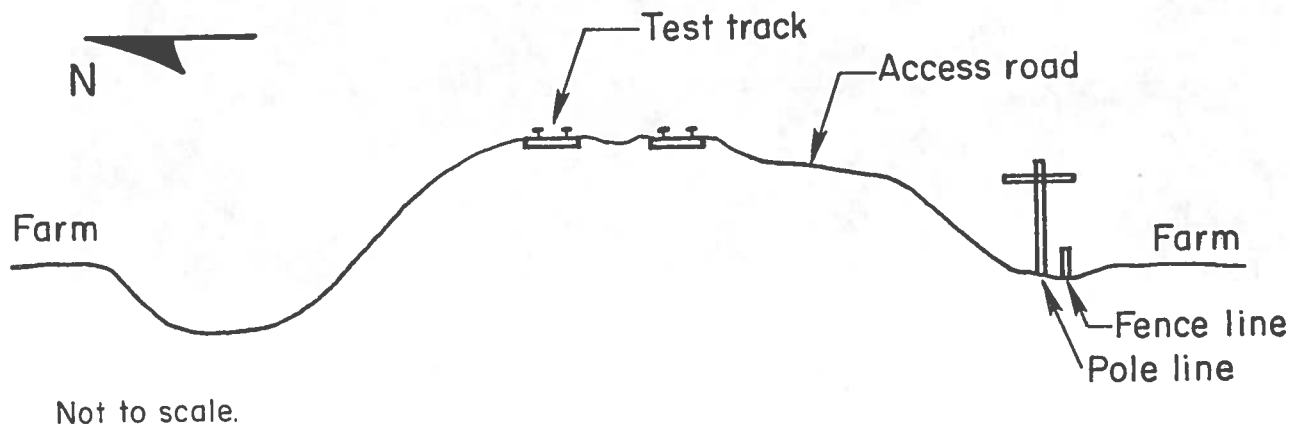


FIGURE 2. LAYOUT OF STREATOR TEST SITES



SECTION A-A - CONCRETE TIE TEST SITE



SECTION B-B - WOOD TIE TEST SITE

FIGURE 3. CROSS-SECTIONS OF TRACK AT STREATOR SITE



FIGURE 4. AT&SF CONCRETE TIE TEST SITE, STREATOR (LEEDS), ILL.,  
WITH WESTBOUND GEOMETRY CAR

### 3.3 Chessie System Site Near Richmond, Virginia

The Chessie System concrete tie installation is located in central Virginia, in the suburbs eleven miles west of Richmond. (Chessie calls this section Lorraine.) The track is part of the C&O line between Richmond and Lynchburg. The test site, located just east of the foot of Gaskins Road between mileposts 11 and 12, is on the north bank flood plain of the James River. The test site area has reportedly been flooded several times since the railroad was built. However, it has not flooded since the installation of the concrete ties in 1974. As shown in Figure 5, the concrete tie installation is located near the middle of a reverse curve. The short tangent portion of the reverse curve is intersected by the Gaskins Road crossing. Figure 6 is a photograph of the test section leading west towards Gaskins Road. The James River Golf Club lies just north of the right-of-way.

A conifer wooded area extends south of the right-of-way to the James River. During the measurement period, water was standing throughout portions of this area. A sketch of a typical cross-section of the track can be seen in Figure 7.

The concrete ties are installed in a 3.0-degree curve with 3.0-inch superelevation. The test zone is about 550 feet long and was divided into 3 sections; counting west:

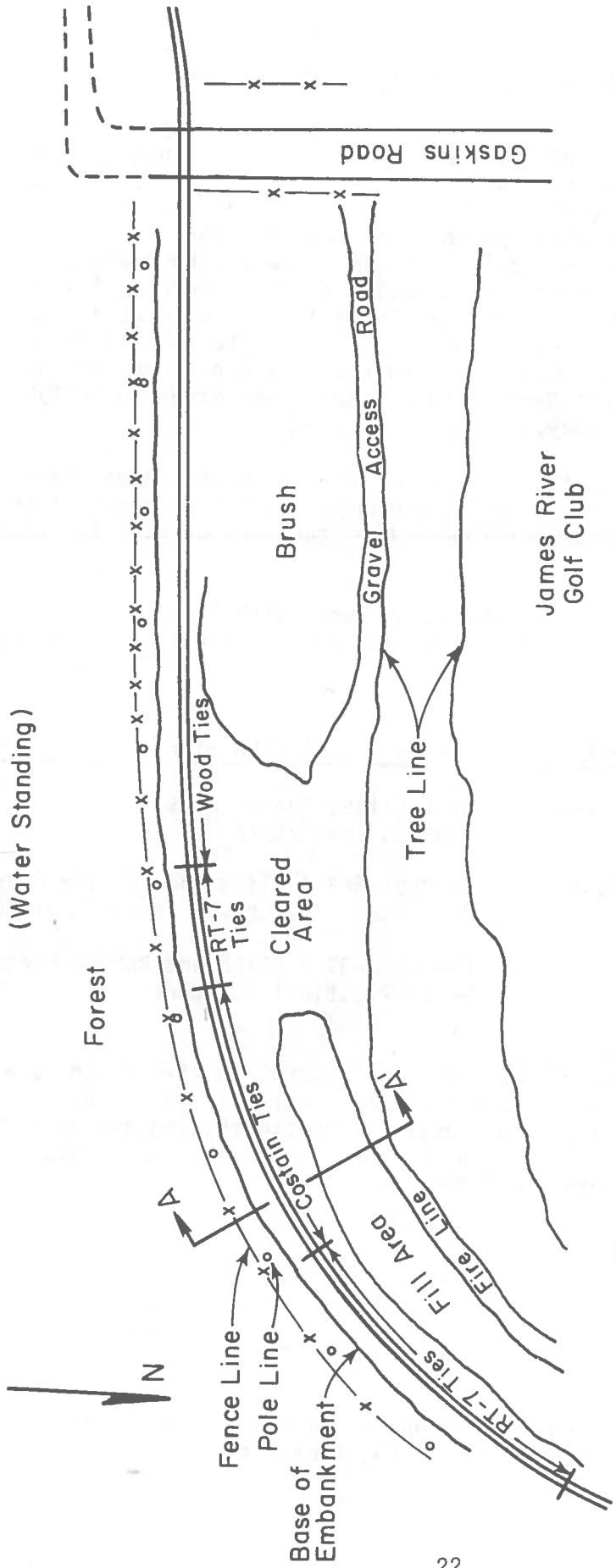
| <u>TIE NO.</u> | <u>TIE TYPE</u>            | <u>FASTENER TYPE</u>   |
|----------------|----------------------------|--|
| 001 - 106      | Gerwick RT-7S              | CS-5 Clips, Rubber Pads,<br>Plastic Insulators                                 |
| 107 - 124      | Gerwick RT-7S              | Pandrol 607 A Clips and Fabrika Pads,<br>Insulated with Epoxy-Coated Shoulders |
| 125 - 224      | Conforce-Costain<br>CC244* | Pandrol 607 A Clips and Rubber Pads,<br>Metal/Plastic Insulators               |

An additional 44-tie section at the west end contains RT-7S ties which were originally installed at the Sabot test site. These were excluded from detailed inspection per a request from Chessie. The tie spacing averaged 25 inches. At the time of the site visit in December 1979, the cumulative tonnage over the test section was 150.9 MGT.

---

\*The CC244 tie has 26 prestressing tendons, while the CC244C has 28 tendons. The ties were designed to the same strength requirements.

James River Flood Plain  
(Water Standing)



Not to scale.

FIGURE 5. PLAN VIEW OF CHESSIE / RICHMOND TEST AREA



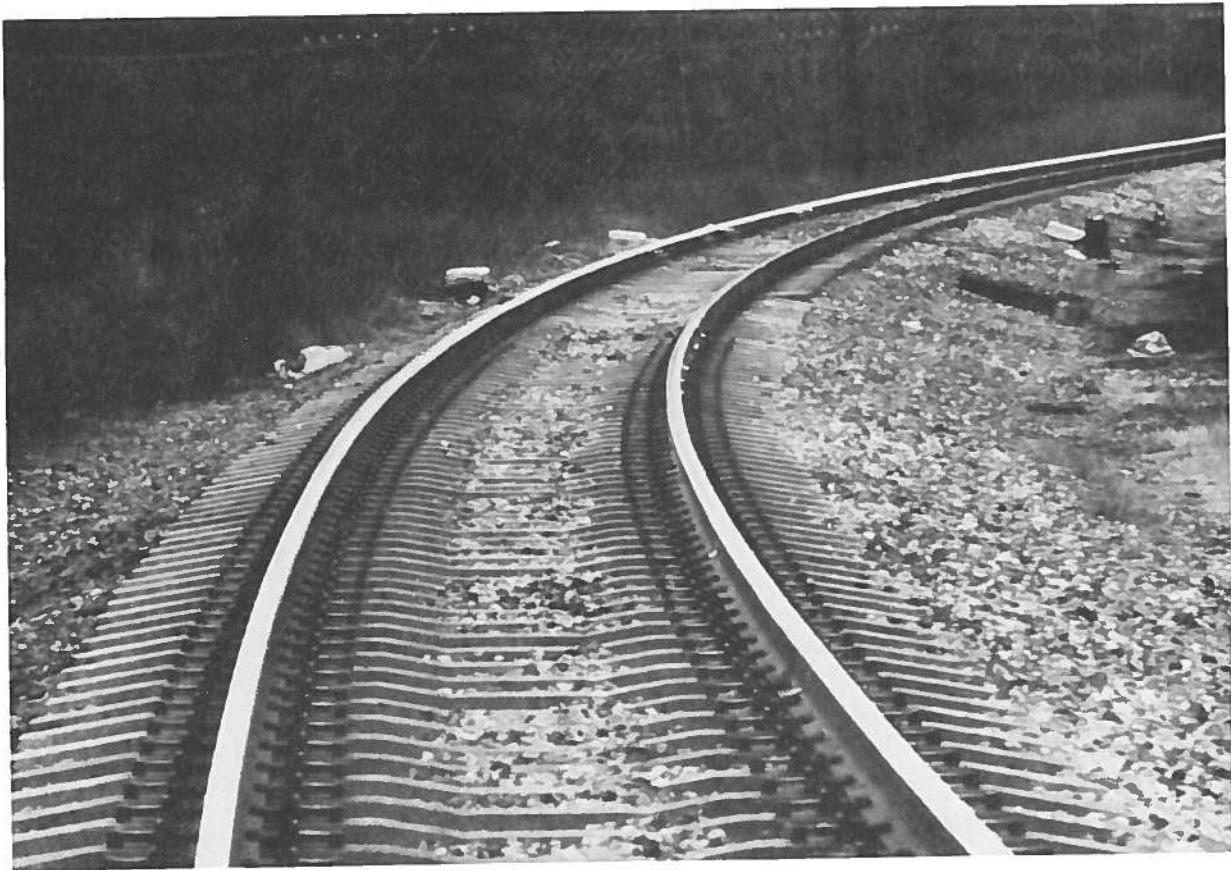


FIGURE 6. CHESIE CONCRETE TIE TEST TRACK, RICHMOND (LORRAINE), VA.,  
(3 DEGREE CURVE)

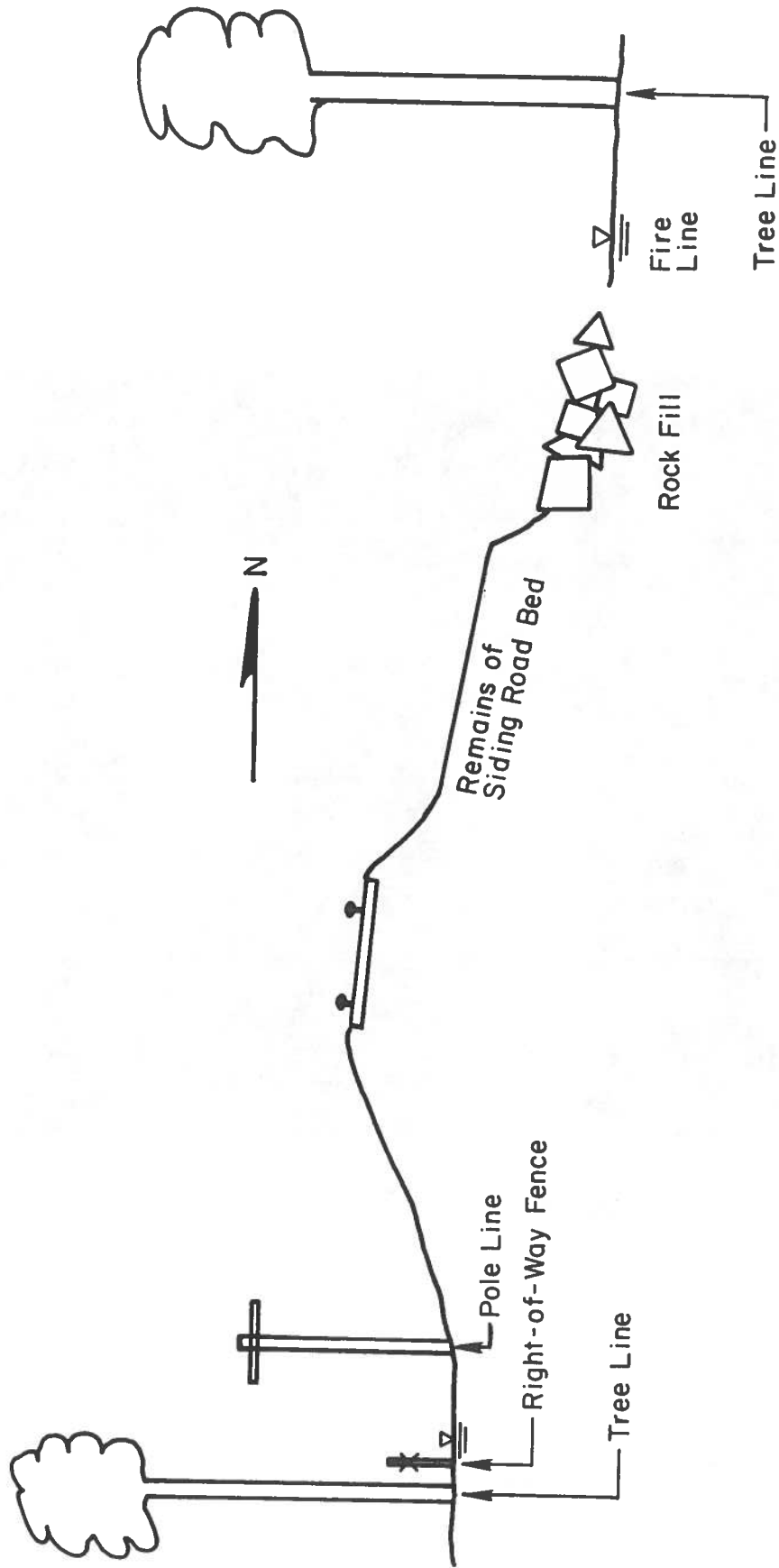


FIGURE 7. CROSS-SECTION OF CURVE AT RICHMOND TEST SITE (SECTION A-A') (REF. 3)

### 3.4 Amtrak Northeast Corridor Site Near Aberdeen, Maryland

#### 3.4.1 Location

The Northeast Corridor site is located approximately three miles southwest of Aberdeen, Maryland. The site lies between mileposts 68.7 and 68.9, where milepost zero is located in the center of Philadelphia. As shown in Figure 8, the site is accessed from Michaelsville Road at Perryman and is adjacent to a concrete pipe plant on the west side of the track. The Aberdeen Proving Grounds border the east side of the track. Although the railroad runs northeast-southwest through the test area, the traffic directions are designated North (toward Aberdeen) and South (toward Baltimore).

Three mainline electrified tracks in the test area are numbered Track 2 (easternmost) through Track 4 (westernmost). Track 2 carries predominantly northbound traffic. The center Track 3 carries traffic in both directions along with all daytime freight traffic, and the concrete tie Track 4 carries mostly southbound traffic. North of the test site, the tracks are tangent for about two miles. The first curve to the south is approximately one mile from the test site. Timetable speeds through this area are 110 mph for Metroliner service, 90 mph for other passenger trains, and 60 mph for freight trains.

#### 3.4.2 Physical Layout

Figure 9 shows a photograph of the test site. The RT7SS-2 concrete ties are equipped with Pandrol elastic clips, external nylon insulators and EVA pads which are notched to fit around the fastener shoulders. These components are the standard equipment of the original Northeast Corridor concrete tie installation, which began in 1978 with a 10-mile section through Aberdeen.

The test site is essentially at grade, and the area surrounding the site is rather flat. The track itself is on a small embankment of about 4 ft, which is an old trackbed that has been raised and reballasted many times over the years.

### 3.5 The Norfolk and Western Site Near Roanoke, Virginia

The Roanoke, Virginia test site, designated Kumis by the N&W Railway Company is located to the west of an overpass on US Rt. 460 about 15 miles west of Roanoke. The N&W has two mainlines in this vicinity allowing it to direct eastbound, loaded coal trains down a long grade which is 0.38 percent at the concrete tie test site. The eastbound traffic crosses from Montgomery to Roanoke Counties about midway through the test site in this rural area. Timetable speed is 45 mph through this area and because of the downgrade, service braking is required.

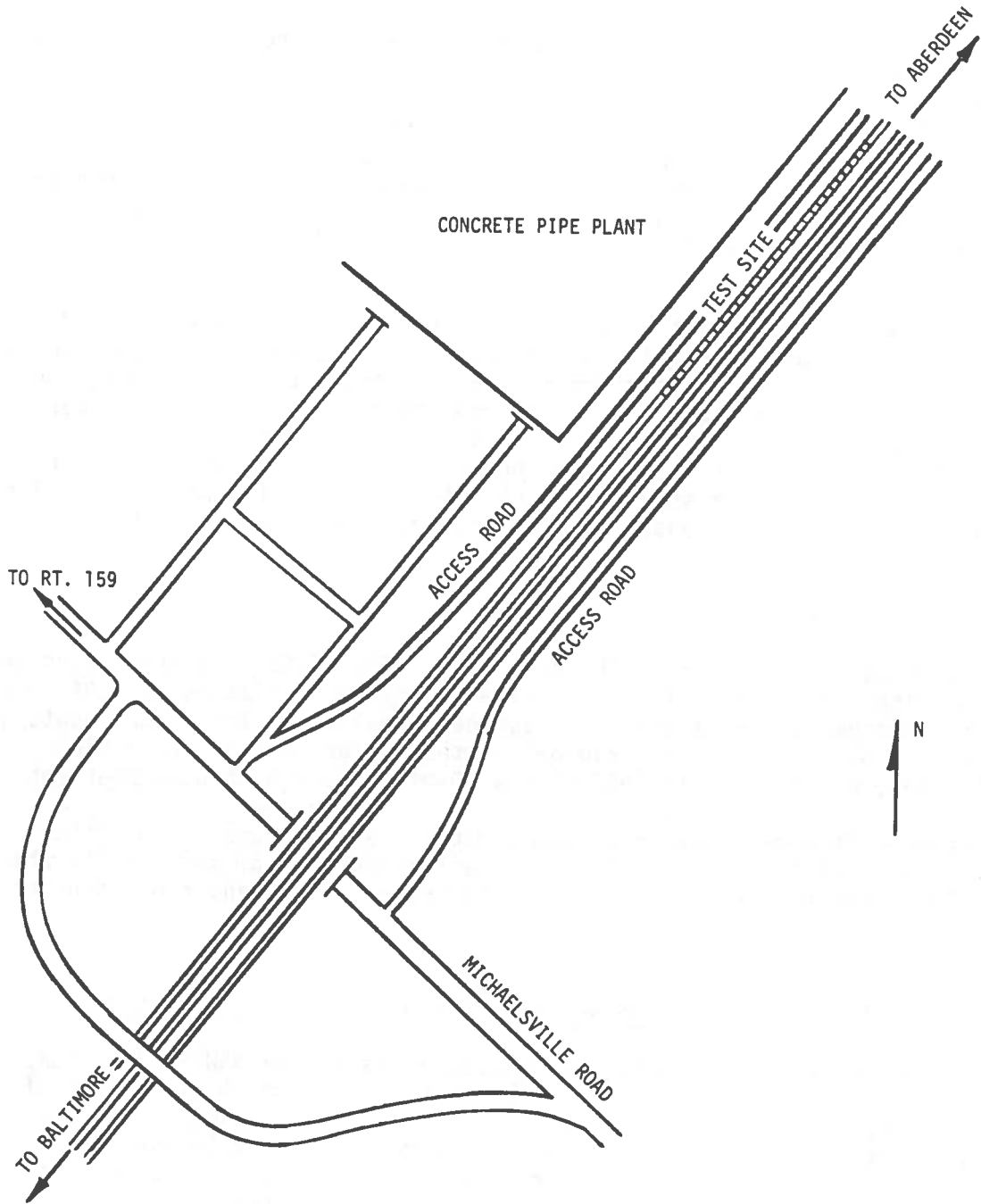


FIGURE 8. LOCATION OF NORTHEAST CORRIDOR TEST SITE AT ABERDEEN, MD

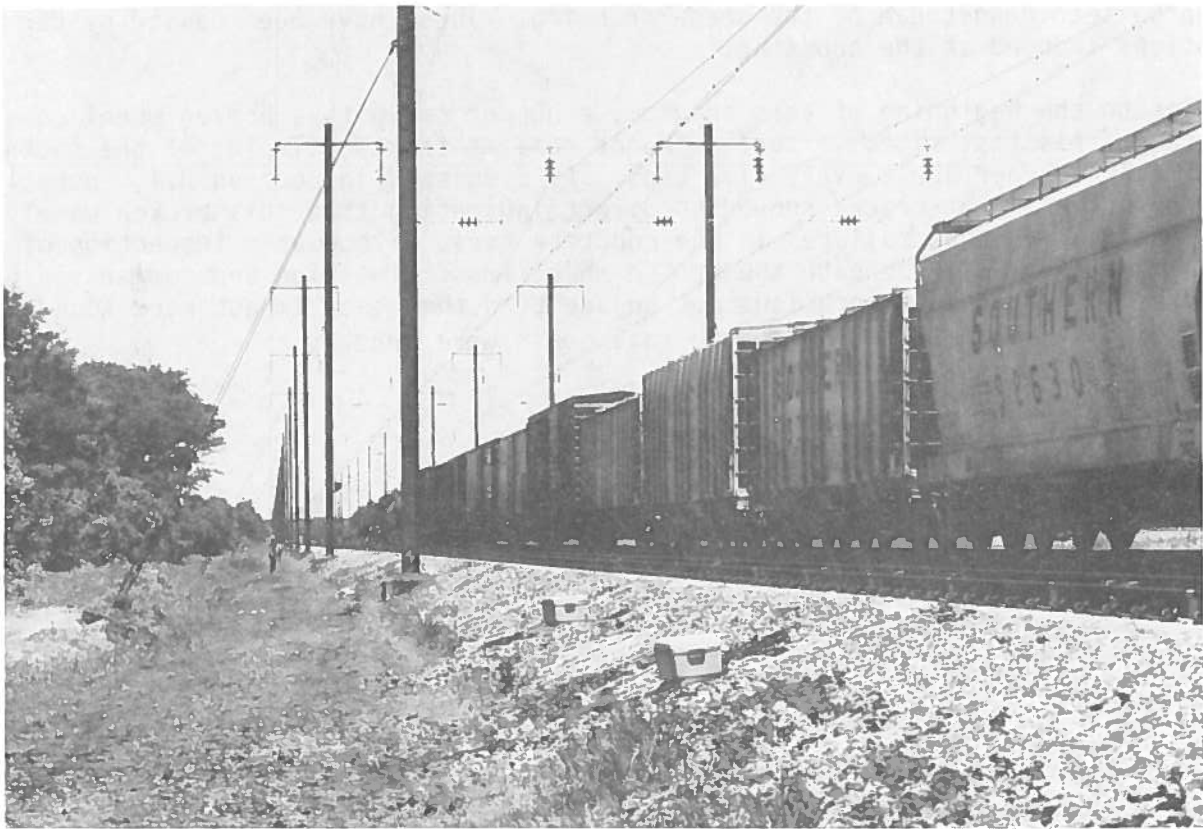


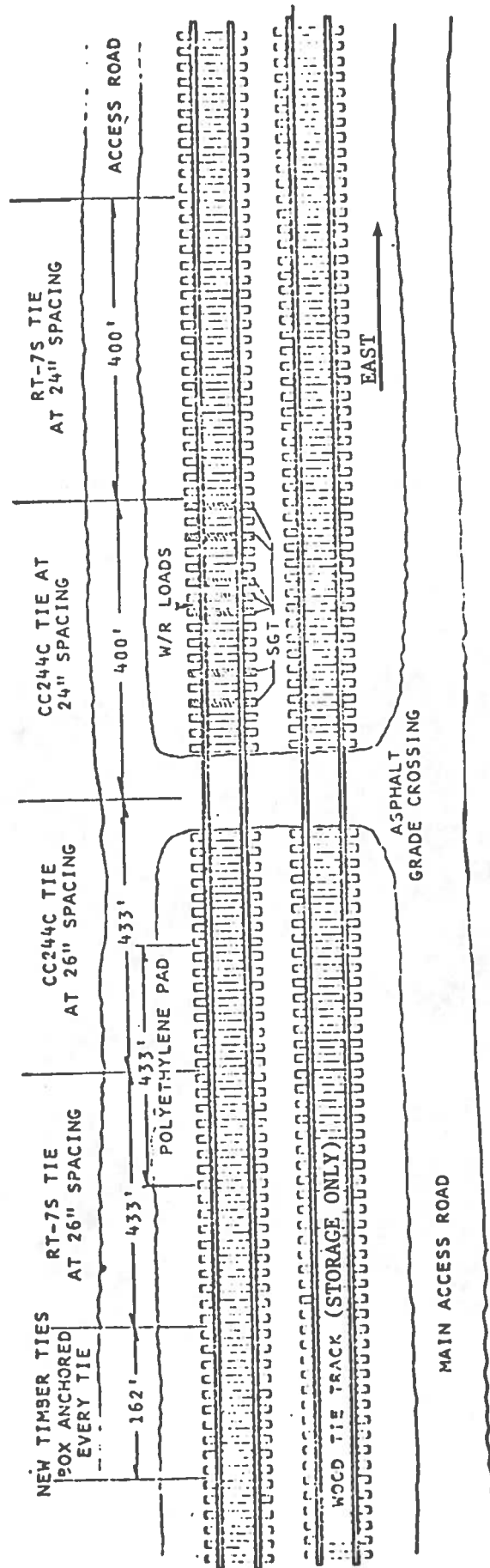
FIGURE 9. VIEW OF ABERDEEN TEST SITE LOOKING NORTHEAST

As shown in Figures 10 and 11, the N&W test track is a 1666-foot section on tangent track paralleled by a two-mile-long passing siding. This site is bisected by a grade crossing and a culvert immediately to the east of the crossing. To the west of the grade crossing, ties are spaced at 26-inch intervals while to the east, ties are at 24-inch intervals. Each half of the site contains 200 RT-7S and 200 CC244C ties.

The random selection of instrumented ties began at the eastern end of the zone containing CC244C ties on 24-inch spacing and progressed westward. This allowed selection of the seven instrumented ties under the same conditions of tie length and spacing as the other test sites, while it avoided a rough spot further west in that same zone near the culvert.

The concrete tie test section has not received any maintenance, such as surfacing or undercutting since it was built, except for some spot maintenance around the culvert. Several long-wavelength undulations of the track surface can be seen downstream of the grade crossing. These have been caused by car motions induced at the crossing.

Prior to the beginning of this program, a hopper car with a broken wheel came through this test site. Visual evidence remains from scalloping of the south rail gage corner about every five ties. As discussed in Section 8.1, inspection for rail seat cracks showed no direct indication that this broken wheel produced any unique failures in the concrete ties. Systematic inspection of rail seats directly beneath the broken wheel impact location and comparison of those results against locations not adjacent to the wheel impact were found inconclusive because all inspected rail seats were cracked.



NORFOLK & WESTERN  
 ROANOKE, VIRGINIA

BALLAST: 18" CRUSHED GRANITE  
 RAIL SIZE: 132  
 TRAFFIC: MIXED FREIGHT & UNIT COAL (HEAVY EASTBOUND)  
 TONNAGE: 40 - 50 MGT/YR  
 FASTENER: PANDROL  
 PAD: KONVEX (EXCEPT AS NOTED)

FIGURE 10. LAYOUT OF CONCRETE TIE TEST SECTION AT ROANOKE, VA

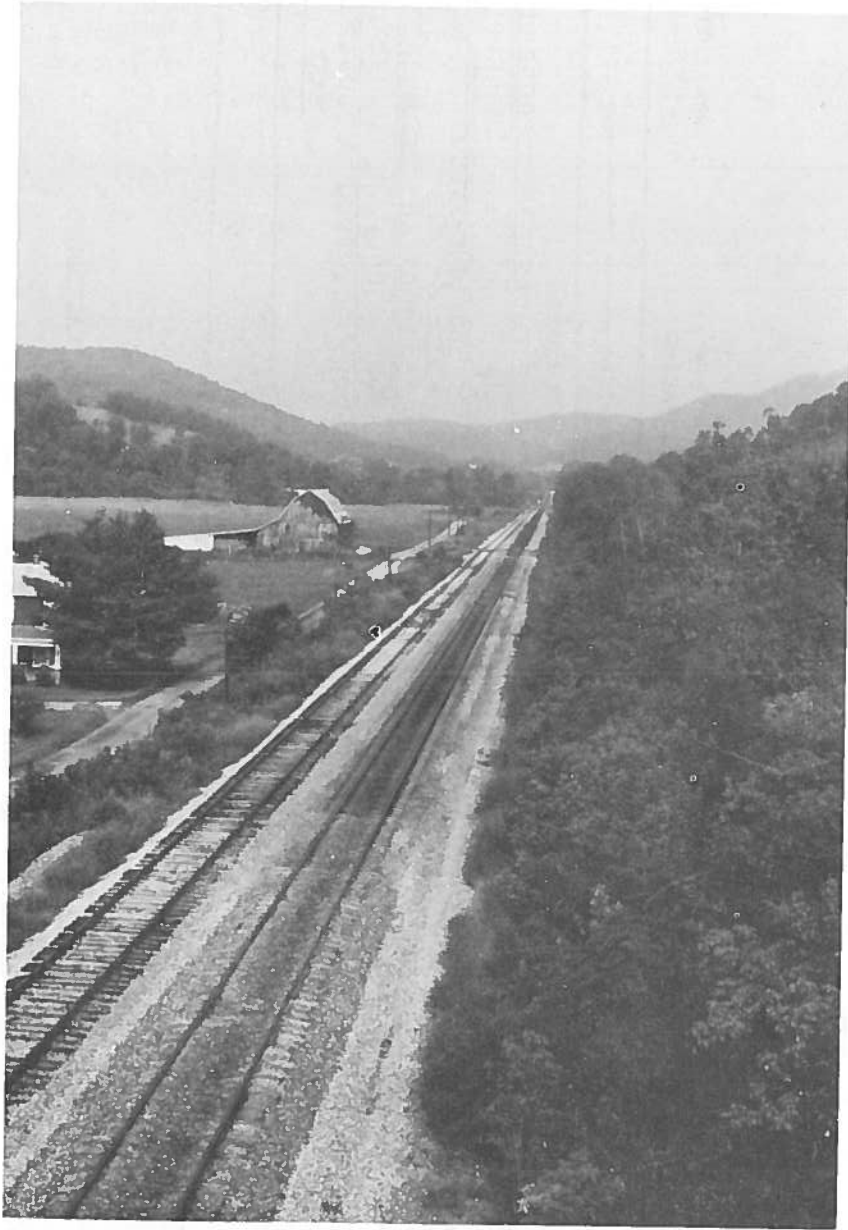


FIGURE 11. N&W CONCRETE TIE TEST SITE, NEAR ROANOKE, VA., LOOKING WEST



#### 4.0 CORRELATION MEASUREMENT PLAN

The general approach of the correlation analysis was to evaluate the dependence of track degradation on loads, track structural characteristics, climatic conditions, and maintenance practices at FAST and in revenue service. An ultimate objective was to develop the ability to predict analytically long-term performance from a given set of operating conditions. However, the current state of the art in analytical prediction is limited, even for the simulation of very short-term phenomena such as track response to given loads. Therefore, the correlation test plan was designed to gather the information which would permit the evaluation of long-term performance on two levels:

- a. by direct comparison of the conditions that cause track degradation (loads, ballast and subgrade support characteristics) with measurements of track degradation (track geometry, settlement, component wear)
- b. by analytical simulation of long-term settlement. This objective required the collection of ballast and subgrade samples on which laboratory tests were performed to determine behavior under repeated loads.

This report summarizes the results of the efforts under (a) and (b), for which a detailed measurement and analysis plan was developed [1]. Volume II covers in detail the work required to achieve (b). Volume III describes the field measurements, data acquisition, and analyses needed to support the performance evaluations.

#### 4.1 Summary of Measurements

The data required for a correlation study at either of the previously described levels can be grouped into the following categories:

- a. construction and maintenance history
- b. traffic data
- c. track loading and response under load
- d. mechanical and material properties of ballast and subgrade
- e. performance indicators.

In Table 1 the types of data collected from the railroads and the measurements conducted during the visits to each revenue service track site are summarized. The data have been applied to the site descriptions which appear in Section 3. Each measurement is defined in more detail in following subsections, as well as in greater detail in Volume III.

TABLE 1. SUMMARY OF MEASUREMENTS AND DATA REDUCTIONS

| MEASUREMENT                                      | REQUIRED DATA   | DATA REDUCTIONS   |
|--|---|---|
| 1. CONSTRUCTION AND MAINTENANCE RECORDS          | Construction and maintenance history of test section from installation of concrete ties through correlation test period.  | Summary of test site construction and maintenance history.  |
| 2. TRAFFIC DATA                                  | For one month of traffic spanning each site visit:<br>(1) Date and time of train passage<br>(2) Type of each car<br>(3) Gross weight of each car and of train<br>(4) Direction of travel and track if multiple-track line | Classification of traffic:<br>(1) Percent empties vs. fulls<br>(2) Percent travelling each direction<br>(3) Types of cars and locomotives |
| 3. TONNAGE ACCUMULATION                          | For period of time starting with installation of concrete ties and extending through correlation test program: date vs. accumulated tonnage.  | Tonnage accumulation is a basic independent variable for performance plots.   |
| 4. WHEEL/RAIL LOADS<br>a. Vertical<br>b. Lateral | Vertical and lateral wheel/rail loads on both rails at one site in each test section, for all axles passing over the site during the dynamic data collection period.  | Cumulative probability distributions and probability densities of train loads.  |
| 5. TIE BENDING MOMENT                            | Tie bending moment at one rail seat and at tie center for seven ties, 3 consecutive and 4 isolated (randomly selected) in the test section.   | Cumulative probability distributions<br>Bending moment vs. loads  |
| 6. RAIL/TIE ACCELERATIONS                        | Simultaneous measurement of acceleration on the tie and adjacent rail base, for several ties per site   | Transfer functions defining degree of attenuation from rail to tie, principal vibration frequencies of rail/tie system                    |
| 7. WHEEL DETECTOR AND SPEED                      | Six channels for wheel detection<br>Measured distances between detectors  | Train speed, wheel identification   |
| 8. VERTICAL TRACK MODULUS                        | Vertical load, applied simultaneously to both rails, and corresponding vertical deflections measured from fixed reference, at 7 - 10 locations per test section   | Variation in ballast stiffness with type of construction, tonnage accumulation and surfacing  |

TABLE 1 (Cont.) SUMMARY OF MEASUREMENTS AND DATA REDUCTIONS

| MEASUREMENT  | REQUIRED DATA  | DATA REDUCTIONS   |
|--|--|---|
| <p>9. BALLAST DENSITY (IN-SITU)</p>  | <p>Volume of displaced ballast (of water to fill hole) and weight of ballast sample for 18 tests, 9 at each of two tie locations in the test section:</p> <ul style="list-style-type: none"> <li>● 2 in ballast crib</li> <li>● 3 under tie at ballast surface</li> <li>● 2 at top of subballast layer</li> </ul>                | <p>Variation in density over width and depth of track, to compare with other ballast characteristics</p>  |
| <p>10. PLATE LOAD RESISTANCE</p>   | <p>Applied vertical plate bearing load and corresponding deflection for 18 tests, 9 at each of two locations:</p> <ul style="list-style-type: none"> <li>● 3 in ballast crib</li> <li>● 3 under tie at ballast surface</li> <li>● 3 at top of subballast layer</li> </ul>  | <p>Variation in ballast stiffness over width and depth of track, to compare with other ballast characteristics</p>  |
| <p>11. BALLAST GRADATION (INDEX)</p>   | <p>Percent weight of ballast sample passing through each of 14 sieves, for 6 samples per test section</p>  | <p>Cumulative "percent finer than" plots, for ballast classification</p>  |
| <p>12. BALLAST MATERIAL PROPERTIES</p> <ol style="list-style-type: none"> <li>a. Liquid &amp; Plastic Limits</li> <li>b. Specific Gravity</li> <li>c. Water Absorption</li> <li>d. Chemical Composition</li> <li>e. Angularity, Sphericity</li> <li>f. Hardness</li> </ol> | <p>One complete test series per test section</p>   | <p>Complete tabulated data set</p>  |
| <p>13. SUBGRADE PENETRATION TESTS</p> <ol style="list-style-type: none"> <li>a. Dutch Cone Test</li> <li>b. Standard Tests (Disturbed Samples)</li> <li>c. Material Identification and Stratification</li> </ol>   | <p>(Penetration resistance vs. depth)<br/>                     Tests at intervals of 50 - 100 feet through test section, to depths of 20 - 25 feet<br/>                     Two tests in each section to depths of 20 - 25 feet. Collect samples.<br/>                     Visual identification of soil material and strata</p> | <p>Plots of depth vs. penetration force<br/>                     Plots of depth vs. penetration force<br/>                     Charts of stratification vs. depth</p> |
| <p>14. SUBGRADE MATERIAL PROPERTIES (Undisturbed Samples - Laboratory Tests)</p> <ol style="list-style-type: none"> <li>a. Shear Strength</li> <li>b. Resilient Modulus</li> <li>c. Permanent Strain</li> <li>d. Moisture</li> <li>e. Density</li> </ol>                   | <p>Two 4" - 6" diameter borings to depth of 5 - 10 feet, starting at top of subballast layer.<br/>                     45 tests per track section:</p> <ul style="list-style-type: none"> <li>● 3 test sites</li> <li>● 3 materials (ballast, subballast, subgrade)</li> <li>● 5 samples per material</li> </ul>                 | <p>Measured properties tabulated by test site, material and depth.</p>  |

(Continued Next Page)

TABLE 1 (Cont.) SUMMARY OF MEASUREMENTS AND DATA REDUCTIONS

| MEASUREMENT   | REQUIRED DATA  | DATA REDUCTIONS   |
|---|--|---|
| <p>15. MOISTURE MONITORING &amp; SAMPLING</p> <p>a. Oven samples - Ballast, Subballast &amp; Subgrade</p> <p>b. Moisture sensors for subgrade</p> | <p>Moisture content of ballast, subballast and subgrade</p> <p>Variety of samples to come from penetration tests, plate load and density tests, ballast gradation tests and samples taken during installation of moisture sensors.</p> <p>Readings of "apparent capacitance" due to moisture variations at intervals of one week for six sensors per test section.</p> | <p>Tabulations by depth, material and time of measurement</p> <p>Variation of moisture content through test period</p>  |
| <p>16. TRACK GEOMETRY CAR MEASUREMENTS</p>  | <p>Runs of railroad track geometry car at the same frequency as site visits, with positive identification of the test section. It is especially important to have runs before and after surfacing maintenance.</p>   | <p>Data reductions normally produced by railroad (exception reports, etc.)</p> <p>Strip charts of deviations vs. time</p> <p>5-percent level of exceedance of deviations, vs. MGT</p> |
| <p>17. SURVEY-TO-BENCHMARK</p> <p>a. Vertical</p> <p>b. Lateral</p> <p>c. Longitudinal</p>  | <p>Elevation, lateral and longitudinal position of points on rail located approximately every 10 ties.</p>   | <p>Rates of settlement, lateral shift and rail movement vs. MGT</p>   |
| <p>18. TIE/FASTENER/PAD/INSULATOR INSPECTIONS</p>   | <p>Records of tie cracks, tie damage, movement, dislocation and damage of fastener clips, pads and insulators. All tie tops inspected and 10 percent of cribs opened.</p> <p>Note rail corrugations and evidence of rail creep and tie movement. Creep markers installed at first site visit.</p>  | <p>Rates of cracking, damage, dislocation and failure of components</p> <p>Verbal descriptions of rail corrugations and tie movement</p>  |

## 4.2 Measurement Locations

Most of the measurements of Table 1 required the selection of discrete locations at the test site where instrumentation was applied, material samples were collected, or observations were made. Tie surface and fastener inspections were performed on all ties in the designated test section. Crib inspections were performed at intervals through the site in sufficient number to form a large statistical sample. However, cost constraints required the selection of the fewest number of instrumentation and material sampling sites that could satisfy the test objectives.

These numbers of measurement locations were summarized in Table 1. As an example, wheel/rail loads were measured at only one crib per test section. Care was taken to see that this location avoided unusual track conditions such as battered welds or joints between welded rail strings. Previous experience with this measurement had shown that when bad track conditions were avoided, the effect of spatial variation on loads is small, on the order of  $\pm 10$  percent. Since the test objective was only to characterize the traffic loads at the site, the single measurement site was deemed adequate. Additional discussion of the choices of measurement location appear in the procedure descriptions of Volume III, Sections 5 - 7.

All of the measurements listed in Table 1 were performed at three sites: Streator, Richmond, and Aberdeen. The dynamic measurements of wheel/ rail load and tie bending moment were made periodically in Sections 17 and 22 at FAST. Due to cost constraints and conflicting test plans at the N&W, the measurements at Roanoke did not include the ballast and subgrade studies.

## 5.0 DYNAMIC MEASUREMENTS

Several measurements were made to characterize the dynamic behavior of the track structure under service loading. Strain gauge circuits were applied to the rail to measure vertical and lateral wheel/rail loads. Strain gauge coupons were applied under the rail seats and the tie center of selected ties in each section. These were calibrated in place to measure tie bending moments. Because of the variability of support conditions which are known to occur within the track structure, a total of seven, randomly selected ties were instrumented. To maintain a sufficient statistical base by which valid comparisons could be made between sites and within separate populations of events at each site, a minimum of 20,000 axles were recorded for each test condition.

Accelerometers were attached to the rail base and to the adjacent tie surface to simultaneously measure rail and tie accelerations. These were used to define the attenuation of vibratory loading offered by the tie pad. Transducer installations are illustrated in Figure 12. Figure 13 defines a typical layout of dynamic measurement locations in a test section.

Details of installation and calibration of the transducers, data acquisition, and data reduction are all included in Volume III.

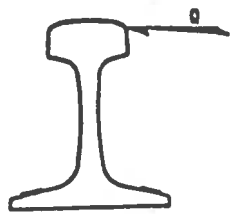
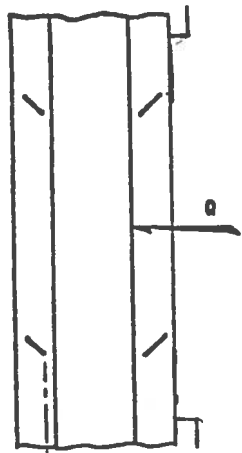
### 5.1 Traffic Loads

As discussed in Section 3.0, the traffic loads at each revenue test site were expected to be sufficiently different in character to afford a comparison of load conditions. These different loading conditions would produce differing responses in the track structure, both in terms of tie performance as well as track settlement.

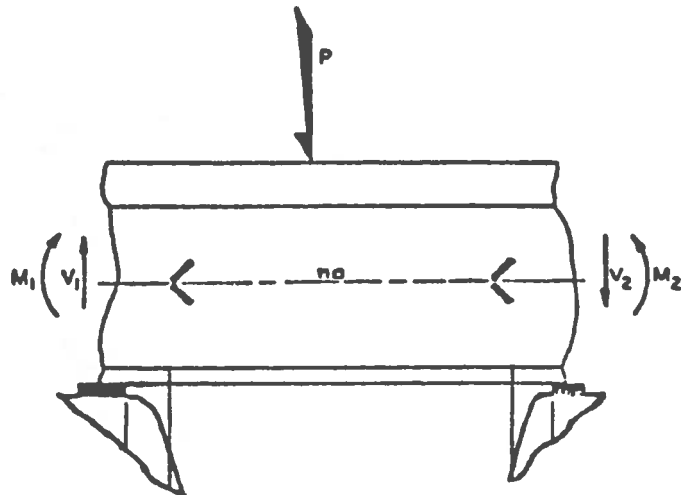
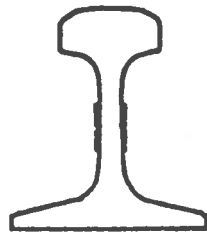
Once characterized, selected values of traffic loads at each site could be used for correlation of track settlement through laboratory tests and analytical model runs.

Traffic density and cumulative tonnage data were acquired from each railroad. Listings of the individual train consists were acquired through their computerized data systems.

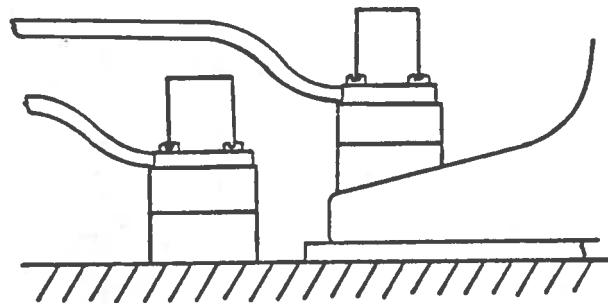
By acquiring consist lists throughout the period of the revenue data collection and tabulating the gross loads of the cars listed on these consists, it was possible to develop static load distributions. By comparing these against the dynamic wheel load distributions, it was possible to make direct comparisons between static and dynamic loads without direct knowledge of the static weights of the individual axles. Figures 14 through 18 are the resulting pairs of static and dynamic wheel load distributions for each of the 5 test sites including FAST. The variation between the static and dynamic load curves at any one point can be caused by four factors: (1) static weight distribution to each wheel on any car will rarely be exactly 1/8 of the gross load listed on the train consist sheet. Uneven car loading as well as imperfect load distribution within the trucks' suspensions will cause a



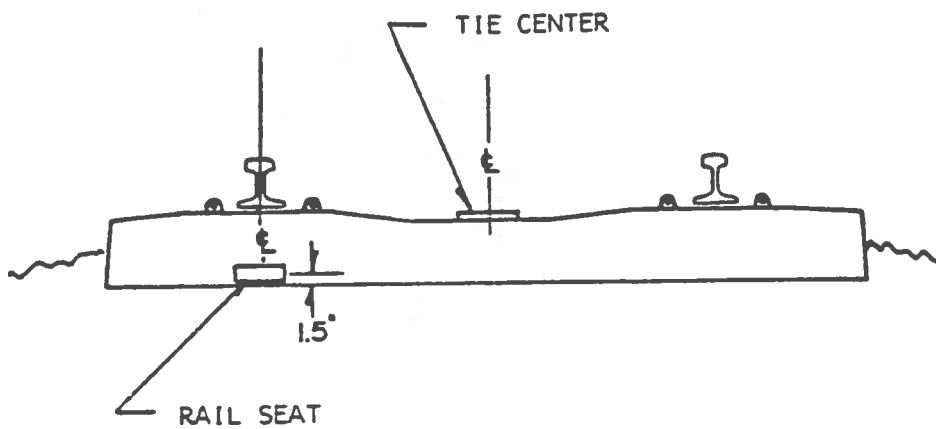
Lateral Load



Vertical Load



Rail and Tie Accelerations



Tie Bending Moments

FIGURE 12. RAIL AND TIE INSTRUMENTATION FOR DYNAMIC MEASUREMENTS

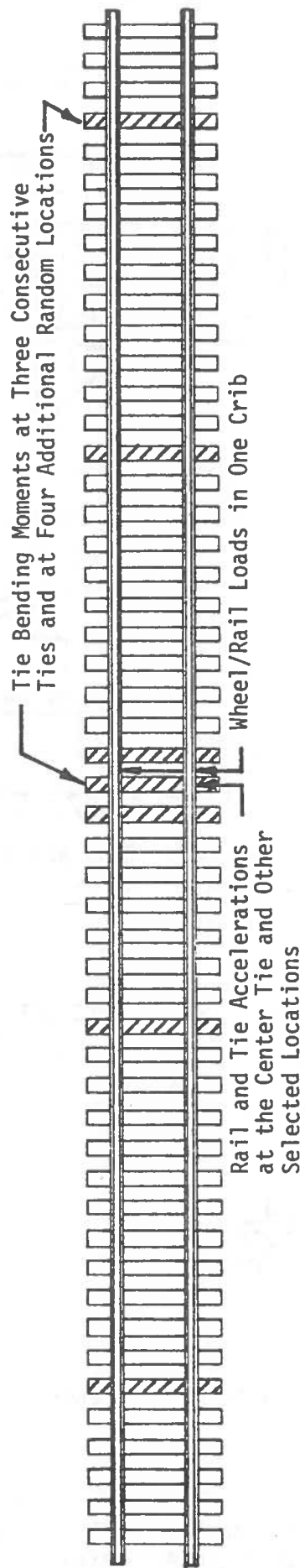


FIGURE 13. TYPICAL LAYOUT OF DYNAMIC MEASUREMENTS IN A TEST SECTION



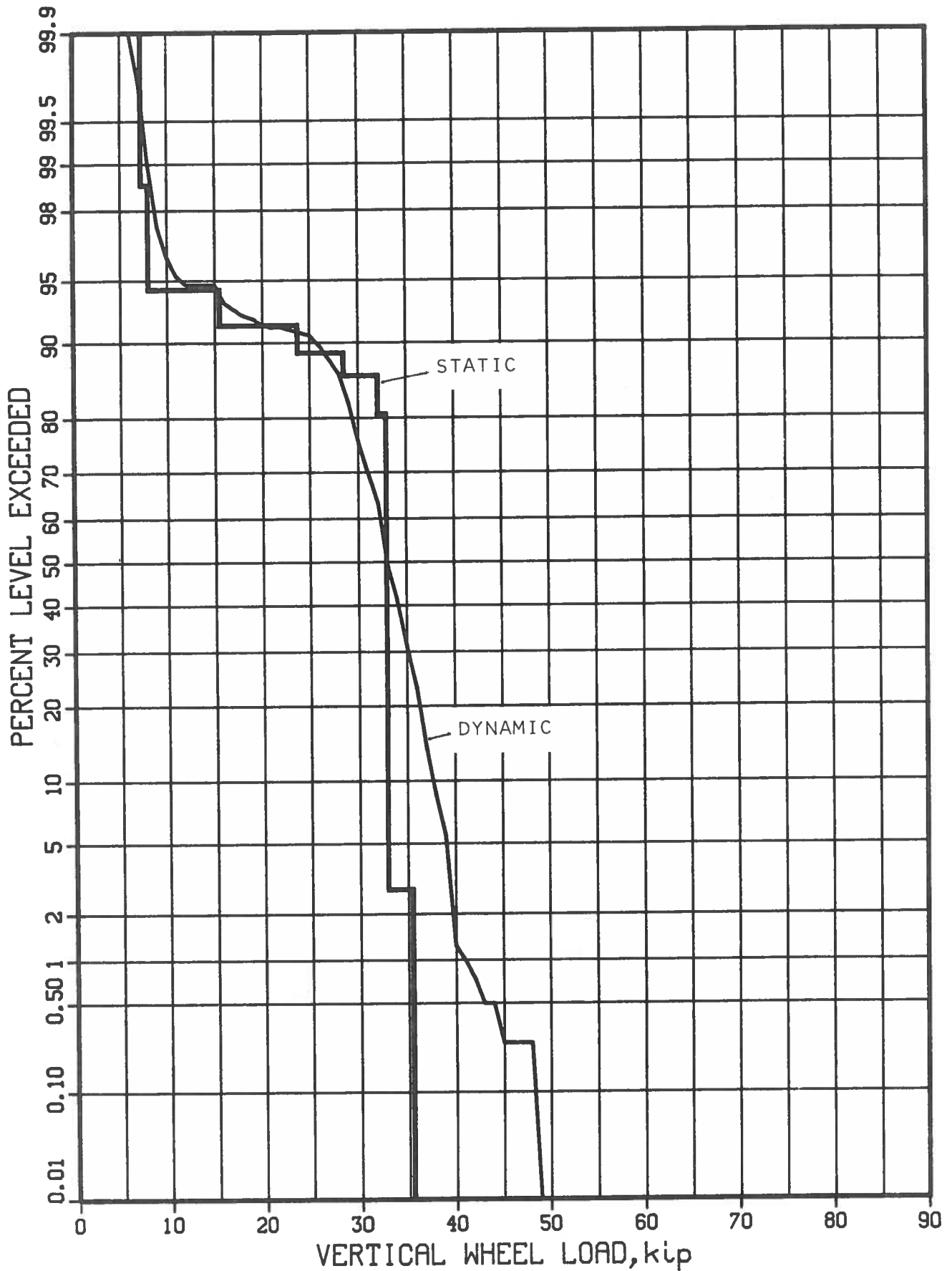


FIGURE 14. STATIC AND DYNAMIC WHEEL LOADS AT FAST, SECTION 22

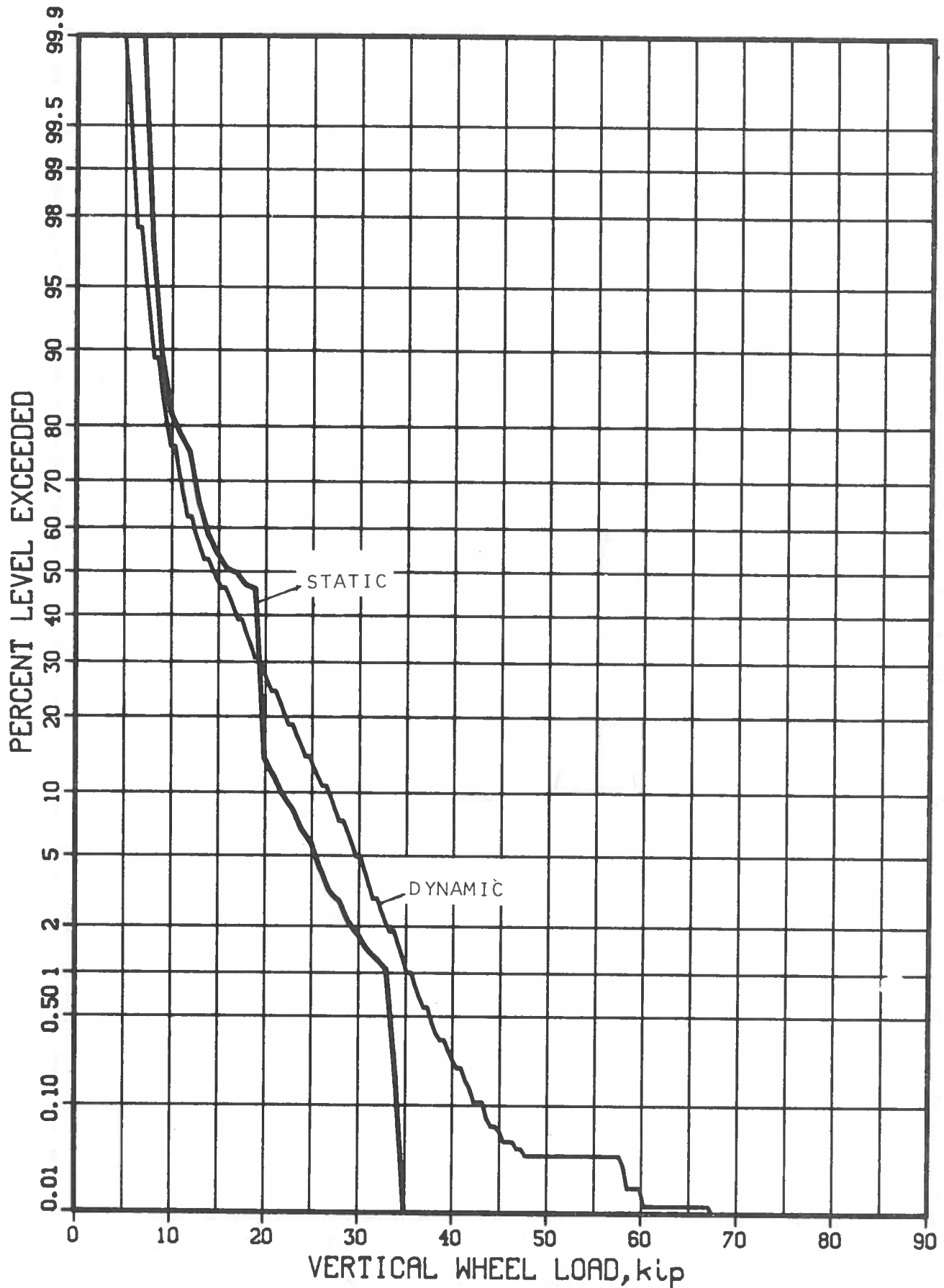


FIGURE 15. STATIC AND DYNAMIC WHEEL LOADS AT STREATOR (SANTA FE)

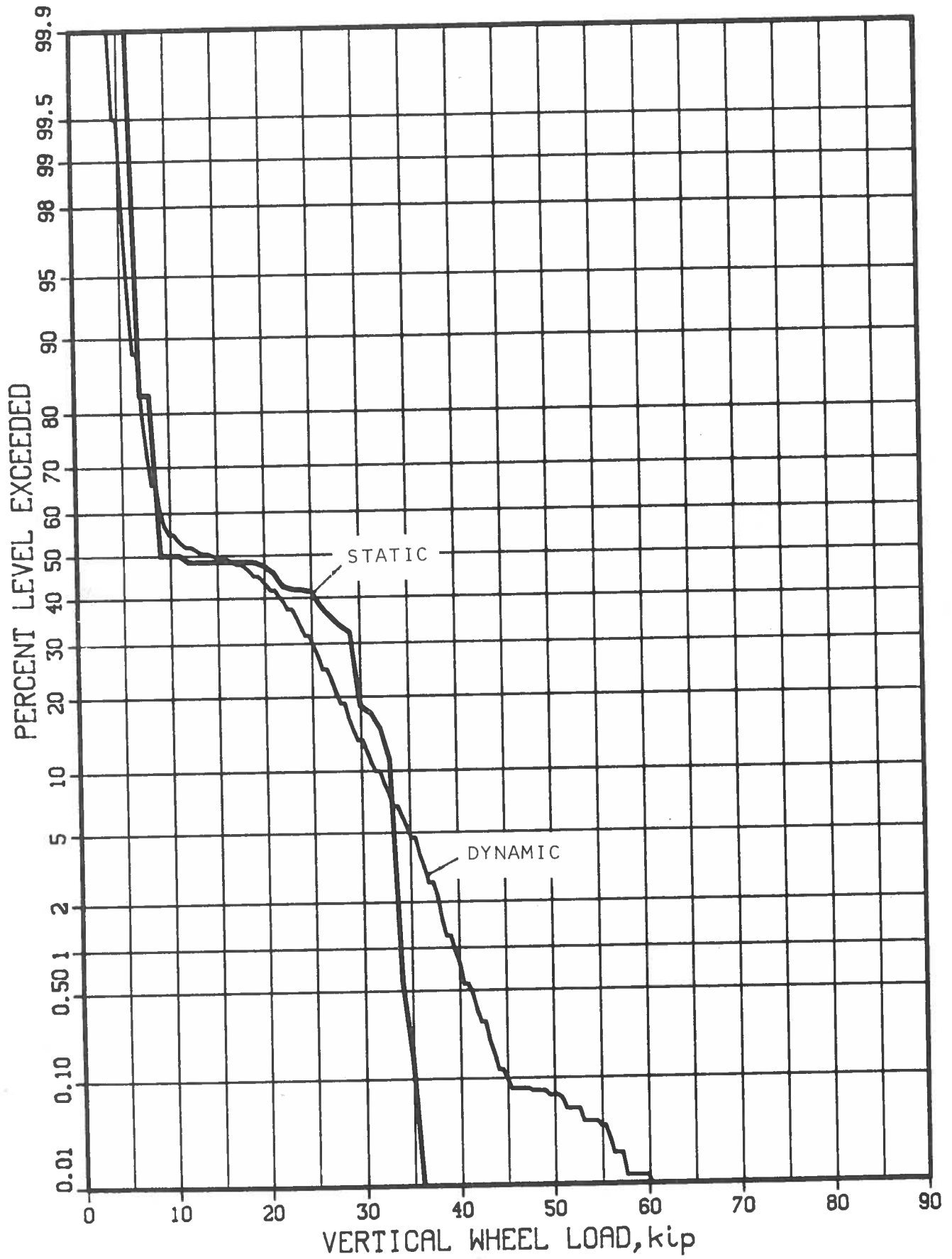


FIGURE 16. STATIC AND DYNAMIC WHEEL LOADS AT RICHMOND (CHESSIE)

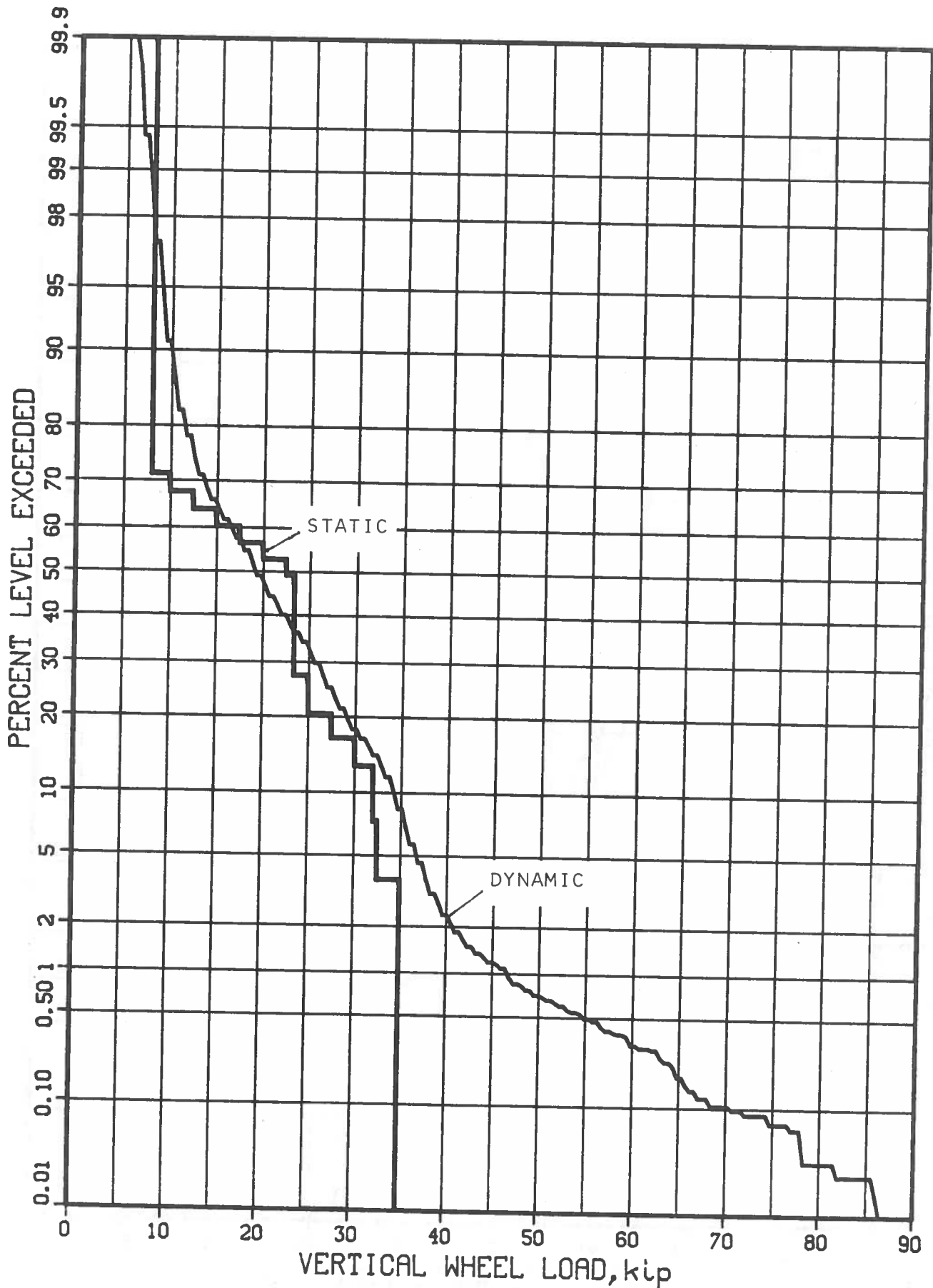


FIGURE 17. COMBINED PASSENGER AND FREIGHT STATIC AND DYNAMIC WHEEL LOADS AT ABERDEEN (AMTRAK AND CONRAIL)

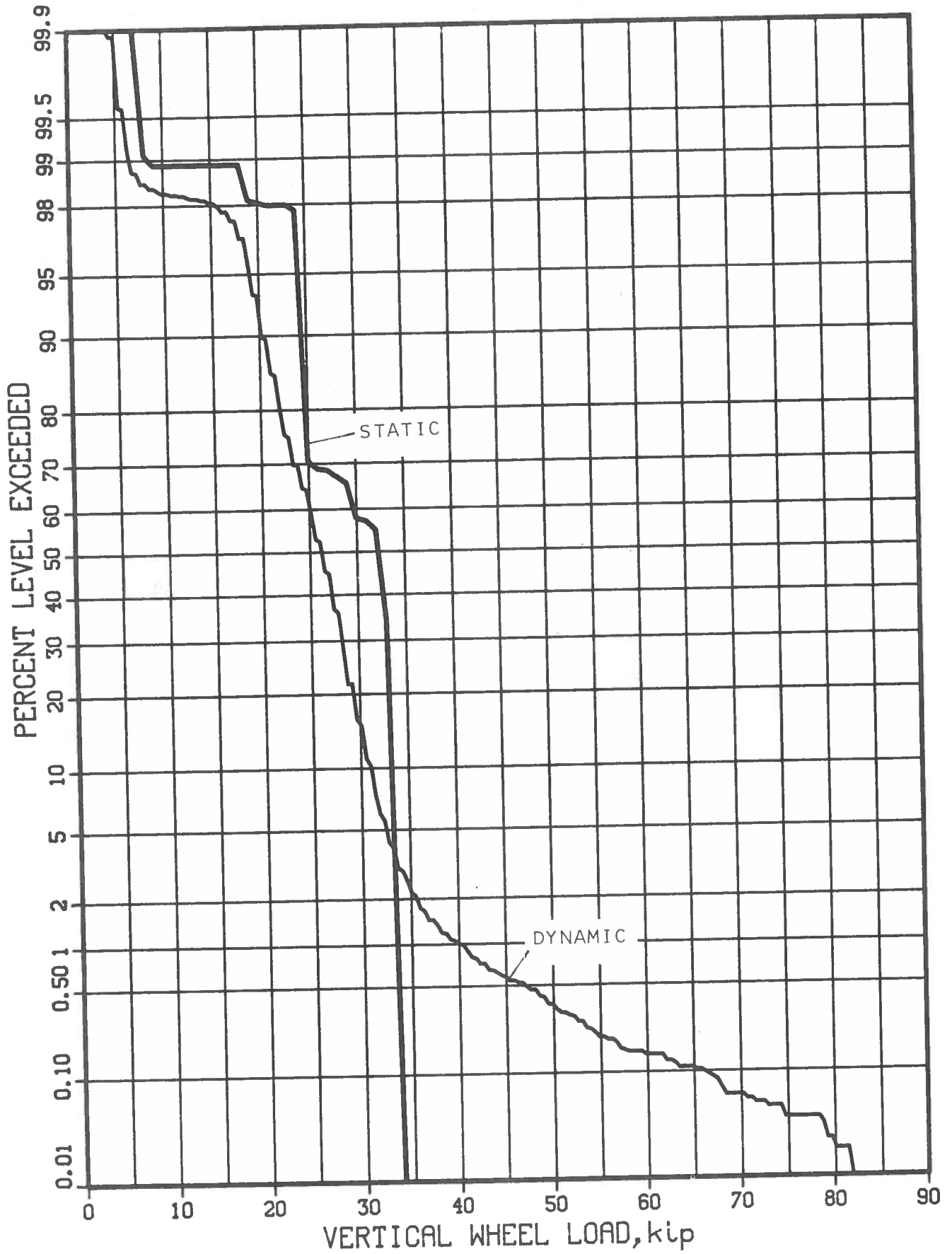


FIGURE 18. STATIC AND DYNAMIC WHEEL LOADS AT ROANOKE (N&W)

variability in the loads seen at each wheel, (2) dynamic wheel impacts caused by irregularities in either the wheels or rail surfaces, (3) variation of wheel force due to vehicle/track interaction, such as curving imbalance and pitch and bounce, (4) differences in calibration between the scales used to measure the gross carloads and the circuits used to measure the dynamic wheel loads.

As can be seen from examining Figures 14 through 18, there is a relatively close matching of the loads determined statically and dynamically over 90 to 95 percent of the axles. On the static curves, the near vertical line segments represent subpopulations of vehicles which are listed in the consists as having identical gross loads. The corresponding segments of the dynamic curves typically have finite slopes indicating the normal scatter in actual wheel loads about the average of these subpopulations. In the lower portion of each plot, static and dynamic loads begin to diverge significantly, particularly in Figures 17 and 18, because of the superposition on the dynamic load curve of an additional subpopulation of loads from wheels having irregularities including spalled and eccentric profiles, and slid flats. Although a direct interpretation of the two curves in this low-probability, high-load region would tend to imply that these higher loads caused by wheel irregularities are being superimposed only on the heaviest nominal wheels, a detailed examination of the wheel load data shows that nominally lighter wheels contribute equally to these incremental dynamic loads.

#### 5.1.1 FAST Loads

As the lower portion of Figure 14 indicates, the FAST consist exhibits almost no wheel tread irregularities, evident by only small differences between the heaviest static wheel loads and the corresponding dynamic wheel loads. The FAST train primarily consists of 100-ton cars loaded to capacity, with a few selected cars switched in and out for specific tests. The break in the curve at the 90th percentile level indicates that approximately 10 percent of the vehicles carry less than the rated maximum loads including a few empty cars. This is very close to the maximum unit train condition expected where all cars are 100-ton capacity and fully loaded.

#### 5.1.2 Streator Loads

The vehicles on the Sante Fe as seen at Streator consists primarily of trailer-on-flat cars and container-on-flat cars (TOFC/COFC). The large segment of this population, indicated on the static curve in Figure 15 between 15 and 45 percent, represents the nominal, loaded capacity of the TOFC/COFC cars. The actual mix of these cars along with the variation in empty conditions (with and without two trailers, etc.) produces the uniform range of wheel loads from about 7 to 27 kip per wheel. The remainder of the fleet is a mix of general freight, both loaded and empty, which will range in load between 5 and 35 kip per wheel. A very small percentage of flat wheels indicated at the bottom of the curve in Figure 15 shows an overall high quality of wheel maintenance exceeded only by that at FAST.

### 5.1.3 Richmond Loads

At the Richmond site, Chessie primarily runs unit coal trains: loaded in one direction and empty in the opposite direction. This is characterized in Figure 16 as two curve segments separated at the 50th percentile. The empties are represented by the upper curve segment between 6 and 8 kip and the loaded unit trains dominate the lower 50 percent. The rounded off region between the 50th and about the 15th percentile includes smaller capacity hopper cars and an occasional mixed freight. The divergence at the bottom of the curve between the 0.1 and 0.5 percentile characterizes the portion of the fleet with wheel irregularities.

### 5.1.4 Aberdeen Loads

Figure 17 is a composite of the static and dynamic loads acquired at the Aberdeen test site. Freight consist data were not acquired from Conrail directly, however Amtrak provided detailed tonnage data used to document the traffic over Track 4 at Aberdeen. Both passenger and freight loads could therefore be characterized by reconstructing the statistics in a form similar to the data acquired at the other sites. The dynamic data were also apportioned in a manner to reflect the correct cumulative balance between passenger and freight traffic over Track 4. This resulted in a relatively close match between static and dynamic loads down to about the 2 percent level. The subpopulation of large wheel loads below the 2 percent probability level are caused almost entirely by the passenger car fleet. This is especially significant because the nominal wheel loads of the passenger cars are relatively low at about 23 kips and the speeds are relatively high; between 80 and 110 mph. These large dynamic wheel loads compromised tie performance as discussed in detail in Section 8. Another research program was initiated to determine, in detail, the causes and solutions to the effects of wheel flats on concrete ties [5].

### 5.1.5 Roanoke Loads

Figure 18 shows the static and dynamic loads for N&W traffic at Roanoke. These curves are unique in that the static loads are consistently shown to be greater than the corresponding dynamic loads down to about the 3 percent level of exceedance. For this to occur, the last two of the four previously discussed factors affecting static and dynamic wheel load measurements may be causing some discrepancy. Either there was a small but effective dip in the running surface of the rail at the location that wheel loads were measured dynamically or there was a fundamental discrepancy between the scale used to weigh the gross loads of the vehicles and the calibration of the rail circuit at the test site. The vehicle population on the N&W consisted entirely of loaded hopper cars in the 70- and 85- and 100-ton capacity range. The static curve clearly shows that 55 percent of all the vehicles are the 100-ton class and, correspondingly, about 15 percent are 85-ton class and about 18 percent are 70-ton class. Comparing this to the dynamic response curve would indicate that for the heavy loads there exists about a 5 kip underestimation of the nominal static loads. This is of little consequence, however, when compared to the strong influence of wheel irregularities that affect the lower 3 percent of the exceedance curve. If the error is in the dynamic wheel load circuit calibration, there may be a corresponding underestimation of the dynamic loads at the extreme values.

### 5.1.6 Load Summaries

Figure 19 is a summary plot of the same five dynamic wheel load exceedence curves allowing direct comparison of the five sites. In addition, Table 2 summarizes the statistical values at the median load level and at the 10, 1, and 0.1 percent levels of wheel load. By coincidence the large variation in both the nominal wheel loads and the extreme value loads can be seen to "cross over" at about the 2 percent level. It will be shown later that the relatively large, median loads at FAST will have little effect on the tie cracking performance, whereas the large, low probability loads seen at Aberdeen and Roanoke will dominate the tie performance.

Because wheel circumferences are on the order of 9 to 10 ft and wheel loads were measured only over a 10-12 in. zone, the actual population of wheel irregularities can be assumed to be about 10 times greater. Generally, maximum dynamic wheel loads can range from as low as 1.5 times the static weight on smooth tangent track (as seen in the statistics from FAST) to extreme values between 3 and 5 times the static weight as seen on passenger equipment at Aberdeen. (Although well beyond the linear range of the data system some events have been estimated at greater than 125 kips.)

### 5.1.7 Speed Effects

All data were analyzed to determine the effect of speed on the loads measured at the wheel/rail interface. The relatively narrow range of speeds encountered at most test sites (Figure 20) did not provide for a thorough examination of the speed effects. However, the results do indicate a small speed effect for freight traffic between 20 and 50 mph, although this effect can be ignored because of its minimal influence on the performance of the track structure. The data acquired at Aberdeen, however, revealed a dramatic speed effect for passenger traffic over that site. Originally, data were sorted for the passenger equipment into two speed bands, above and below 70 mph. When a significant speed effect was evident, a more detailed examination of the speeds above 70 mph showed what appeared to be a peak response in the 80 to 90 mph band due to the wheel irregularities. Track model evaluations of wheel impacts have supported the possibility of a resonance effect between the unsprung mass of the vehicle and that portion of the mass in the upper track structure which responds to the impact [6]. However, two groups of passenger equipment are involved: the new Amfleet coaches and the older, "heritage" equipment. It has been shown that these two classes of equipment exhibit different types of wheel irregularities which, when combined with different operating speed ranges, do not allow for a direct verification of the speed effect. In particular, the "heritage" equipment generally runs between 80 and 100 mph, while the Amfleet equipment which exhibits lower extreme loads will run up to 110 mph.



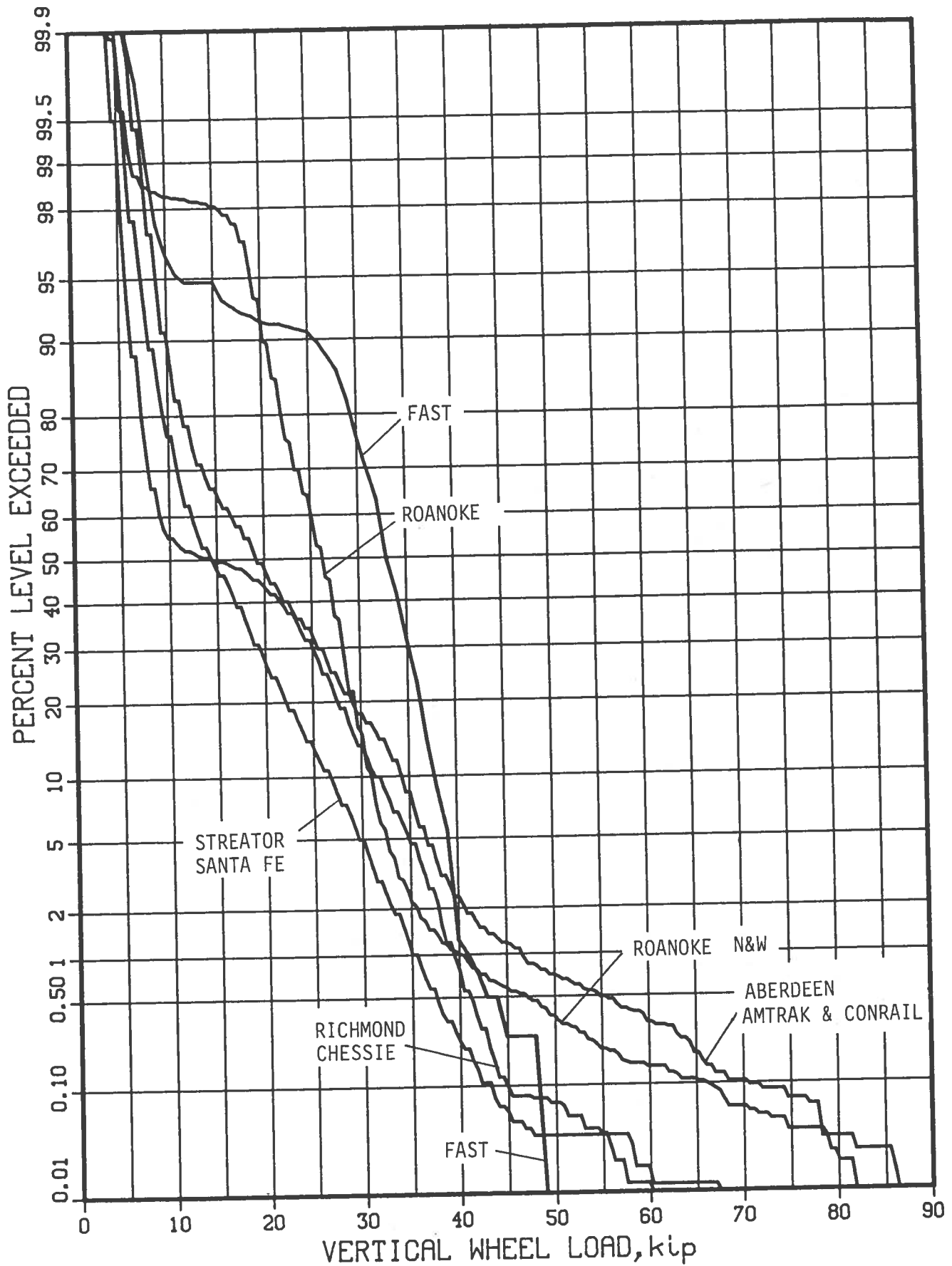


FIGURE 19. SUMMARY PLOT OF DYNAMIC WHEEL LOADS AT ALL SITES

TABLE 2. DYNAMIC WHEEL/RAIL LOAD STATISTICS SUMMARY

| PERCENTILE<br>LOAD | SITE                |          |          |         |
|--------------------|---------------------|----------|----------|---------|
|                    | FAST                | STREATOR | RICHMOND | ROANOKE |
| 50 <sup>(1)</sup>  | 32.8 <sup>(2)</sup> | 15.0     | 15.0     | 26.6    |
| 10                 | 38.3                | 27.3     | 32.0     | 31.4    |
| 1                  | 40.5                | 35.7     | 39.8     | 41.0    |
| 0.1                | 48.0                | 43.5     | 45.0     | 66.5    |

- 1) Percent of Axle Loads Exceeding Stated Value.
- 2) Single Wheel Load in Kips (thousands of pounds).
- 3) Combined Passenger and Freight.

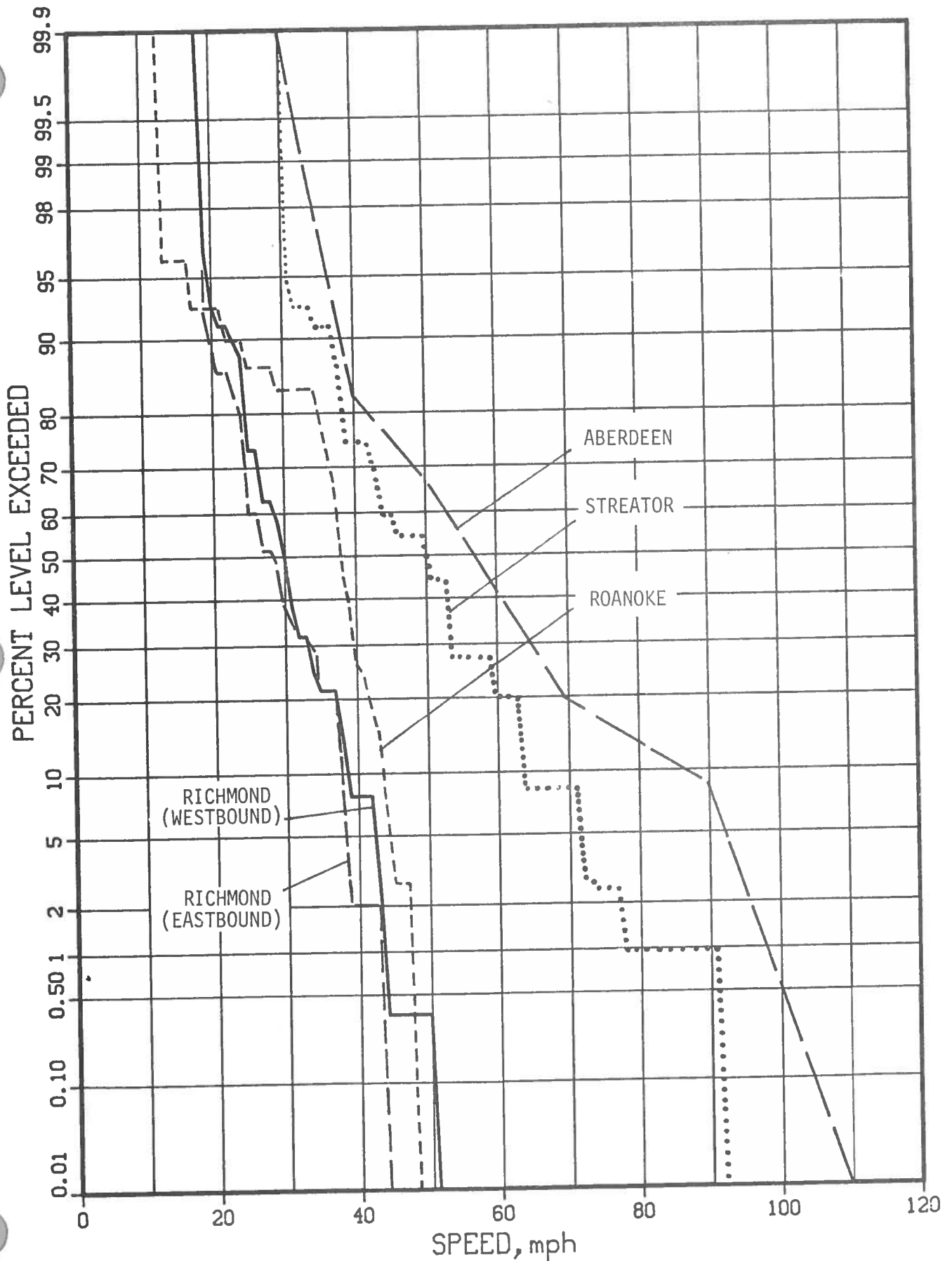


FIGURE 20. DISTRIBUTION OF TRAIN SPEEDS AT EACH SITE

Another observation made during other related tests at Aberdeen [5] indicates that the effective dynamic stiffness of the track can be controlled by the tie pad stiffness. When flexible pads were installed, there was a detectable reduction in the magnitude of the wheel impacts measured at the wheel/rail interface. This is consistent with basic mechanics principles which say that more flexible support conditions will lower the impact loads. It can be assumed that all data summarized in Figure 19 and Table 2 were collected on comparable track structures having essentially rigid rail seat pads and track moduli greater than 4000 lb/in/in.

#### 5.1.8 Effects of Vehicle Weight

All statistically analyzed dynamic data were sorted by nominal weight classes: empties, moderate loads, heavy loads, and locomotives. Classifying vehicles by weight from the dynamic wheel loads is difficult because of the large impact loads caused by wheel irregularities. Several techniques have been used in other programs to minimize the effect of having lighter cars pushed into heavier categories because of wheel impacts. These data were processed by averaging the values acquired for each wheel on an axle, then testing for the difference in left and right wheels. When the difference exceeded 7 kips, the axle was assigned to the next lower weight class. While intuition might indicate that impacts would occur at nearly the same instant, particularly from slid flats, data from Aberdeen showed that whenever a large impact occurred on one wheel, there was rarely a comparable impact on the opposite wheel.

The results of this sorting process is not perfect, so that it is difficult to have high confidence in comparisons of the influence of nominal car weight on the wheel impact phenomenon. However, wheel impacts clearly dominate the loading spectrum to the point of significantly reducing the importance of the nominal weight classes. Only under conditions of well-maintained wheels would nominal weight classes become significant. (No attempt was made to address the effects of weight on rail wear and other related issues that clearly show such trends.)

Although it has not been identified quantitatively, there is an apparent effect of nominal wheel load on the response of a concrete tie. On well-consolidated track there may be a small void under the rail seat which will normally be squeezed out under the larger wheel loads. If a light wheel with an irregularity impacts the rail over this tie, then the tie will respond by "ringing" (prolonged vibrations) at one or more natural frequencies. Thus, the clearances under the rail seat cause the tie to appear lightly damped. Alternatively, if a heavy wheel rolls over the tie and generates an impact, then the small gaps under the tie will be eliminated, causing a constrained response with a significant reduction in the duration of the tie vibration.

## 5.2 Rail Seat Bending

Tie responses to wheel/rail loads were measured with full-bridge strain gauge coupons developed for this program. Techniques described in detail in Volume III allowed for installation of these coupons on ties within the test sections without appreciably disturbing the consolidation\* naturally occurring around the test ties. At each test site, seven ties were randomly selected within a 200 ft test zone, well away from the ends of the concrete tie section to avoid any effects of the transition zones. Each of the selected ties was then instrumented on one rail seat and at the tie center. The tie instrumentation was calibrated in place using a fixture which was proven in the lab to closely approximate the responses recommended by the AREA specification.

Analysis of data collected on both consolidated and freshly surfaced track shows that rail seat bending responses tended to be greatest when track was freshly surfaced, while tie center responses tended to increase with accumulated traffic. These trends however, did not appear to be strong for the combinations of conditions observed at these test sites.

Although it was originally assumed that a 300 Hz data bandwidth was sufficient to characterize bending moments, a detailed examination of the dynamic response of the ties at Aberdeen (at the maximum recorded bandwidth of 2000 Hz) showed that data must be analyzed to bandwidths near 1200 Hz to achieve 95 percent of "true" strain amplitudes experienced in ties excited by wheel impacts. The resulting rail seat bending moment distributions from each of the sites are shown in Figure 21. They are generally similar in nature to the load distributions shown previously in Figure 19. Of the five sites measured, only Aberdeen and Roanoke exhibited very large bending moments\*\*. These large moments at the lower probability levels easily exceeded the cracking strength of the ties. The nominal cracking strength of most ties is between 350 and 375 kip-in. in the rail seat region, which is well above the current 300 kip in. AREA specification for ties installed on 30 in. centers (the highest tie strength specified).

The summary curves shown in Figure 21 are the responses that would be experienced by an average tie in each test section. These were determined by computing the mean response of the seven instrumented ties at each level of exceedance. Variations in support conditions under each tie can be assumed to

---

\* The term "consolidation" is used here in the normal railroad context of compaction by normal traffic because the more proper, technical term "compaction" is often interpreted as a process performed by a special machine (which can actually reduce the degree of compaction).

\*\*Note however, that the Roanoke tie bending data are greater than that at Aberdeen at the higher levels while the converse is true for the wheel load data. This may be a result of a non-linear response of the cracked ties at Roanoke where all (including the instrumented ties) had advanced cracks. This could not be verified by the in-site calibration which could not apply bending moments above the pre-stress limit.

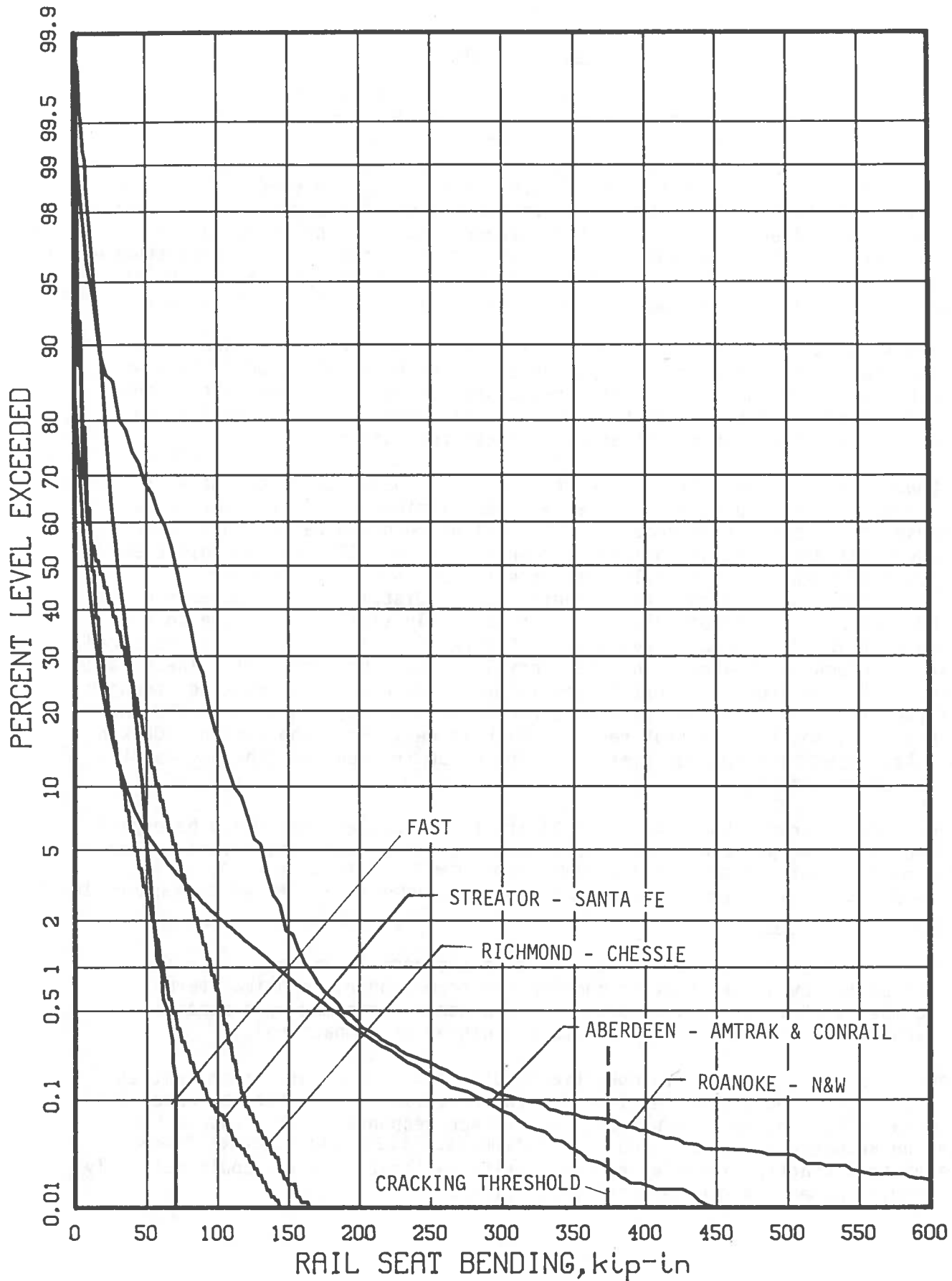


FIGURE 21. SUMMARY OF TIE BENDING AT ALL SITES

be the primary cause for deviations from the mean bending moment response. As an example of the range of variability seen at different test sections, Figure 22 shows that at Streator, the plus-one-standard-deviation curve fits within about 10 percent of the mean curve at the 0.1 percent level of exceedance, thus indicating uniform loading and/or support conditions for the recently surfaced track. On the other hand, Roanoke data in Figure 23 show a plus-one-standard-deviation curve about 25 percent higher than the mean curve at the 0.1 percent level of exceedance and proportionally larger values than that in the upper part of the curve for track which is thoroughly consolidated. This observation is contrasted by the results of the static stiffness tests, discussed in Section 6, where freshly tamped track shows considerably more variation in static stiffness than consolidated track. Unfortunately, no subsurface investigations were performed at Roanoke to provide a possible explanation for this variability, but it is assumed that the main effect is the support condition at the tie/ballast interface.

Another possible cause for the large variations in tie responses encountered at Aberdeen and at Roanoke may be experimental error. As discussed in Section 8.1, a high percentage of the ties at Aberdeen were found to have small-to-medium rail seat flexural cracks at the time that data were collected. At Roanoke, it was determined that 100 percent of ties were cracked prior to instrumenting these same ties. Previous lab tests have shown that when a strain gage coupon is installed adjacent to or over a flexural crack on a prestressed concrete tie, the response will be similar to that of an uncracked tie up to the point that the prestress limit has been exceeded. Above that, a new coupon sensitivity may occur.

Generally, if the coupon's active area bridges the crack, the apparent sensitivity of the coupon will increase slightly. On the other hand, if the crack lies outside the sensitive region of the coupon, there will be a reduction in sensitivity caused by the stresses being concentrated near the top of the cracked region. Because the calibration fixture was not capable of loading the ties to levels above the prestress limit, it was not possible to verify the high level strain sensitivities. It can be assumed that at very high levels of strain the coupon slightly overestimates the magnitude of the bending moment. In general, however, levels of bending moment up to the cracking threshold are of primary interest.

The cracking threshold bending moments were shown in Figure 21 to be exceeded frequently at Aberdeen and Roanoke. At Aberdeen this occurrence happens about once every 1 to 2 days at an average tie location, while at Roanoke it occurs as often as 5 times per day. If the plots for Streator and Richmond were extended to the lower probability, higher bending moments (which would require more data to accurately characterize), they would also show levels exceeding the cracking limit as is evidenced by the observed cracked ties. Wheel inspection techniques in maintenance programs on each railroad will determine at which point on this otherwise ever expanding scale that the curve truncates. At FAST where every wheel is frequently inspected and well maintained, the curve can be seen to truncate at or below the 0.1 percent level. Although similar heavy haul traffic exists on Chessie and N&W, the data indicate a relative difference in wheel conditions on these two railroads. Some of this difference may be attributed to the curved track at the Chessie site which may

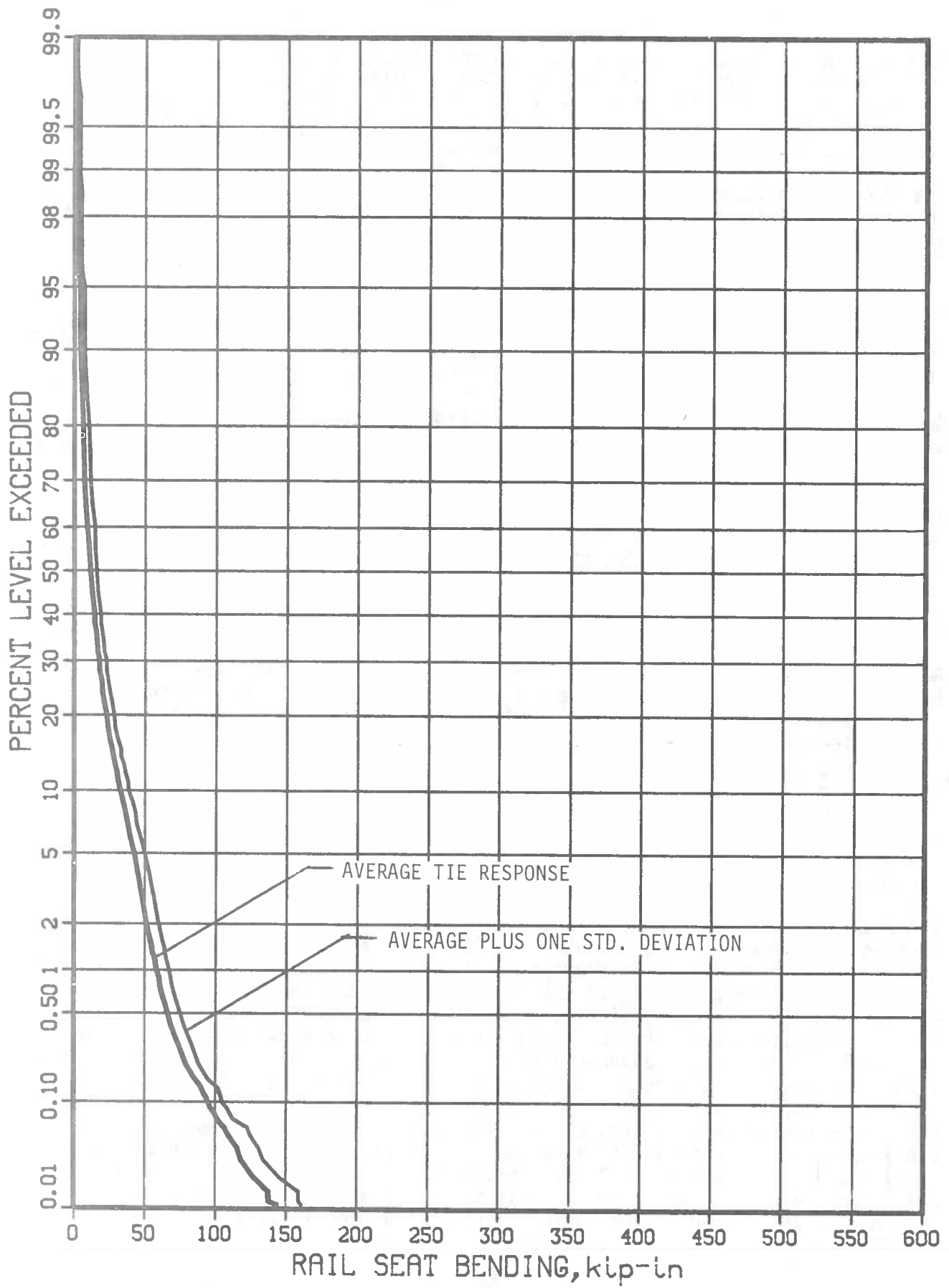


FIGURE 22. STATISTICAL RAIL SEAT BENDING RESPONSE AT STREATOR-CONCRETE



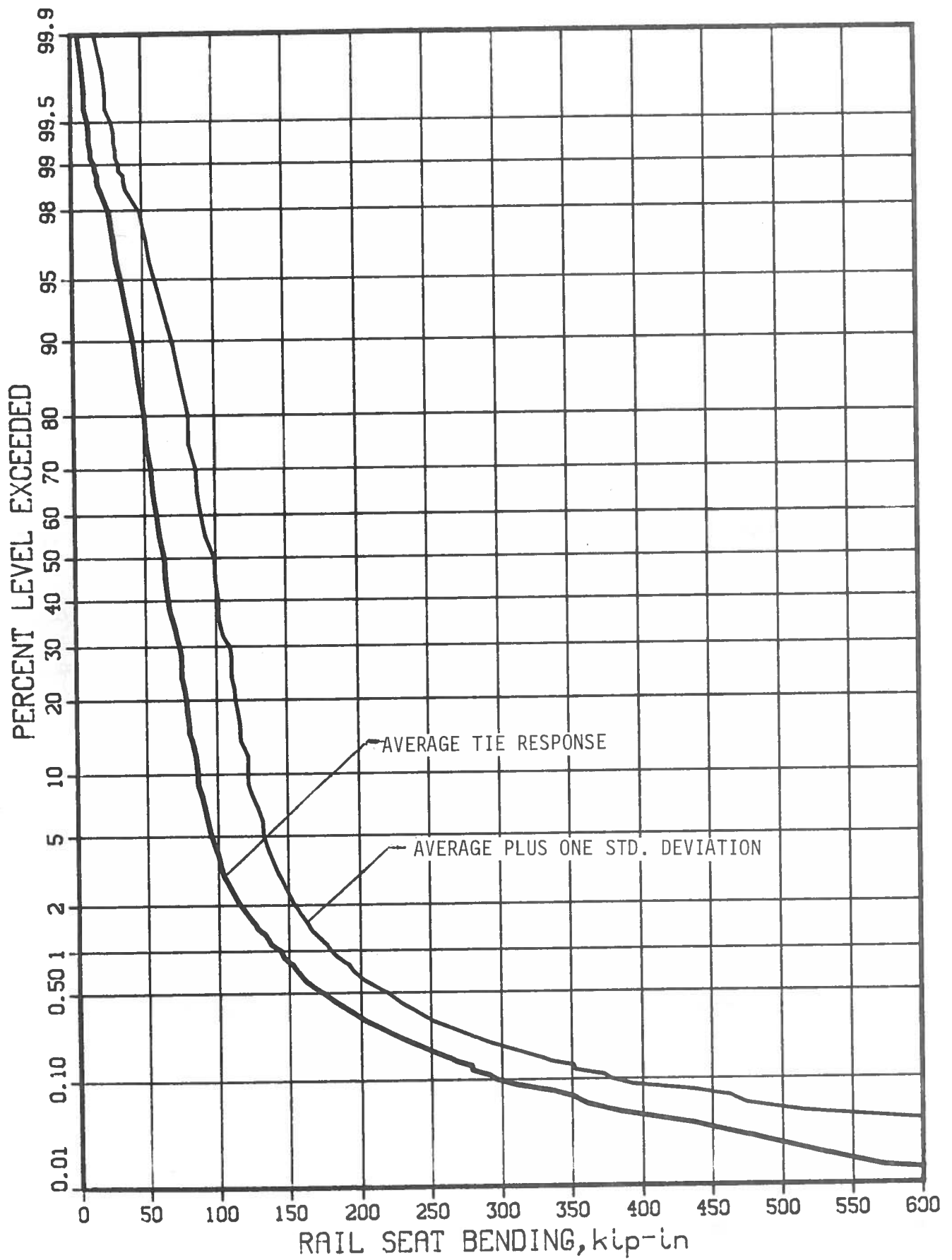


FIGURE 23. STATISTICAL RAIL SEAT BENDING RESPONSE AT ROANOKE

tend to reduce the severity of the wheel impacts by causing a shift in lateral position of the wheels away from the regions of maximum irregularity.

### 5.3 Tie Center Bending

Figure 24 shows a summary of the tie center bending moments measured at the five test sites. At three of the five sites, the center bending moments are quite small, being limited to a range of  $\pm 50$  kip-in. These ties were designed to a specification of 200 kip-in., of negative center bending moment, and typically test to levels above 250 kip-in. before crack initiation. As before, the two sites where significant levels are achieved were Aberdeen and Roanoke. The Aberdeen data show that tie center impacts occur at about the same level of exceedance as the rail seat bending impacts (about 3 percent) and cause bending moments that approach the cracking limit of the tie center. Roanoke data demonstrate that center-bound conditions exist along with the impact problem. This results in relatively large loads being exerted by all the 100-ton equipment, along with the contribution from the bad wheel population.

Because of the low center bending load levels encountered at FAST, Streator, and Richmond, there was little variability in the tie center data acquired. As shown in Figure 25, however, at Roanoke, where the center bound condition was developing, there were large variations observed. There were in fact, two groups of three ties, one group which showed no appreciable center binding while the other showed a significant degree of center binding, producing center bending moments between 100 and 150 kip in. under the loaded, 100-ton cars. Several tie centers were cracked at Roanoke; unfortunately extensive ballast cover prevented a valid estimate of total center cracking. An examination of the data from all sites would indicate that for the center-bound condition to develop, may require a combination of large tonnage accumulations without surfacing (perhaps in excess of 100 MGT), combined with a thoroughly fouled ballast that restricts the flow of ballast under the tie center necessary to relieve the stress concentration.

### 5.4 Ancillary Dynamic Measurements

A variety of dynamic measurements were performed to support characterization of the test sites as well as to explore some phenomena not previously understood. Of particular interest is an analysis of the dynamic response of the ties due to the impacts from the flat wheels. In addition, tie pad isolation of impact loads and fastener performance characteristics were considered. However, these data have been examined more thoroughly in other programs.[5, 7]

#### 5.4.1 Tie Bending Modes

Initial examination of dynamic data acquired showed a prolonged vibratory response of the ties under the randomly occurring impacts. This phenomenon had been seen earlier [8], and it was shown to be primarily associated with the first bending mode of the tie. To more accurately characterize this response, a modal analysis was performed on a concrete tie in the laboratory. The results of these analyses were compared with acceleration responses measured

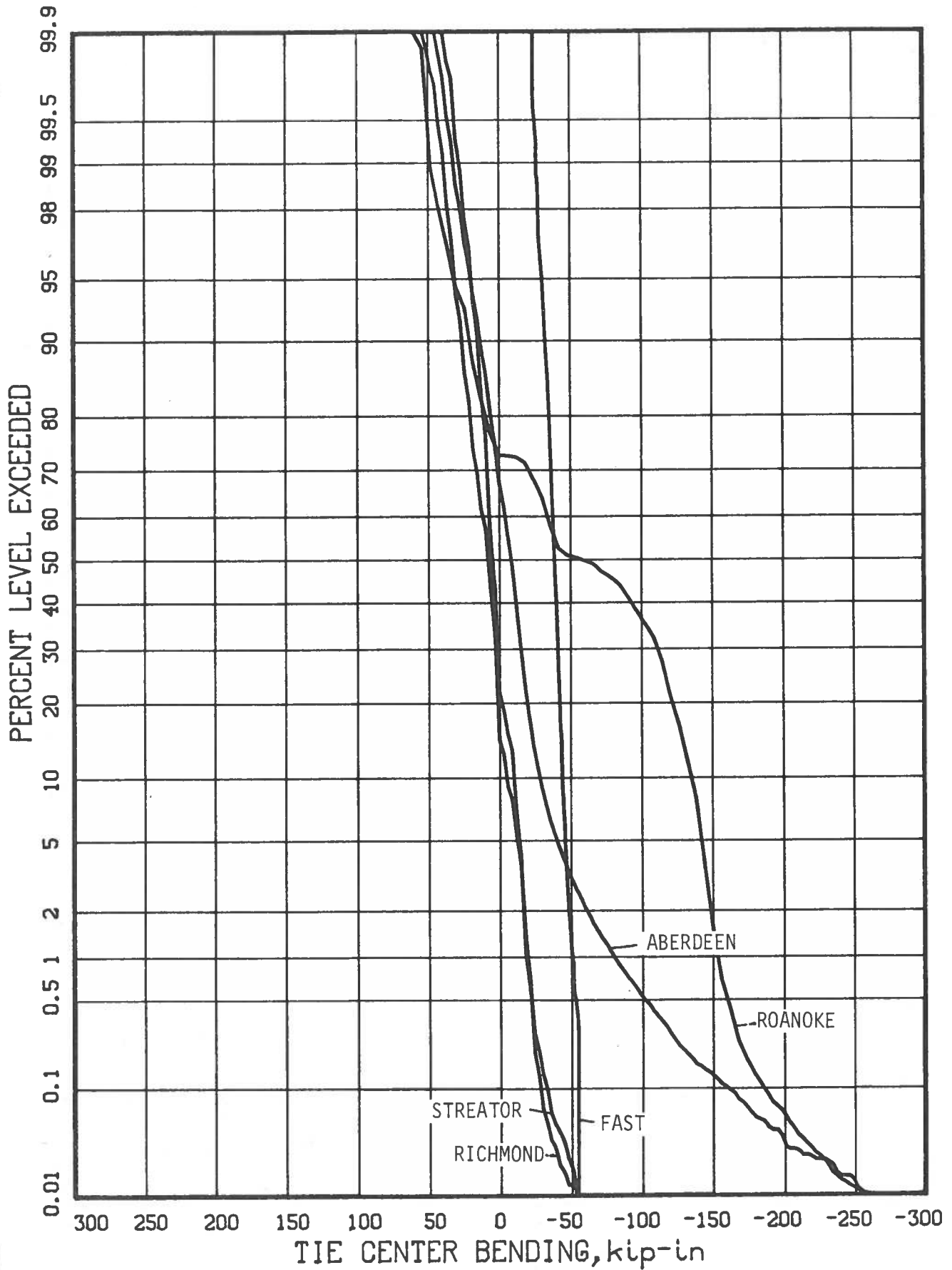


FIGURE 24. SUMMARY OF TIE CENTER BENDING RESPONSE AT ALL SITES

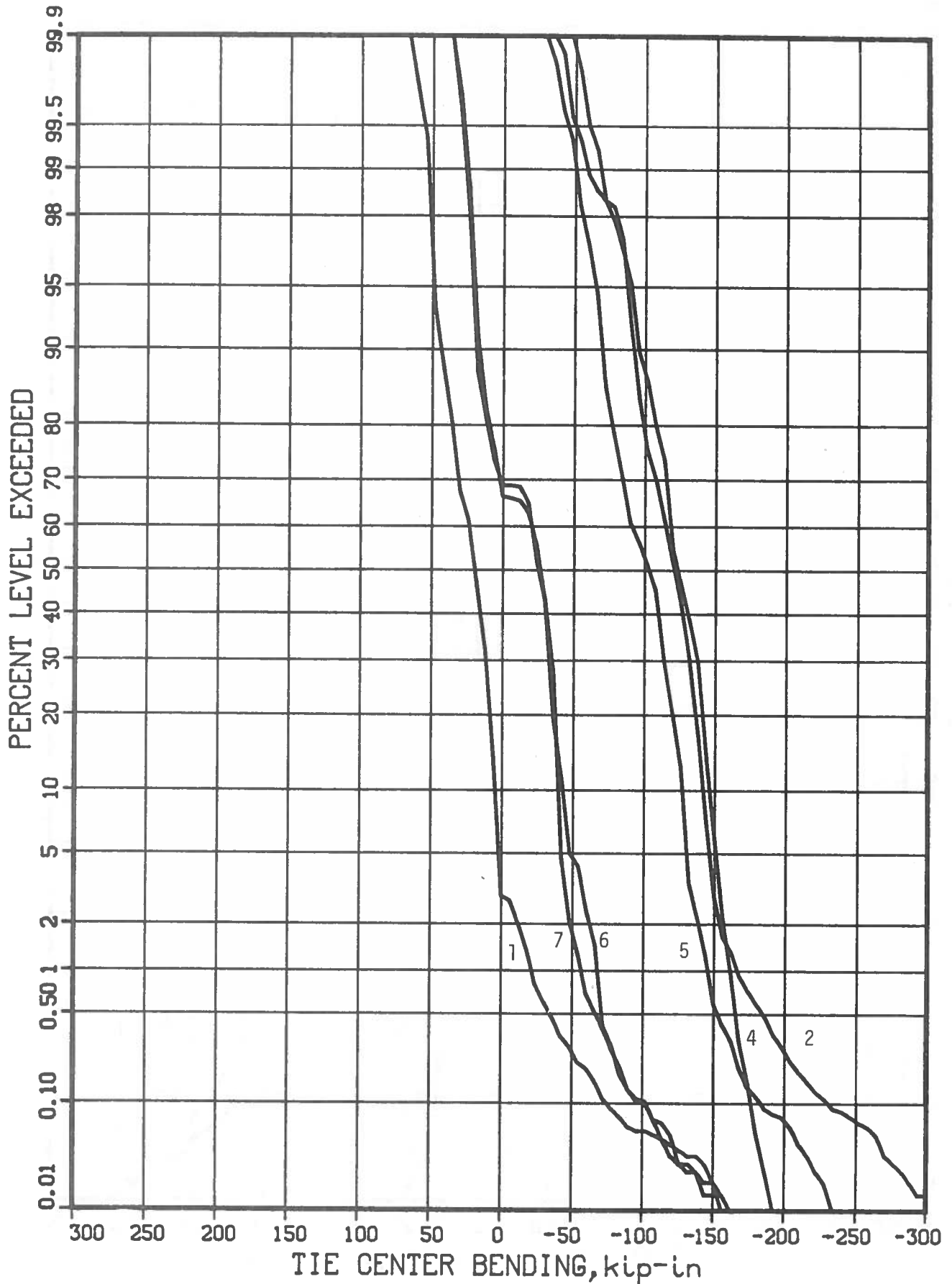


FIGURE 25. TIE CENTER BENDING RESPONSE AT ROANOKE - EACH TIE

under field conditions. The tests showed that there are three primary bending modes which are consistently excited by an impact. As shown in Figure 26A, the first bending mode has its nodes at the rail seat regions and the maximum strains occur at the tie center. Because this is the lowest natural frequency, it is the easiest to excite and can be seen even under relatively smooth wheels, such as those at FAST. Under laboratory conditions this first mode frequency is around 108 Hz, while in the field the variability of nominal wheel loading and support conditions will cause this frequency to vary between about 110 and 130 Hz on the CC244C tie.

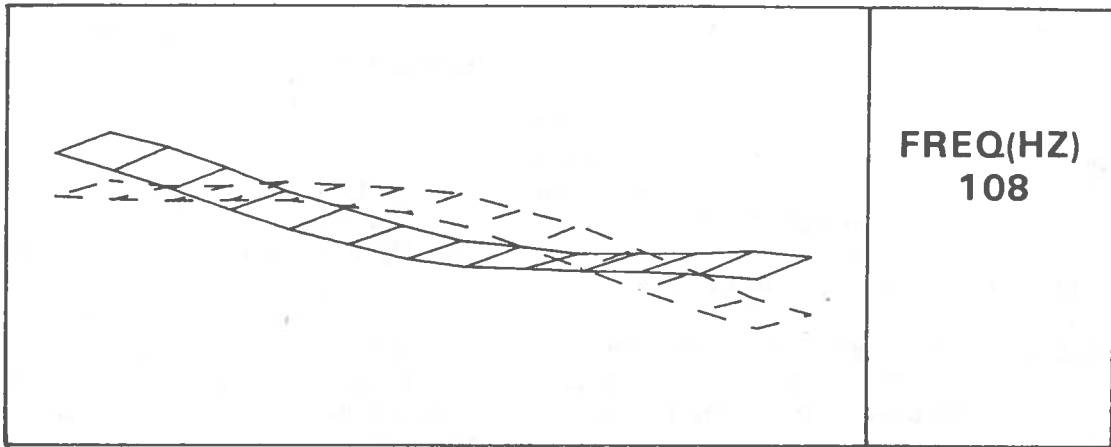
The second bending mode shown in Figure 26B, is the asymmetric mode which occurs at about 330 Hz and causes maximum strains to occur in the rail seat region. As discussed in Section 5.1.2, examination of simultaneous samples of data taken on each rail circuit shows that the probability of occurrence of the high magnitude impact loads is rarely coincident on both rails. This implies that an asymmetric impact (only one wheel causing an impact) has a very high probability of occurrence and this will excite the asymmetric second mode. It also indicates that an impact on one rail seat may cause a crack to occur on the opposite rail seat. This has been shown to occur in laboratory tests.[9] It also implies that reverse bending cracks can occur. While reverse cracks have been observed in the field, no direct proof of the cause has been demonstrated.

The third bending mode seen in Figure 26C is similar to the static deflection curve normally assumed for a tie supported on a uniform foundation with vertical loads at the two rail seats. This mode occurs at about 630 Hz and would be excited by either symmetric or asymmetric impacts. From spectral and time domain analyses of acceleration data from ties in the field it was determined that most large impacts induce combined, second and third mode responses.

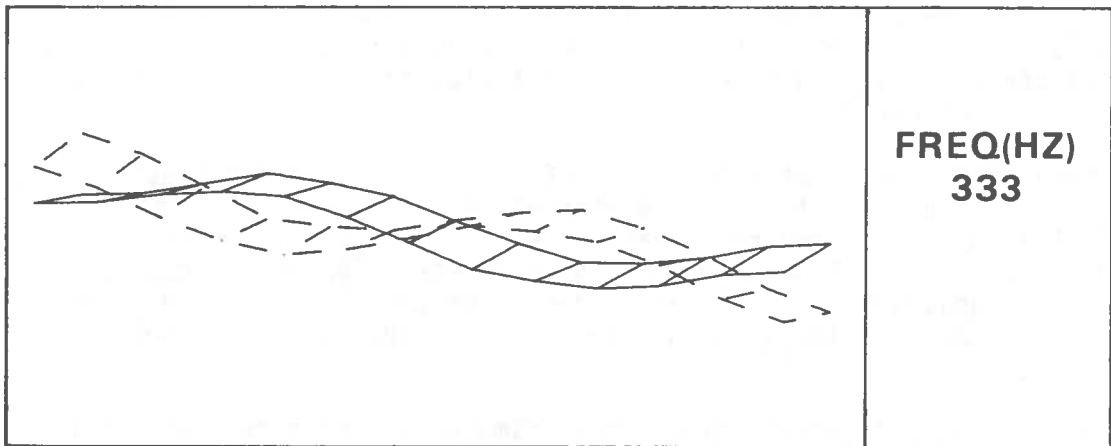
Examination of rail seat bending moment time histories show that a typical impact will cause a strain pulse duration of about 1.5 milliseconds at Aberdeen, while large impacts at Roanoke occurred over durations up to 3 to 4 milliseconds. The 1.5 millisecond duration is characteristic for a 330 Hz, half-sine pulse, while the longer durations seen at Roanoke typically exhibit a more complex wave form which indicates more response at the first mode. This may be in part caused by tie center binding at Roanoke.

#### 5.4.2 Rail and Tie Accelerations

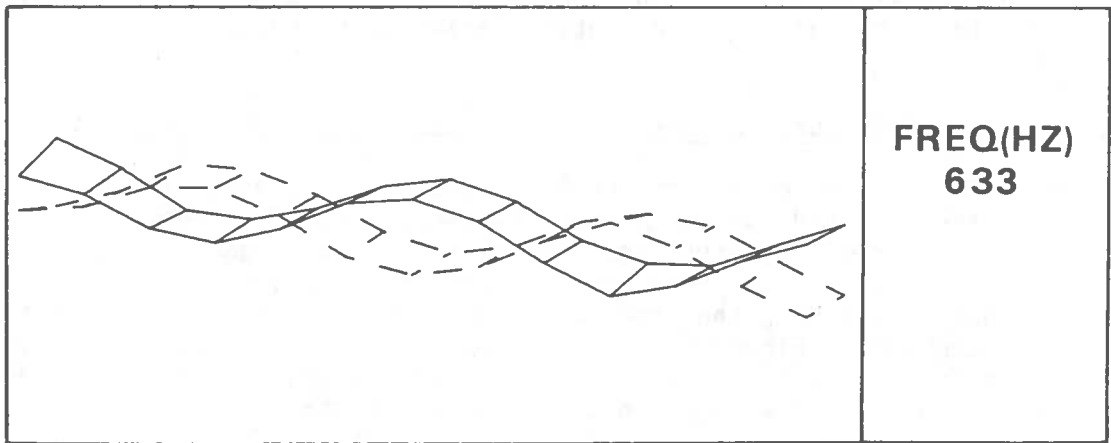
The primary purpose in measuring accelerations was to characterize the influence of the fastener and pad assembly on tie response. Transfer function analysis of accelerometer pairs (one mounted on the rail base and one next to the fastener shoulder on the tie) shows an almost rigid coupling of the rail to the tie out to 400 Hz., thus transmitting almost all impact energy into the tie. Results shown in Figure 27 indicate that flexible pads can significantly reduce the energy transmitted to the tie, particularly in the second and third mode regions which were shown to cause larger strains in the railseat region. The softer pads do tend to transmit more at the first mode frequency. However, this does not contribute significantly to rail seat cracking.



(A) FIRST BENDING MODE RESPONSE



(B) SECOND BENDING MODE RESPONSE



(C) THIRD BENDING MODE RESPONSE

FIGURE 26. SAMPLES OF FIRST THREE BENDING MODES FOR CC-244-C CONCRETE TIE

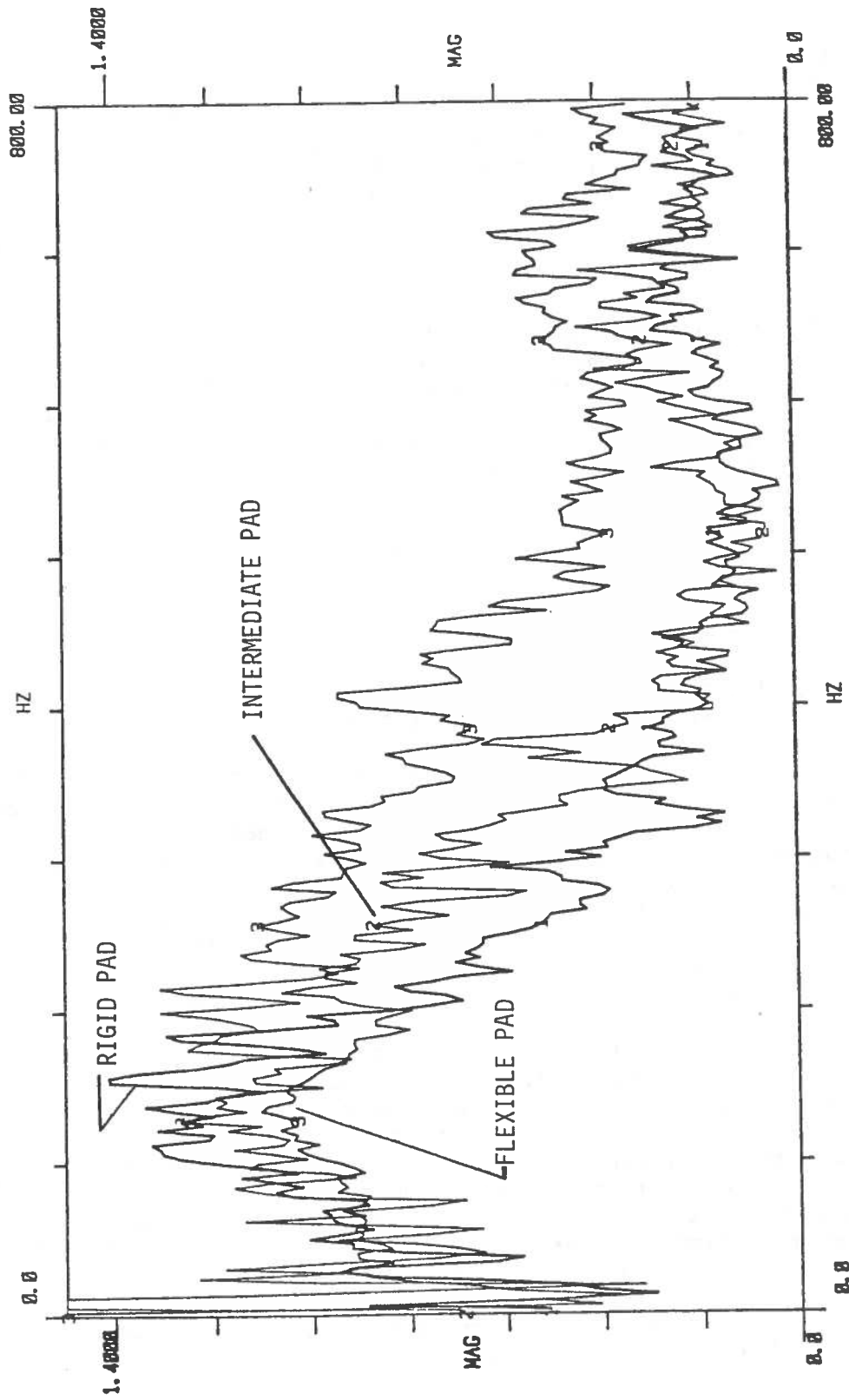


FIGURE 27. TRANSFER FUNCTION OF RAIL/TIE ACCELERATION FOR THREE DIFFERENT TIE PADS

## 6.0 TRACK SYSTEM CHARACTERISTICS AND PERFORMANCE

The overall track structure's mechanical performance is dependent on the properties and performance of the individual elements within the track structure as well as the interaction of these elements under the combined effects of traffic loading and weather. Because of this complex relationship and its affect on track stiffness and strength, vertical track stiffness and permanent settlement were both measured to characterize each site and provide inputs for verification of analytical models.

### 6.1 Track Stiffness/Modulus

Vertical track modulus has long been considered an important means of characterizing track condition. Because of the interaction between stiffness and strength in ballast and subgrade materials, it has been generally considered desirable to have a track with high stiffness because that same track will probably have higher strength. Track modulus is usually calculated from force-deflection measurements applied to the rail head using the equation

$$u = 0.25 [1/EI(P/\delta)^4]^{1/3} \quad \text{units: lb/in/in} \quad (1)$$

where  $P$  = wheel/rail load  
 $\delta$  = rail vertical deflection  
 $EI$  = flexural rigidity of the rail  
and  $P/\delta$  = rail head or track stiffness.

Vertical track stiffness measurements were made both before and after surfacing operations at Streator and Richmond; while at the other locations, measurements were made with whatever degree of consolidation existed. The method used to measure vertical track stiffness was to load both rails at one tie location with a hydraulic jack system suspended beneath a loaded hopper car. Load cells attached to the jacks monitored 6-kip load increments from 0 to 30 kip. Resulting deflections were measured with a surveyor's theodolite sighting a machinist's scale calibrated in 0.01 in. increments. The scale was attached to the rail directly beneath the applied load. The jacks were typically 10 ft. from the nearest wheel on the hopper car. Where possible an initial, zero deflection reading was established prior to moving the work train over the test position. This allowed for verification of any disturbance of the rail position from the adjacent wheels while in the test location. Peak deflections under the hopper car wheels were also noted as a cross check on the measurement scheme. Deflection resolution was approximately 0.003 in. by interpolation. Typical initial offsets due to the influence of adjacent wheels were less than  $\pm 0.01$  in. for the concrete tie track, while the wood tie track at Streator approached 0.10 in. downward. All readings were rezeroed prior to starting the load cycle.

Figure 28 is a summary of the mean track vertical response to the point load application, as determined by averaging 7 to 10 locations at each revenue test



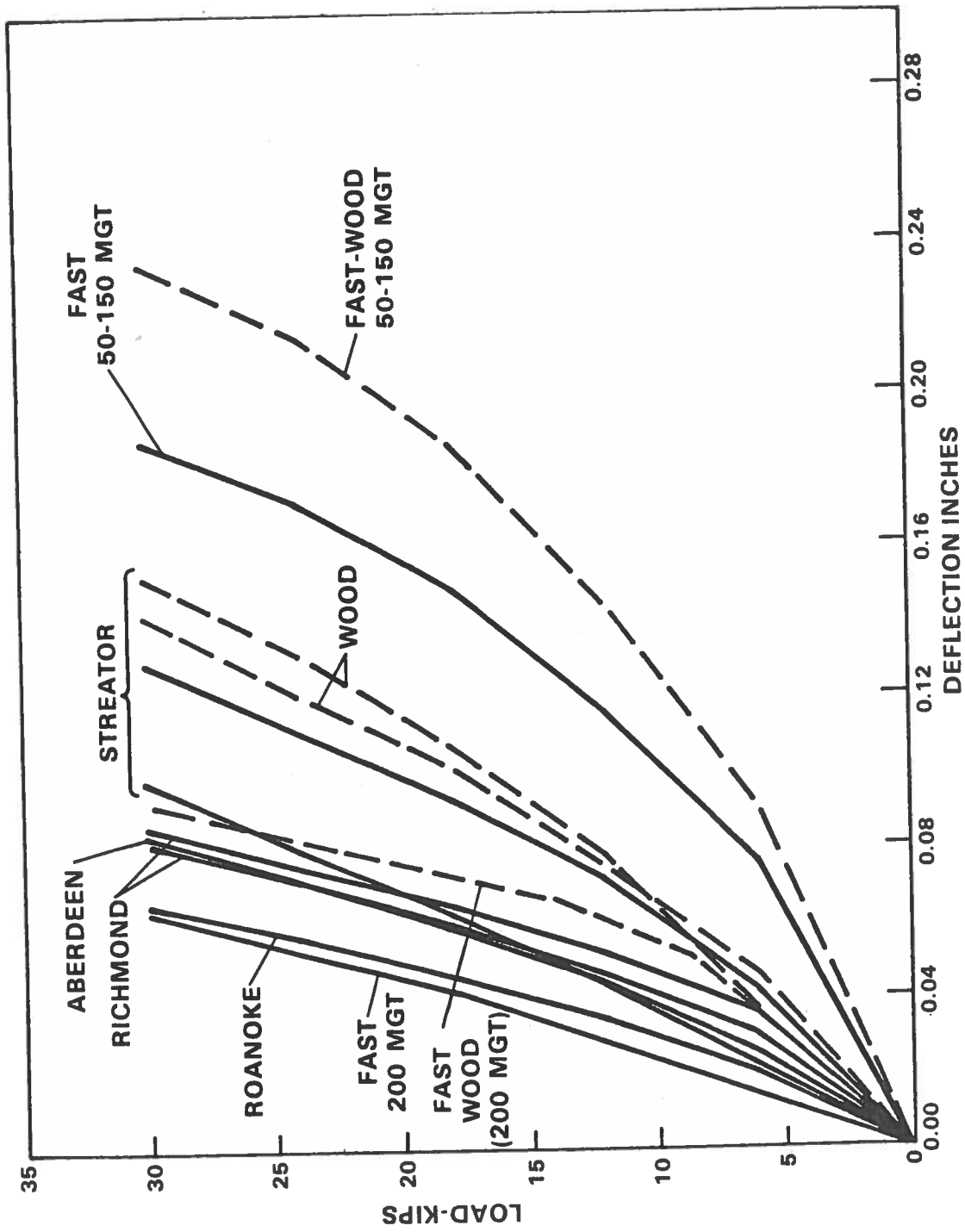


FIGURE 28. SUMMARY OF TRACK STIFFNESS AT ALL SITES

site and by periodic measurements at one location at each test zone in Section 22 of FAST. Note that the consolidated stiffness of the four revenue, concrete tie sites all fall within a small range to the left of the plot. The stiffness of the freshly resurfaced, concrete tie track at Streator as well as the wood tie section at Streator both show more "slack" at the lower load levels resulting in overall, lower secant stiffnesses, about half that for the consolidated concrete tie sections.

Stiffness data acquired from FAST were measured at 50 MGT intervals at only one tie position in each of the two test sections. Four sets of data were acquired for 50 thru 200 MGT. The values acquired at the first 3 intervals indicate a significant amount of "slack" while the fourth and final values acquired are much more consistent with the results acquired at the revenue sites. This large variability would indicate that the technique of selecting single ties for stiffness measurements will not assure average values for the track as a whole.

Note that the Richmond data and the Streator wood tie data indicate no significant change in mean stiffness as a result of the surfacing operation. The data from the concrete tie test section at Streator show that there is a significant loss of stiffness at the lower load levels as a result of surfacing, while the tangent stiffnesses at maximum, nominal wheel load levels are essentially identical before and after surfacing.

A surprising result of comparing data acquired before and after surfacing is that the surfacing operation produces a significant increase in the variability of the support under the ties. Figures 29 through 31 show pairs of curves for before-and-after-surfacing data. The cross-hatched areas indicate the  $\pm$  one standard deviation values before maintenance and the shaded areas indicate the effect of surfacing. Note that the variability nearly doubles in each case. Also note that the slight increase in average stiffness seen in Figure 28 as a result of surfacing the Streator wood tie test section is of minimal significance when compared to the degree of variability indicated at that section. Results of stiffness tests at Aberdeen and at Roanoke show minimal variability: comparable to the pre-maintenance data from Streator concrete.

If the tangent stiffness at the nominal maximum wheel load is not significantly altered by the surfacing operation, then this would indicate that the top layer of ballast directly beneath the tie, which is disturbed in the surfacing operation, does not contribute significantly to the loaded track stiffness. Results from the plate load tests discussed in Section 7.2.2, however, show that there is a substantial reduction in the load-deflection characteristics in that layer resulting from surfacing. This would indicate that there must be a significant change in the contact area between the bottom of the tie and top of the ballast, such that the net reduction in plate load stiffness is offset by a change in the effective bearing area under the tie, under full load conditions. Effective stiffness at low load levels must be strongly affected by a combination of tamping technique and ballast physical states such that Streator-concrete showed a significant reduction resulting from surfacing while Richmond showed no appreciable change.

Table 3 summarizes the track modulus values derived from the track stiffness data. Stiffness and modulus values are shown for three ranges of incremental

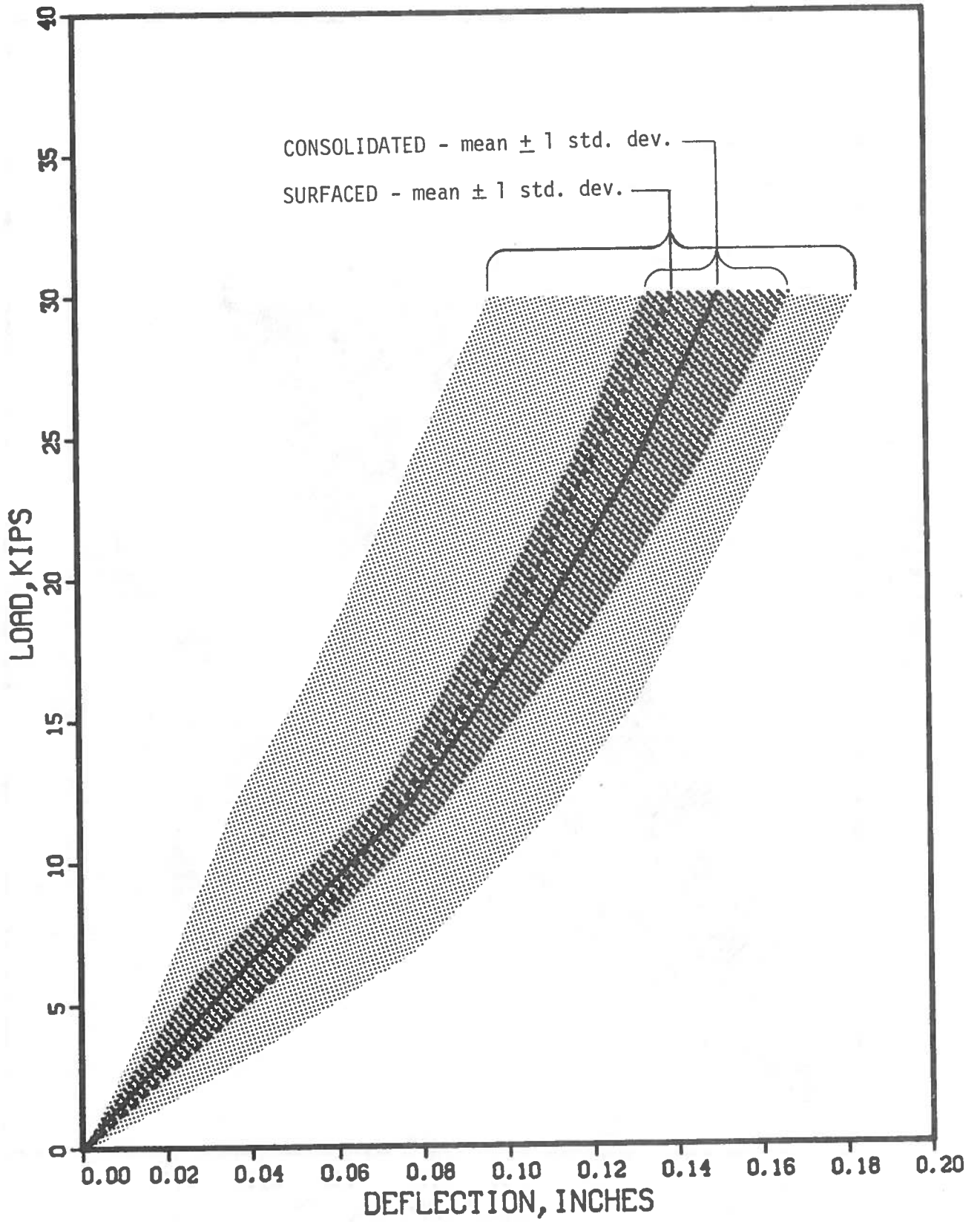


FIGURE 29. TRACK VERTICAL RESPONSE TO POINT LOAD APPLICATION AT STREATOR-WOOD

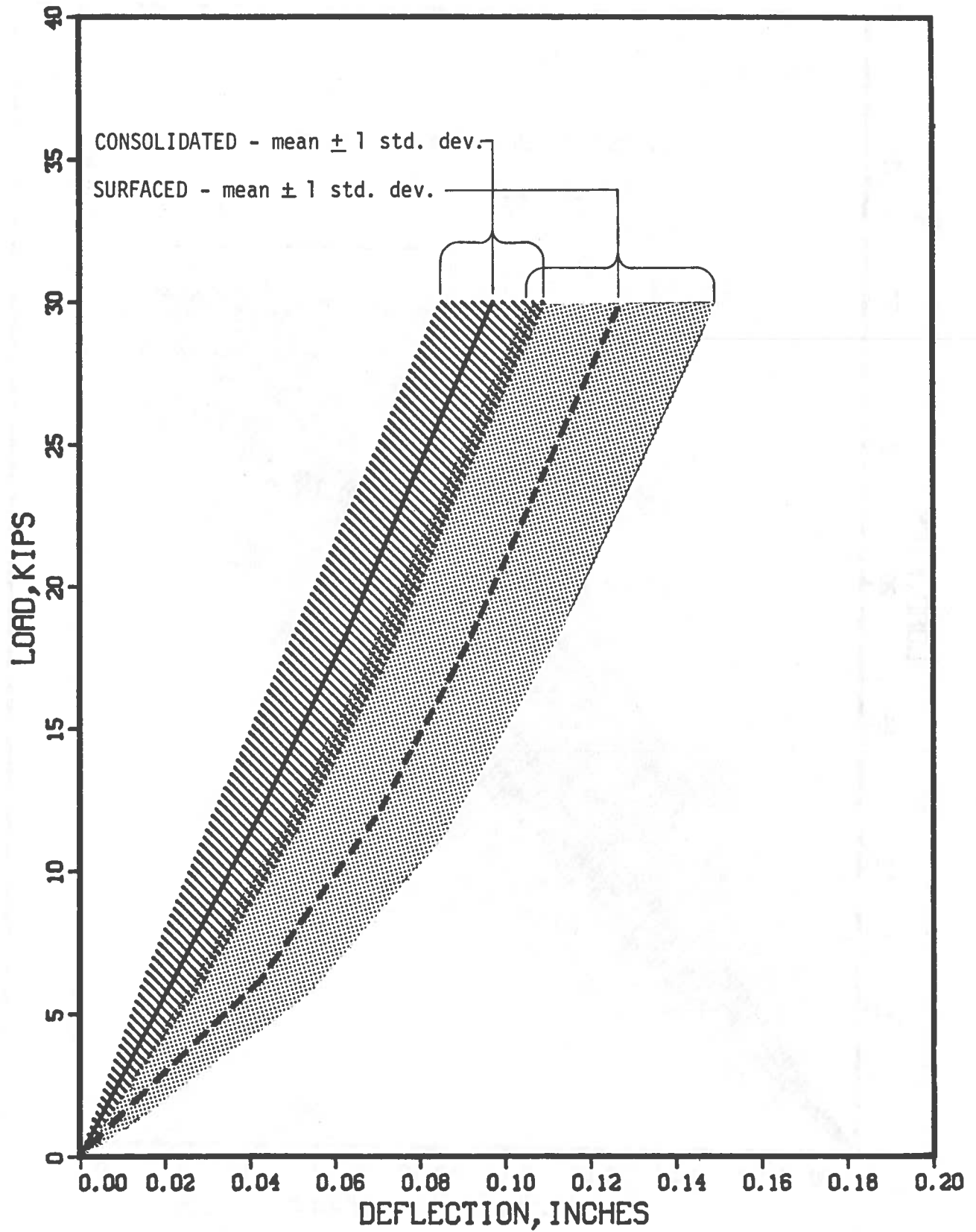


FIGURE 30. TRACK VERTICAL RESPONSE TO A POINT LOAD APPLICATION AT STREATOR-CONCRETE

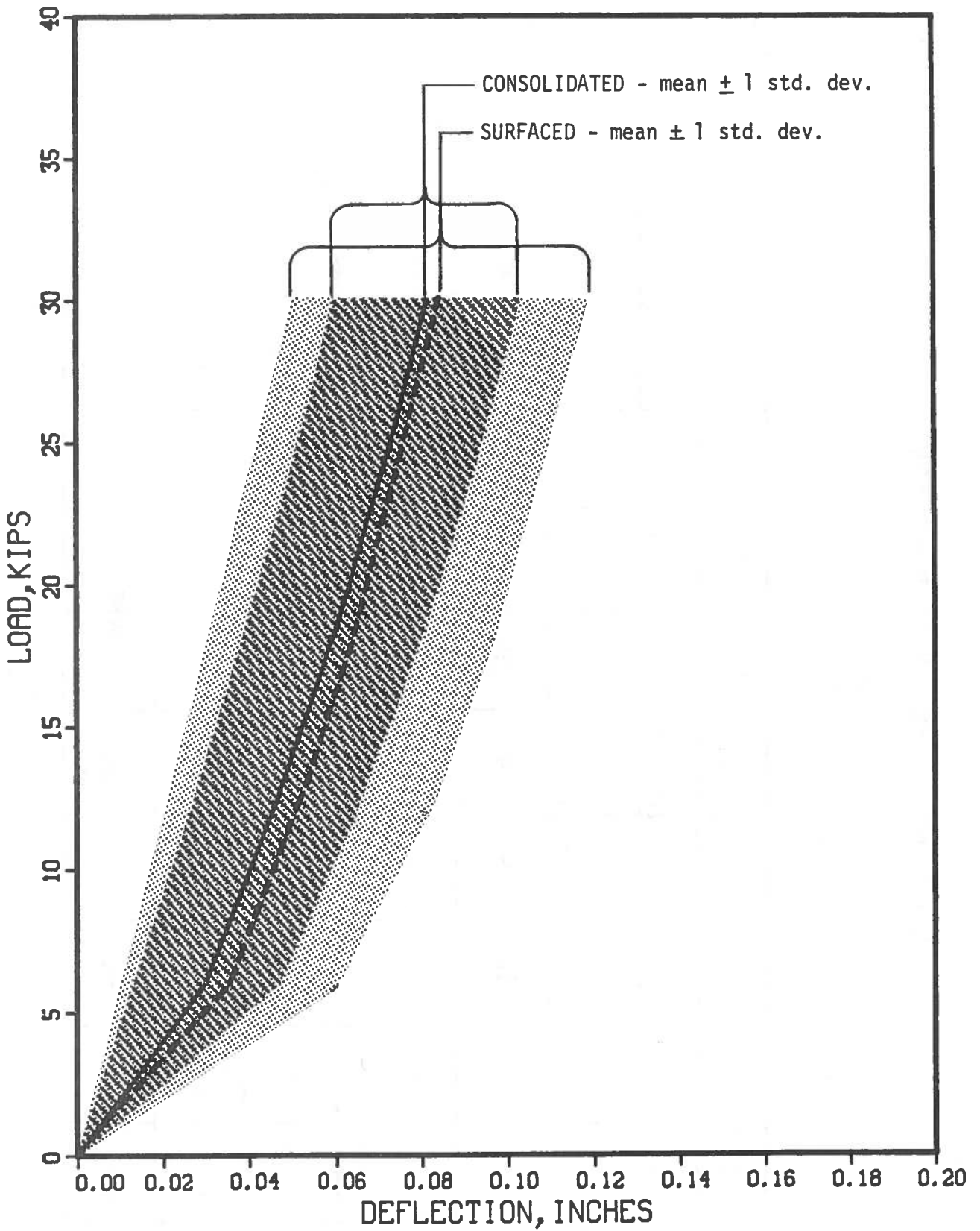


FIGURE 31. TRACK VERTICAL RESPONSE TO A POINT LOAD APPLICATION AT RICHMOND

TABLE 3. VERTICAL TRACK STIFFNESS AND MODULUS

| STREATOR<br>CC-244C | STREATOR<br>WOOD TIES |                    | RICHMOND<br>RT-7S & CC-244 |                    | ABERDEEN<br>RT-7SS-2 | ROANOKE<br>CC-244C | FAST<br>RT-7SS-2 (22-6356) |            | FAST<br>WOOD TIE (22-3056) |            |
|---------------------|-----------------------|--------------------|----------------------------|--------------------|----------------------|--------------------|----------------------------|------------|----------------------------|------------|
|                     | PRE-<br>SURFACING     | POST-<br>SURFACING | PRE-<br>SURFACING          | POST-<br>SURFACING |                      |                    | 50, 100 &<br>150 MGT*      | 200<br>MGT | 50, 100 &<br>150 MGT*      | 200<br>MGT |
| 0 KIP               | 309                   | 235                | 199                        | 213                | 35 MGT               | 270 MGT            | 128                        | 488        | 160                        | 336        |
| 6 KIP               | 317                   | 279                | 210                        | 252                | 417                  | 536                | 167                        | 495        | 214                        | 445        |
| 18 KIP              | 339                   | 333                | 267                        | 298                | 496                  | 622                | 250                        | 533        | 308                        | 710        |
| 0 KIP               | 3680                  | 2560               | 2050                       | 2250               | 4550                 | 6510               | 1140                       | 6780       | 1540                       | 4110       |
| 6 KIP               | 3810                  | 3210               | 2200                       | 2810               | 5470                 | 7860               | 1620                       | 6900       | 2260                       | 6000       |
| 30 KIP              | 4170                  | 4080               | 3040                       | 3510               | 6880                 | 9590               | 2780                       | 7630       | 3660                       | 11170      |

\*Average of single tie data which showed excessive slack at lower loads.

load. The values for the 18-kip to 30-kip loading increment best describes the response of the track to nominal wheel loads.

During the first field tests (at Streator) there was a concern as to whether the technique used to calibrate the concrete ties would have an affect on the track stiffness due to minor disturbances to the ballast. Therefore, during the Richmond tests, two groups of ties were tested for stiffness values, the seven instrumented CC244's and seven randomly selected uninstrumented RT-7S's. Table 4 compares these two sets of data. Note that the secant stiffness values (0 to 30 kip) are increased by the surfacing operation for the undisturbed ties and decreased for the instrumented ties. In contrast, the 18-to-30-kip values are both increased slightly by the surfacing operation. The drop in secant stiffness under the instrumented ties can be explained by a greater loss of compaction associated with the tamping operation. Calibration of the instrumented ties requires excavating a small slot about 2 in. wide by 1 in. deep across the base of the tie 15 in. on either side of the railseat, to allow insertion of a nylon strap. During the surfacing operation, this position is approximately adjacent to the two outer tamping forks for that rail. If the tamper operator squeezes the tamping forks the same number of strokes on that instrumented tie as he does on the adjacent uninstrumented ties, some ballast will flow into the void caused by the excavation. This would tend to reduce the support for that tie at the railseat because overall, less material is available for support. As a result of this finding, stiffness data acquired at Aberdeen and Roanoke were acquired only in undisturbed locations. In fact, dynamic data at Roanoke were acquired with instrumented ties not calibrated until after data collection was completed to avoid any disturbance to the support. This was particularly important at Roanoke because of the thoroughly consolidated ballast section.

## 6.2 Track Settlement/Roughness

Survey-to-benchmark measurements were taken at all revenue sites, except Roanoke, then continued at 6-month intervals. Three benchmarks were installed at each test zone, one at each end and one at the center. The test zones were between 450 and 600 ft long. Because the original test plan called for roughness measurements acquired from geometry cars and only mean settlement values acquired from survey-to-benchmark measurements, the Streator and Richmond sites were initially laid out with approximately 20 randomly located points along the test zone. After the initial site surveys at Streator and Richmond, it was concluded that track geometry car data would not be sufficiently consistent to provide the desired roughness data. Therefore, all sites were laid out with uniform 10-foot intervals, so that both roughness and settlement could be derived from the survey data. The surface of each rail, the corresponding cross level, and the alignment of one rail were measured. The absolute elevation and offset data were then curve fitted and detrended to eliminate overall curvature and grade effects, so that the nominal roughness and settlement could be seen more easily in graphical plots as well as provide more useful statistics. Ten-foot intervals were considered sufficient to develop characteristic roughness, considering that these sites did not have any anomalies in running surface caused by bolted joints or special track work. Comparing the data taken on each visit allowed for evaluation of settlement

TABLE 4. EFFECT OF DISTURBANCE OF BALLAST SUPPORT ON TRACK STIFFNESS AND MODULUS

|                             |                        | Richmond<br>Uninstrumented RT-7S<br>(Undisturbed) |                    | Richmond<br>Instrumented CC-244<br>(Disturbed) |                    |
|-----------------------------|------------------------|---|--------------------|--|--------------------|
|                             |                        | Pre-<br>Surfacing                                 | Post-<br>Surfacing | Pre-<br>Surfacing                              | Post-<br>Surfacing |
| Stiffness<br>$K_r$ , kip/in | 0 Kip<br>to<br>30 Kip  | 400   | 493                | 342  | 277                |
|                             | 6 Kip<br>to<br>30 Kip  | 513   | 583                | 427  | 417                |
|                             | 18 Kip<br>to<br>30 Kip | 583   | 606                | 500  | 561                |
|                             |                        |   |                    |  |                    |
| Modulus<br>$u$ , lb/in/in   | 0 Kip<br>to<br>30 Kip  | 5650  | 7470               | 4580   | 3460               |
|                             | 6 Kip<br>to<br>30 Kip  | 7870  | 9320               | 6160   | 5960               |
|                             | 18 Kip<br>to<br>30 Kip | 9320  | 9830               | 7610   | 8860               |



performance, both qualitatively and quantitatively. Of particular interest, was the absolute settlement of the track and whether or not there was an underlying relationship between increased track roughness as a function of absolute settlement or accumulated tonnage.

Figure 32 shows the characteristic roughness and settlement at FAST, Section 22, for the concrete tie zone after the maintenance at 93 MGT. Note that most of the apparent roughness that develops shows up at one or two distinct locations such as stations +100 and -120. The upper family of curves are the actual detrended elevations while the lower set of curves show the relative amounts of settlement referenced to the original surface. The rapid settlement after only 1.4 MGT is equivalent to the subsequent settlement after an additional 50 MGT.

The survey results shown in Figure 33 for the Streator Concrete tie section reveal almost no change in apparent roughness after 36 MGT in spite of initial roughness indicated, particularly on the left end of the plot. Notice the dramatic difference in settlement between the second and third measurement sets, compared to almost no perceptible settlement for the first and last intervals.

At Richmond, there was also little change in roughness, as seen in Figure 34, in spite of having the greatest total settlement of all sites surveyed. The upper trace is from the original, random interval survey discussed previously. The zero elevation reference mark refers to the average elevation of both the high and low rails from the first survey. Only the high rail data are shown.

The Aberdeen data in Figure 35 clearly show the smoothest track surveyed. Although the last survey indicated one or two locations approaching the lower limits of Class 6 track, it was difficult to see any surface or line errors with the naked eye. Unfortunately, the test section was resurfaced just prior to a fourth survey attempt.

Figure 36 is a summary plot of mean settlement at each test site, beginning with a survey made as close as practical to the moment that the site was freshly surfaced. It has been generally known that track settles rapidly upon the first few load cycles and then begins to asymptotically approach a low, uniform settlement rate controlled primarily by the load spectrum and the performance of the ballast and subgrade materials. In fact, ballast strain data at Aberdeen indicated that essentially all permanent settlement was occurring within the upper 13 in. of the ballast layer. Instances when it was not possible to survey immediately upon completion of surfacing required an estimation of the initial settlement occurring under the first trains passing the test site. However, the resulting characteristic settlement rates of each site once the initial reconsolidation of the upper ballast layer has occurred, still reveal some interesting results. As Figure 36 shows, all sites tend to follow one of two general ranges of settlement rates. A very low settlement rate on the order of 0.002 in./MGT (500 MGT/in.) is seen at the one extreme, and as high as 0.025 in./MGT (40 MGT/in.) at the other. At three of the sections surveyed--Streator concrete, Streator wood, and Aberdeen,--some form of seasonal effect seemed to be causing accelerated settlements during the winter and early spring. Moisture levels measured at the base of the ballast section and

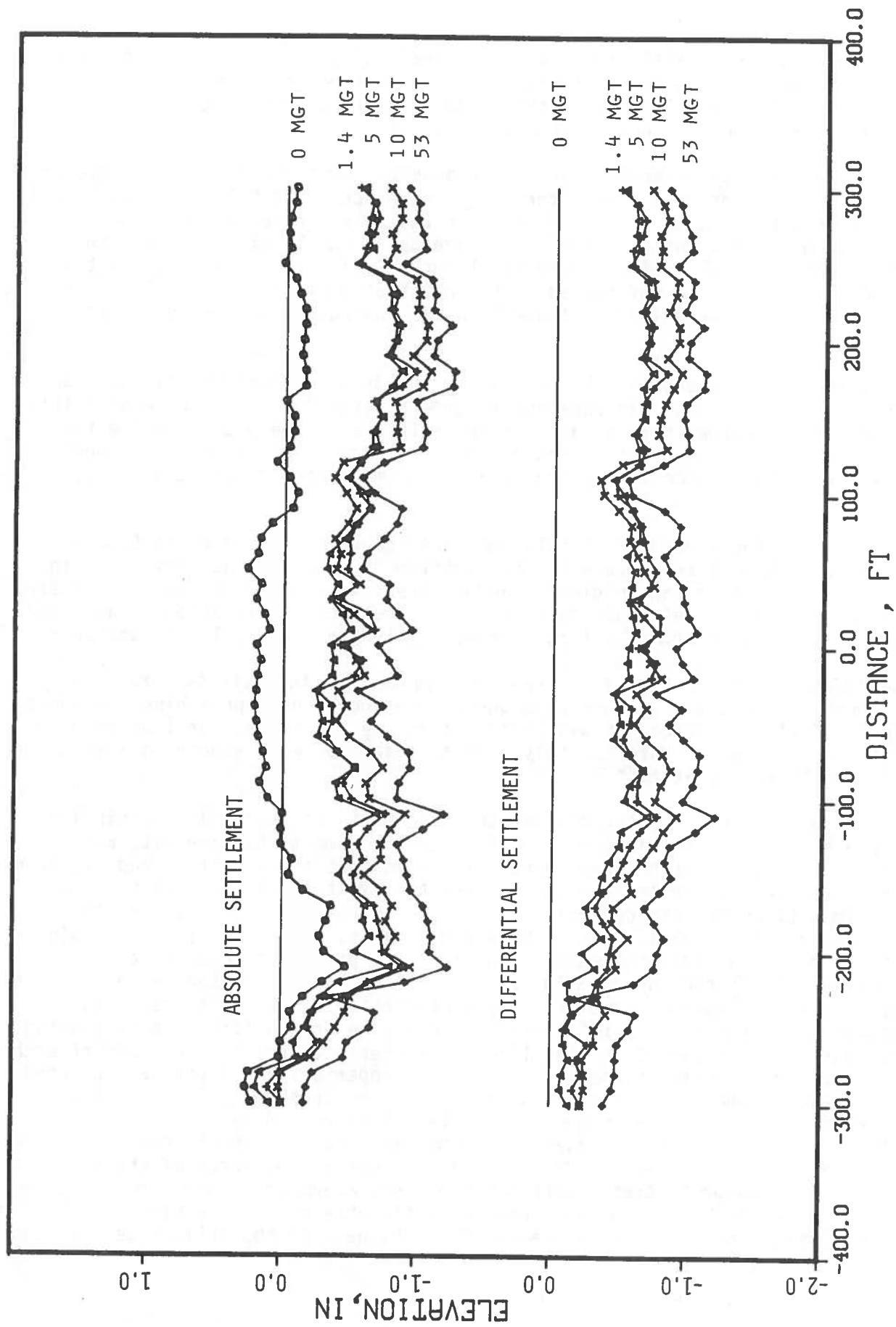


FIGURE 32. CONCRETE TIE TRACK SETTLEMENT AT FAST

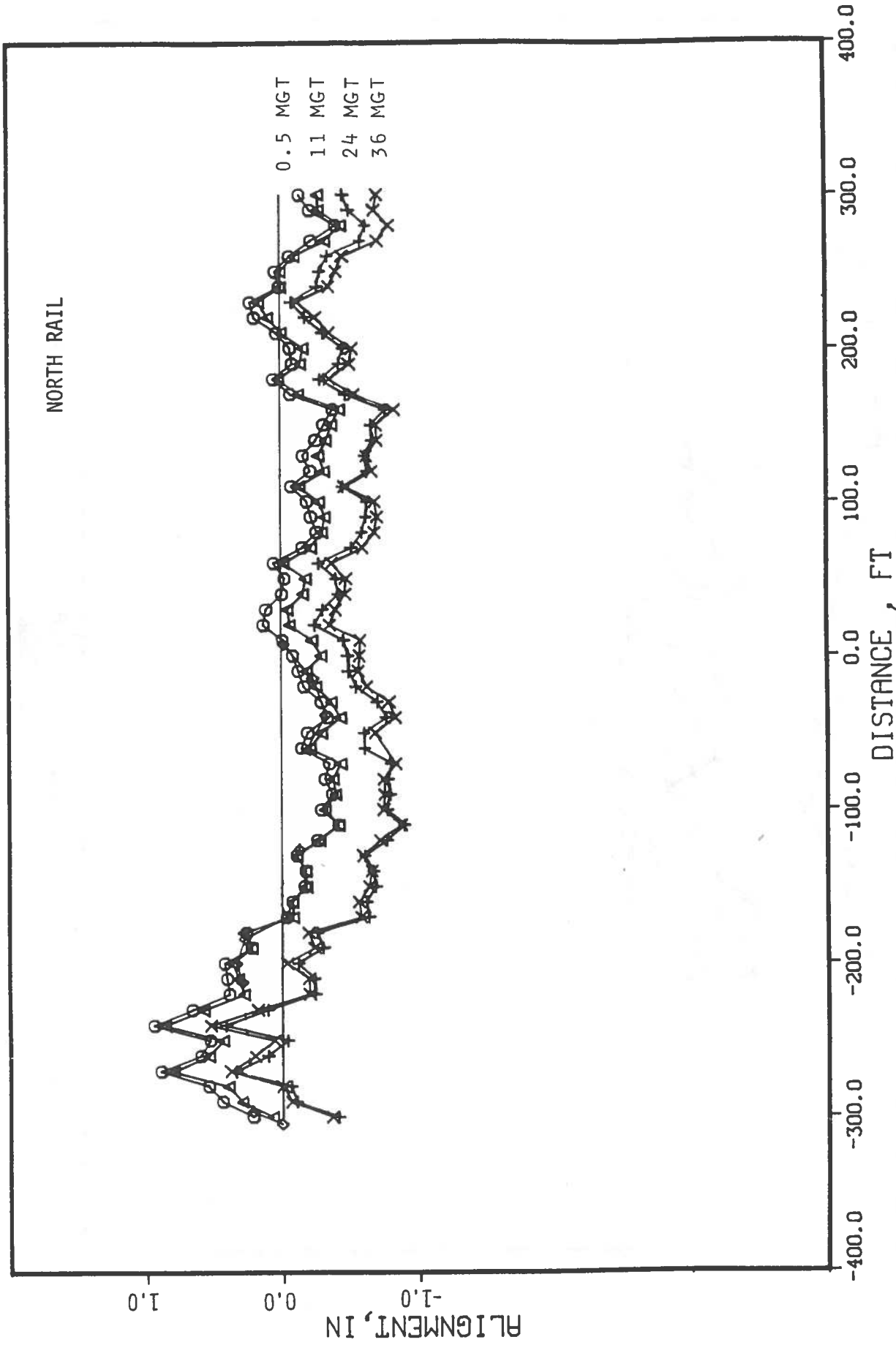


FIGURE 33. CONCRETE TIE TRACK SETTLEMENT AT STREATOR

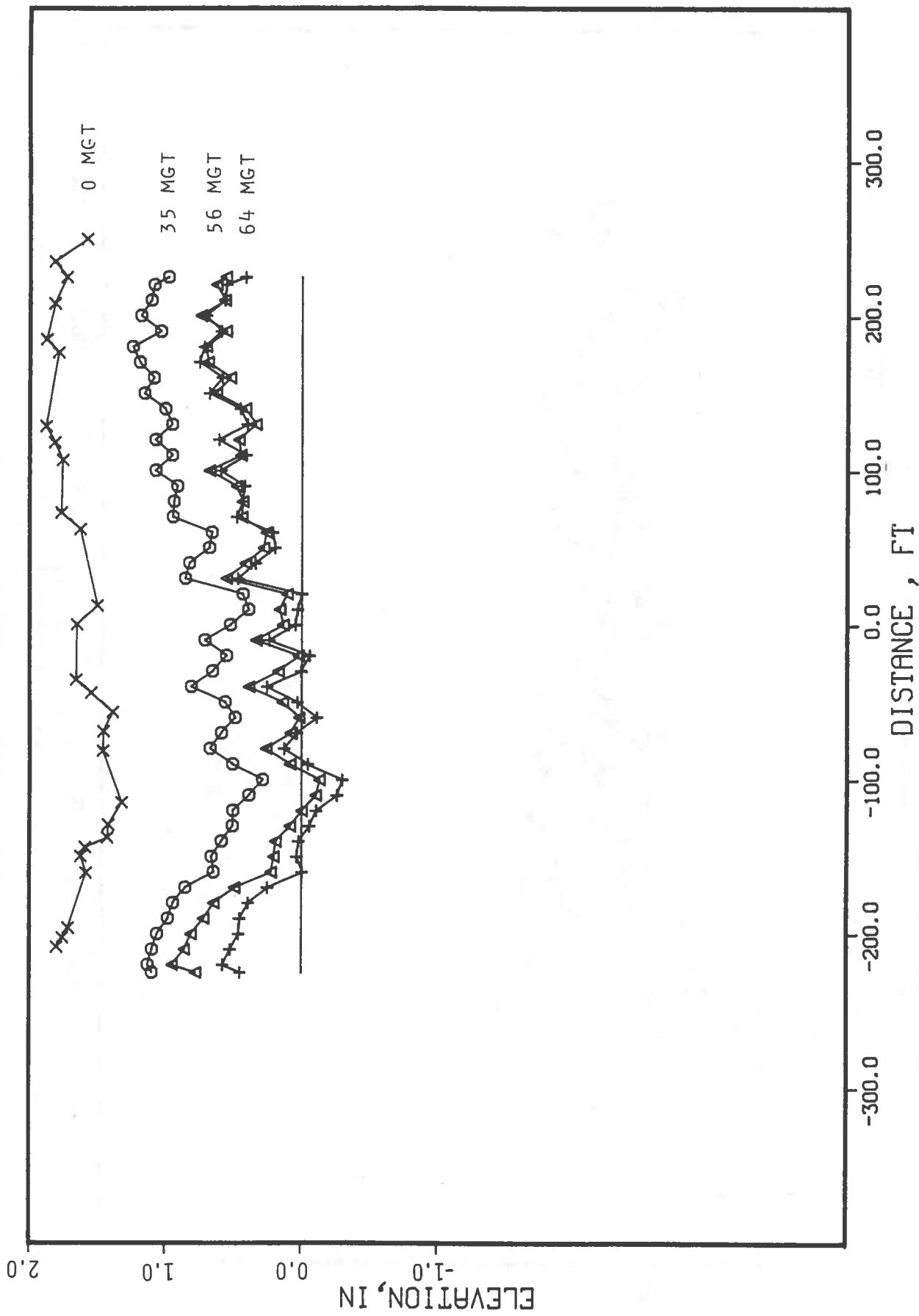


FIGURE 34. CONCRETE TIE TRACK SETTLEMENT AT RICHMOND

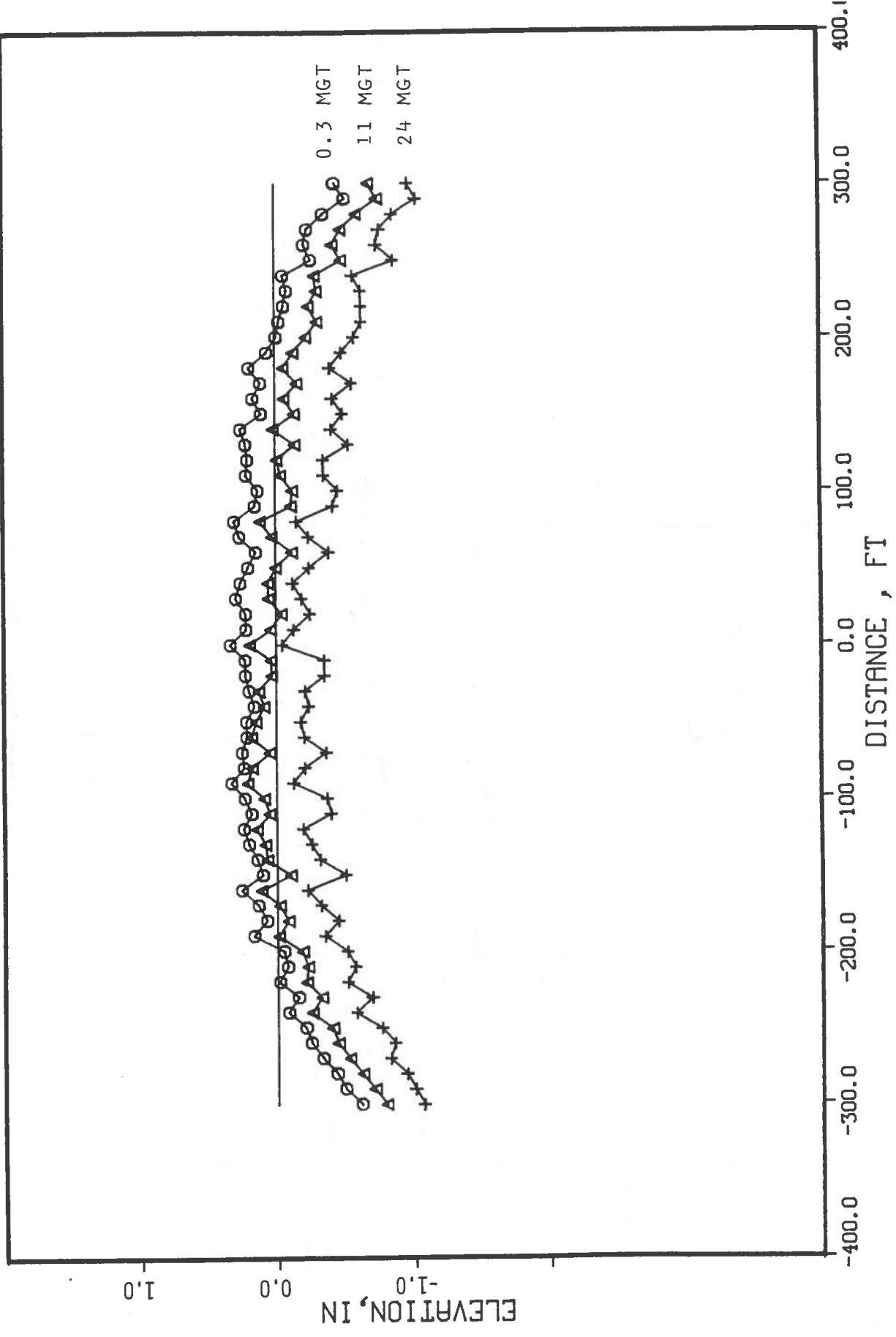
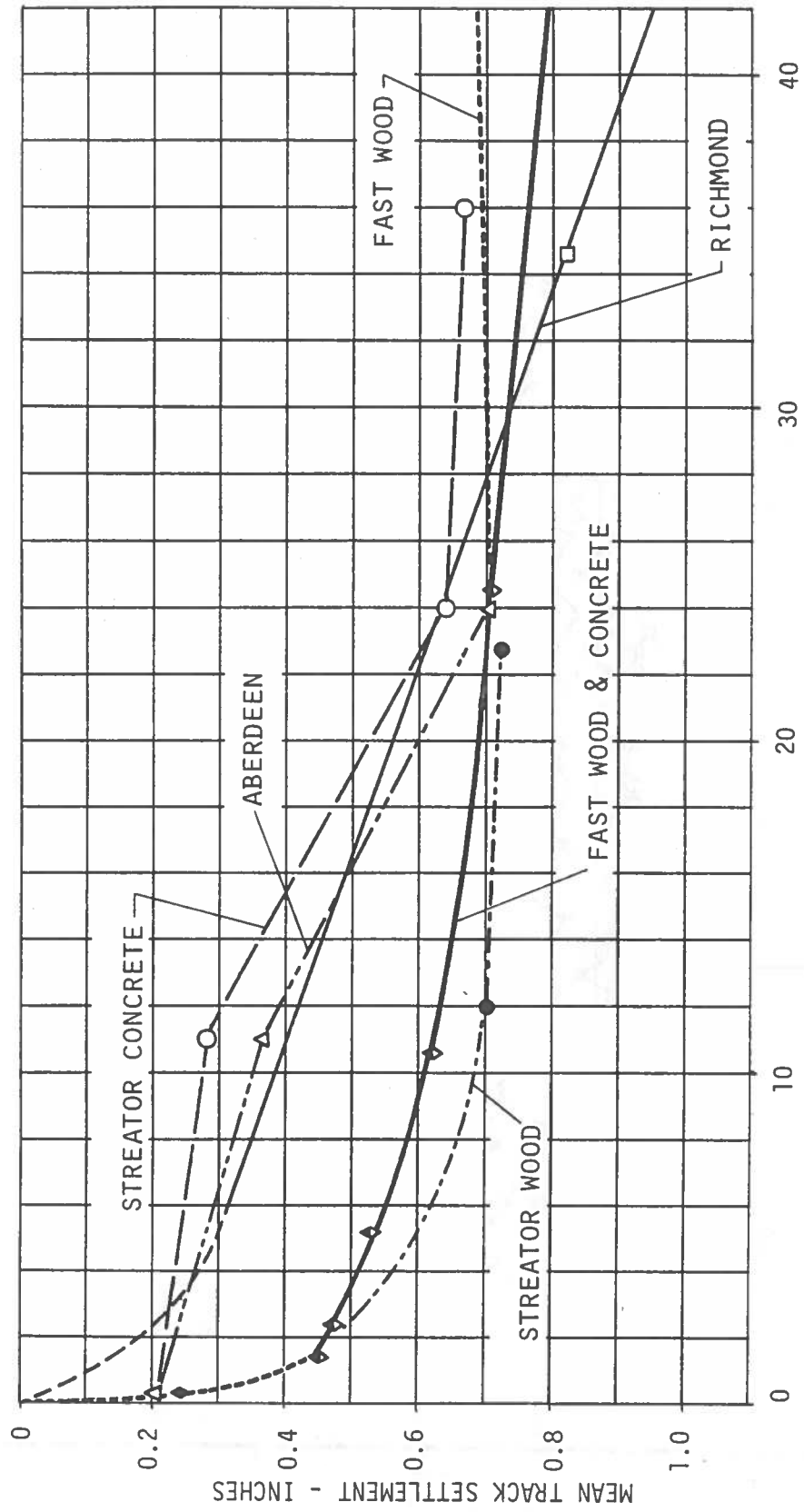


FIGURE 35. CONCRETE TIE TRACK SETTLEMENT AT ABERDEEN



TRAFFIC SINCE SURFACING - MGT

FIGURE 36. SUMMARY OF MEAN TRACK SETTLEMENT

rainfall statistics (discussed in Section 7.3) do not seem to correlate with the seasonal settlement effect. Therefore, it has been assumed that this effect may be associated with either freeze-thaw cycles or perhaps an increased track modulus when the ballast is frozen, causing higher impact loads from wheel irregularities resulting in higher stresses in the ballast and subgrade. There is no indication of a similar trend at Richmond which does not have heavy frost or Pueblo where moisture levels are quite low and no significant impact loads occur.

Survey data derived to characterize track roughness show only a weak correlation between average track roughness and either absolute settlement or accumulated track tonnage. This can be seen qualitatively in Figures 32 thru 35 and is discussed in more detail in Section 9. It must be emphasized, however, that these data were collected over deliberately chosen homogeneous sections of track containing no obvious anomalies such as joints, engine burns, grade crossings, or culverts. Overall, track geometry was also sufficiently smooth to minimize any vehicle dynamics which otherwise might cause fluctuating loads. The lack of correlation with settlement or traffic tends to confirm the assumption that relative track roughness is driven primarily by discrete anomalies within the track structure; either in terms of local imperfections in the running surface or abrupt changes in stiffness or strength in the track structure. None of these anomalies was observed within the surveyed portion of the test sites. However, some transients did develop in the running surface at the ends of the concrete sections where track stiffness changes occurred. This further emphasizes the importance of track uniformity.

Wood tie test sections at FAST and Streator were studied along with the concrete tie sections to compare the relative performance of wood and concrete ties. In Section 22 at FAST, wood and concrete ties were built with new components upon similar subgrades and ballast beds, built and maintained at the same times with common procedures. By contrast, the Streator test sites had different histories. The concrete tie test site was newly built track (1974) with 14-in. of fresh Georgia granite, while the wood-tie control section represented mature mainline track. This original wood-tie track had the expected mix of new and old ties with random lengths and support conditions built on an old 9-in. ballast bed of small, thoroughly fouled slag material. The results of these site comparisons show that when constructed under identical conditions wood ties at the traditional 19-1/2 in. spacings and concrete ties at the currently accepted 24-in. spacing produce almost identical settlement rates and comparable degrees of track roughness. By contrast, there was a slight advantage in quality of surface and line of the concrete test section over adjacent wood-tie section at Streator. This may be attributed primarily to differences in the ballast sections and to tie condition. One clear advantage that the concrete ties have over the wood ties is their ability to maintain a very precise and consistent gauge as seen in Figure 37. Note also that the surface roughness seen in Figure 37 has little resemblance to the surveyed data in Figure 33. This can be explained by the short chord length of the geometry car system which is best suited for spotting dipped joints and other short wave length errors, while the survey-to-benchmark work could not justify a higher density survey than the 10 ft interval. In addition, the geometry car is measuring "loaded" geometry while the survey was taken "unloaded," which would have some influence particularly in the wood tie section due to the cut spike fasteners.

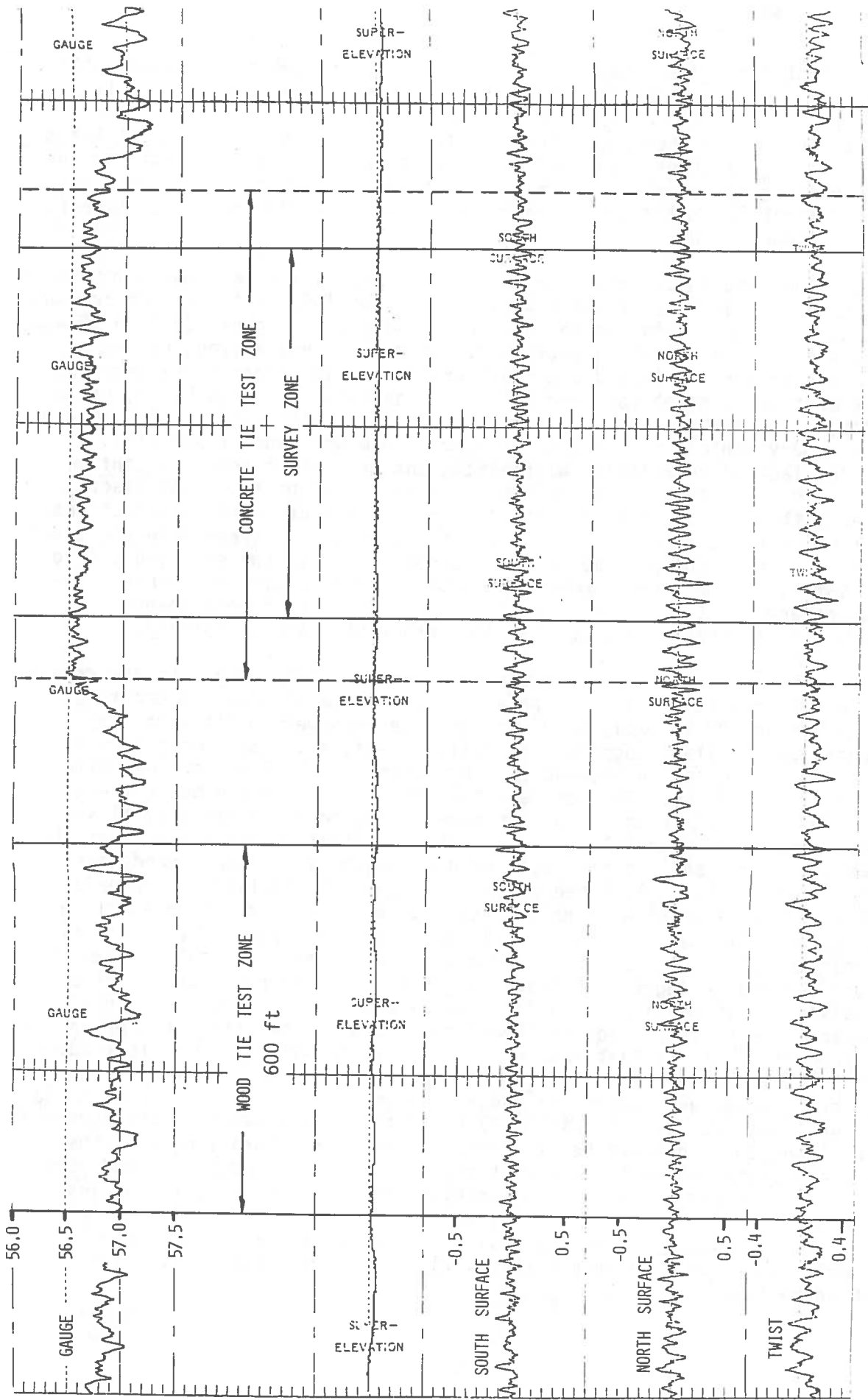


FIGURE 37. TRACK GEOMETRY AT STRACTOR (LEEDS) WOOD AND CONCRETE TIE TEST SITES



## 7.0 BALLAST AND SUBGRADE CHARACTERISTICS

A variety of field tests were conducted at the sites to assess the physical states of the ballast materials as they existed prior to a track maintenance operation. These physical state tests were repeated after surfacing to determine the changes in ballast properties that occurred due to the maintenance. In addition to these tests, standard and Dutch cone penetration tests, and undisturbed tube sampling for laboratory testing were used to investigate the subgrade support characteristics.

The ballast and subgrade materials recovered from the field sites were subjected to a series of index and classification tests. The results were used to develop subsurface profiles describing the composition of the track foundations. Laboratory triaxial tests, both static and repeated load, were also performed on samples of these materials to characterize their stress-strain-strength properties. The results of these triaxial tests were used in the prediction of the vertical track modulus and permanent settlement at each of the field sites. Details of these test results are given in Volume II.

### 7.1 Ballast Descriptions

During the revenue site investigations, it was necessary to remove some of the ties and excavate through the ballast materials in order to position subgrade instrumentation. During the excavations, the descriptions and characteristics of the track formation were logged. The excavation descriptions were combined with the laboratory classification results, ballast and subballast moisture contents, and shallow subgrade auger samples to determine the general ballast profiles for the revenue field sites. These profiles are shown in Figures 38 through 41 for the Streater wood, Streater concrete, Richmond, and Aberdeen test sections, respectively.

At the request of the N&W engineering department, no comparable evaluations were performed at Roanoke on the the ballast and subgrade, because of the possible disruptive effects on its long-term evaluations of track performance. However, clearing of cribs for the tie inspections and installation of strain gages revealed a fouled condition somewhat similar to Richmond. This fouling is caused by the cumulative affects of 270 MGT of loaded, coal trains depositing coal dust into the ballast layer. The resulting mixture of coal fines and granite were sufficiently "cemented" to require extensive use of a pick to break loose the ballast material enough that a ballast fork could be used for removing material from the crib.

A detailed examination of the other sites showed that the crib areas were less fouled than the material below the tie. The water content of the crib materials was very low, generally less than 1 percent, as would be expected. Water content increased as degree of fouling increased. In all of the excavation profiles shown, the first stratum corresponded roughly to the crib materials, and the bottom of the ties are located within a few inches of this first profile boundary shown in Figures 38 through 41. Particle sizes decrease with depth for the field sites. Visible evidence of distinct particle crushing was

Site: Streator (Leeds), Illinois  
Wood Tie Section

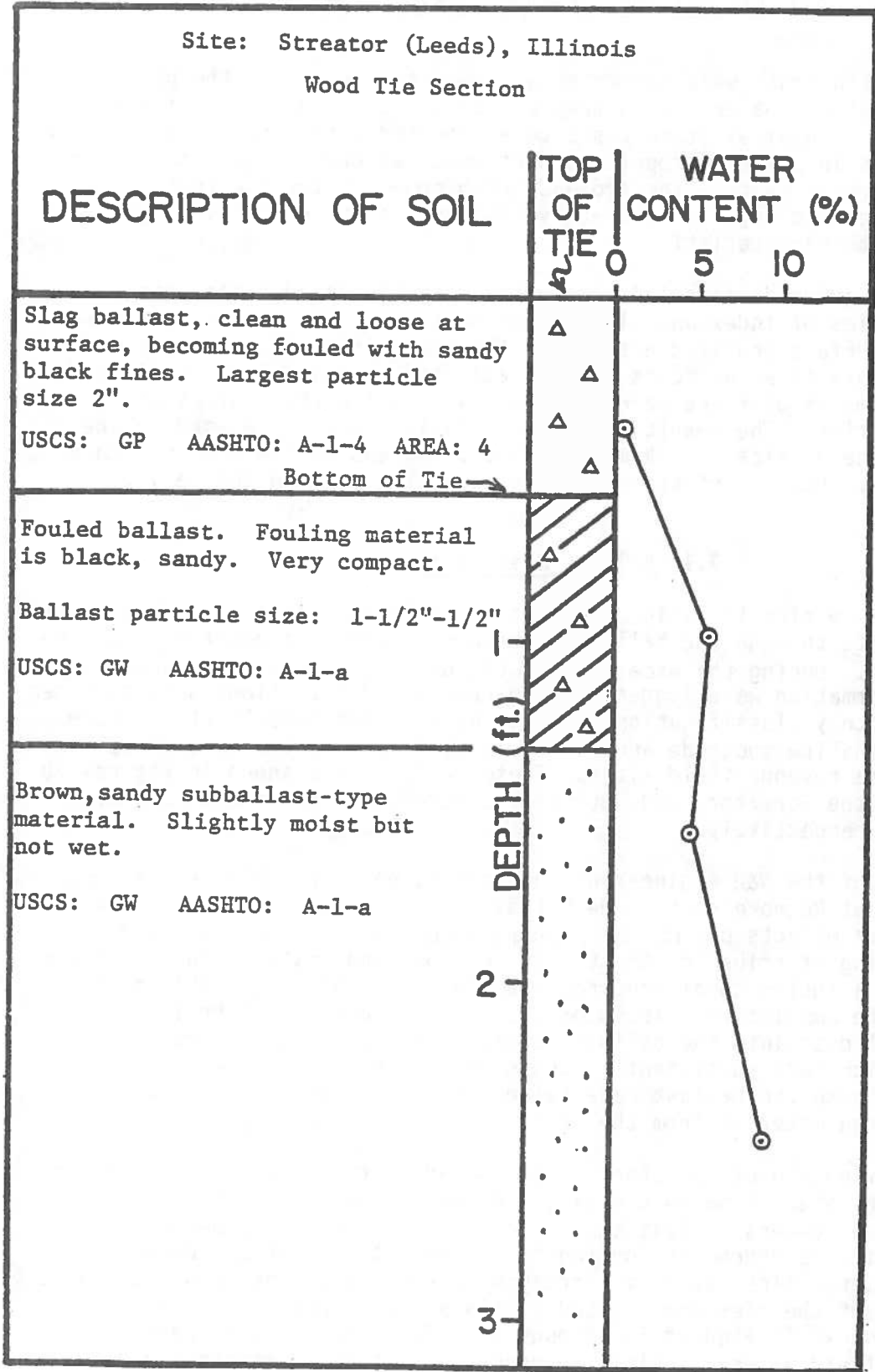


FIGURE 38. BALLAST PROFILE FOR STREATOR WOOD TIE SECTION

Site: Streator (Leeds), Illinois  
 Concrete Tie Section

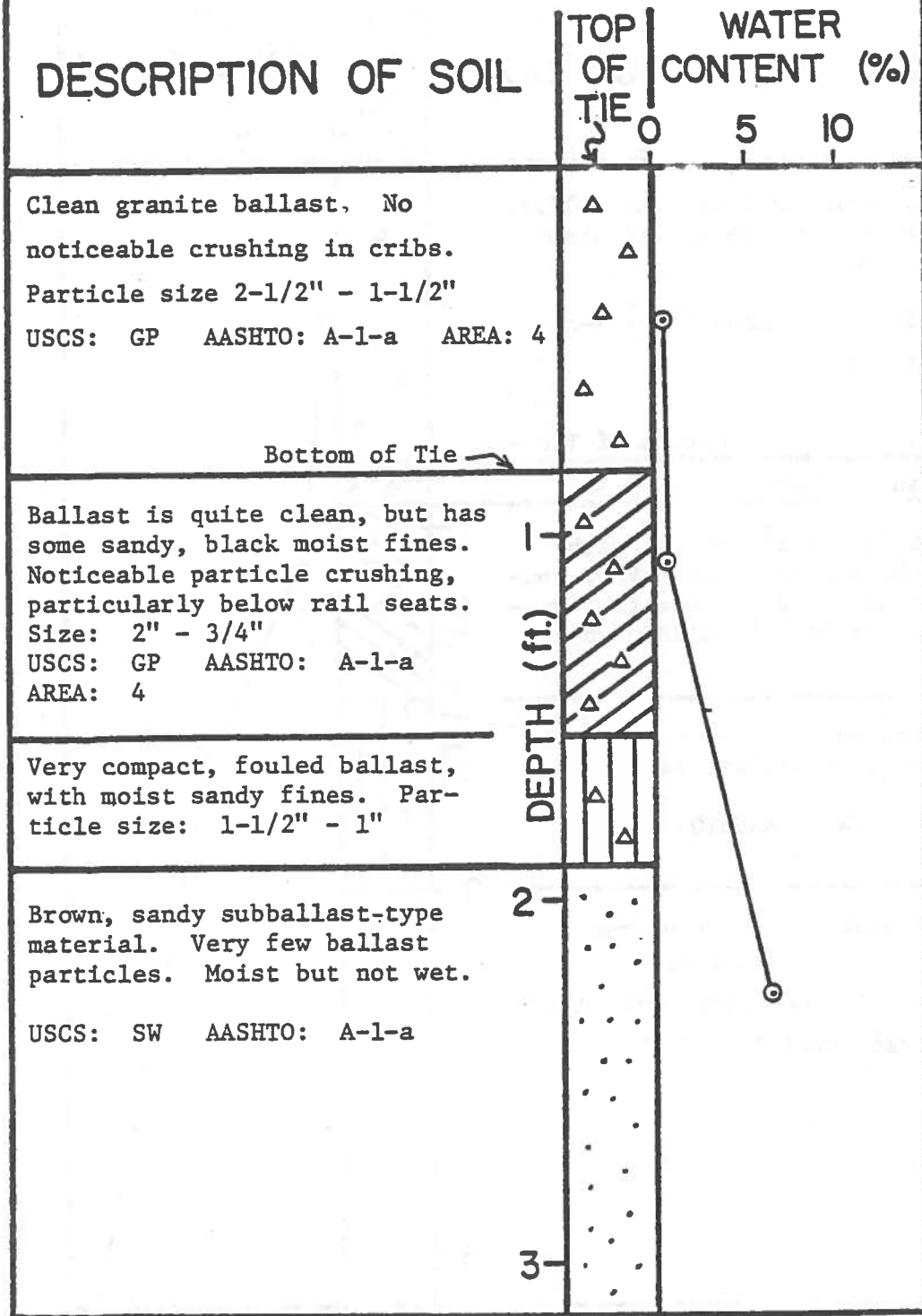


FIGURE 39. BALLAST PROFILE FOR STREATOR CONCRETE TIE SECTION

Site: Richmond, Virginia  
Concrete Tie Section

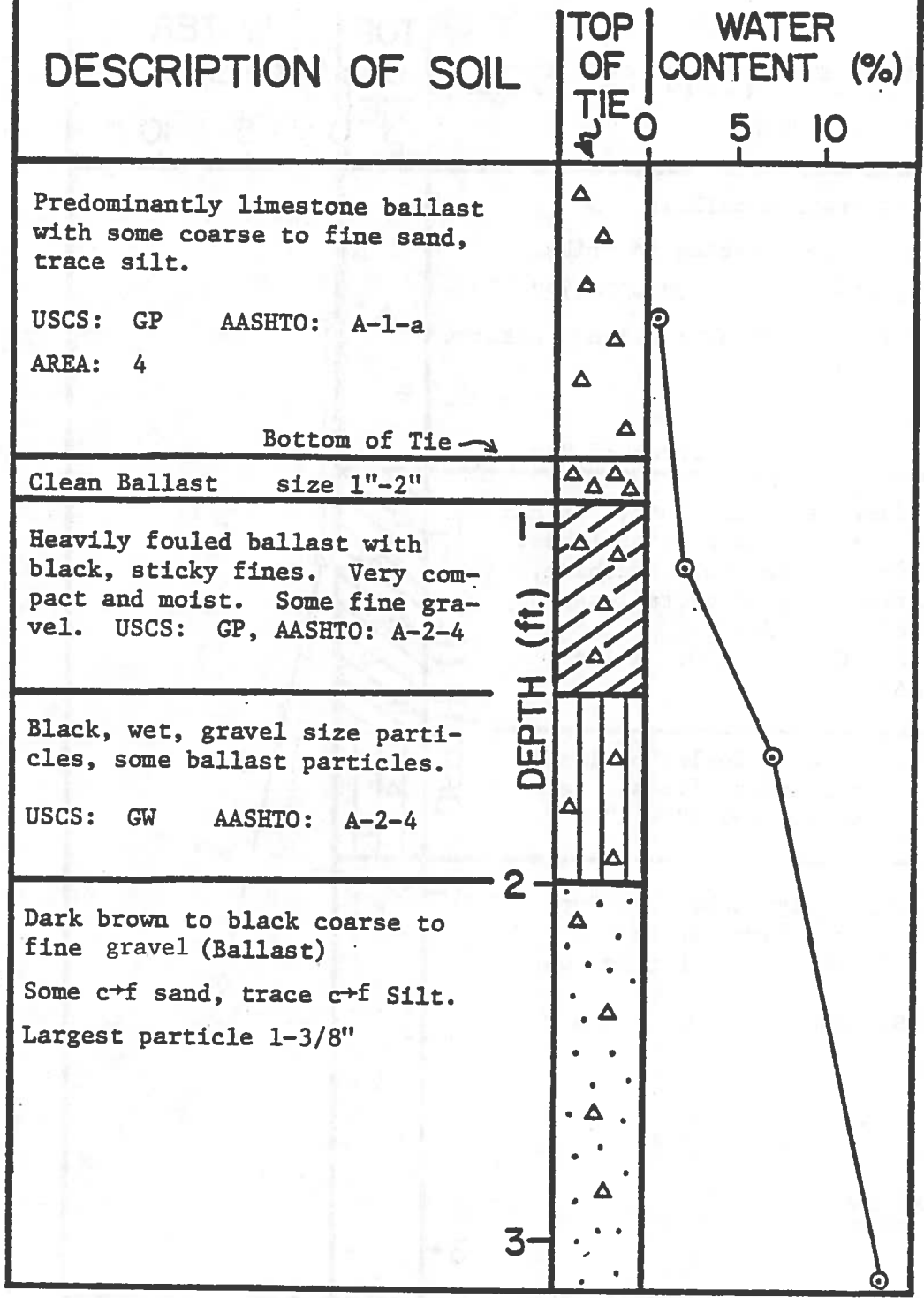


FIGURE 40. BALLAST PROFILE FOR RICHMOND CONCRETE TIE SECTION

Site: Aberdeen, Maryland  
 Concrete Tie Section

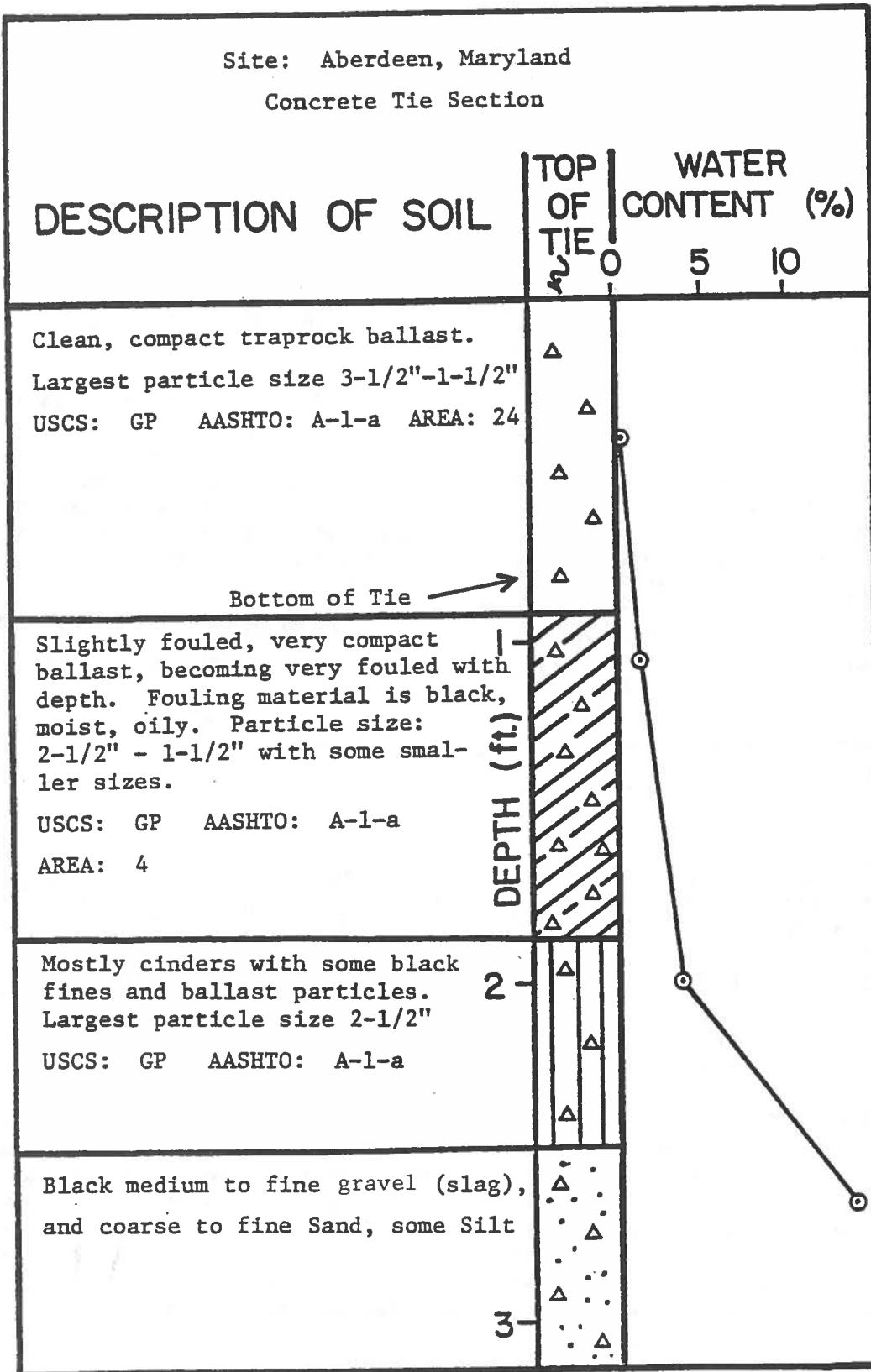


FIGURE 41. BALLAST PROFILE FOR ABERDEEN CONCRETE TIE SECTION

present at the Streator concrete site, particularly near the rail seat areas under the ties. However, gradation comparisons of materials taken from the crib and under-tie areas showed that the crib ballasts were always coarser than the under-tie materials. Thus, breakage undoubtedly occurred at the other sites as well.

A comparison of the gradation curves for the under-tie material in the revenue service sites in Figure 42 shows that the Streator wood tie section ballast was much finer than the other ballasts. The Richmond under-tie material is basically similar to the Streator concrete and Aberdeen material for the coarser particles, say greater than 3/4 in., but contains more particles less than the 3/4-in. size. Aberdeen crib material was classified as AREA 24 material. The crib materials at all other sites, and the under-tie materials at the Streator concrete and Aberdeen sites, were classified as AREA 4. The under-tie materials at the Streator wood tie section and the Richmond site did not fall within any standard AREA classification.

The most appropriate index tests for the specification of acceptable ballast materials are still being debated, although Gaskin and Raymond [10] have attempted to relate certain index properties to track performance. The most commonly used index tests were therefore performed on the ballast materials. There were: (1) specific gravity and absorption according to ASTM standards E-12, C125, C127-73 and C128-73, (2) Los Angeles abrasion according to ASTM C131-69 standards, (3) magnesium sulfate soundness according to ASTM C88 standards, (4) scratch hardness according to ASTM C235-68 standards, (5) petrographic analysis for mineral mode data, Moh's hardness, degree of cleavage and mineral alteration, and (6) particle sphericity, angularity (roundness) and flakiness. The results of these tests are given in Table 5.

It should be noted here that although differences in ballast materials were observed, ballast compaction was a much more important factor in overall track performance.

## 7.2 Physical State Tests

In order to characterize the physical state or structure of the ballast at field test sites, a series of special field tests were performed. Prior to a scheduled maintenance operation, physical state measurements were made at the revenue sites by the University of Massachusetts geotechnical staff. These tests included the ballast density test (BDT), the plate load test (PLT), and the lateral tie push test (LTPT). These physical state tests were repeated after the track was raised and tamped so that quantitative assessments of the change in ballast physical state could be made.

The locations for the ballast density tests were under the tie at the rail seats and in the cribs near the rail seats. A few ballast density tests were also done under the center of the tie. Plate load tests were done in the cribs near the rail seats, and under the ties at the rail seats and tie centers. Measurements of plate bearing index and lateral tie push resistance, both pre- and post-maintenance, were also available for FAST Section 3 and the wood and concrete portions of FAST, Section 22. Ballast density test results for FAST Sections 3 and 22 were not available. The determination of

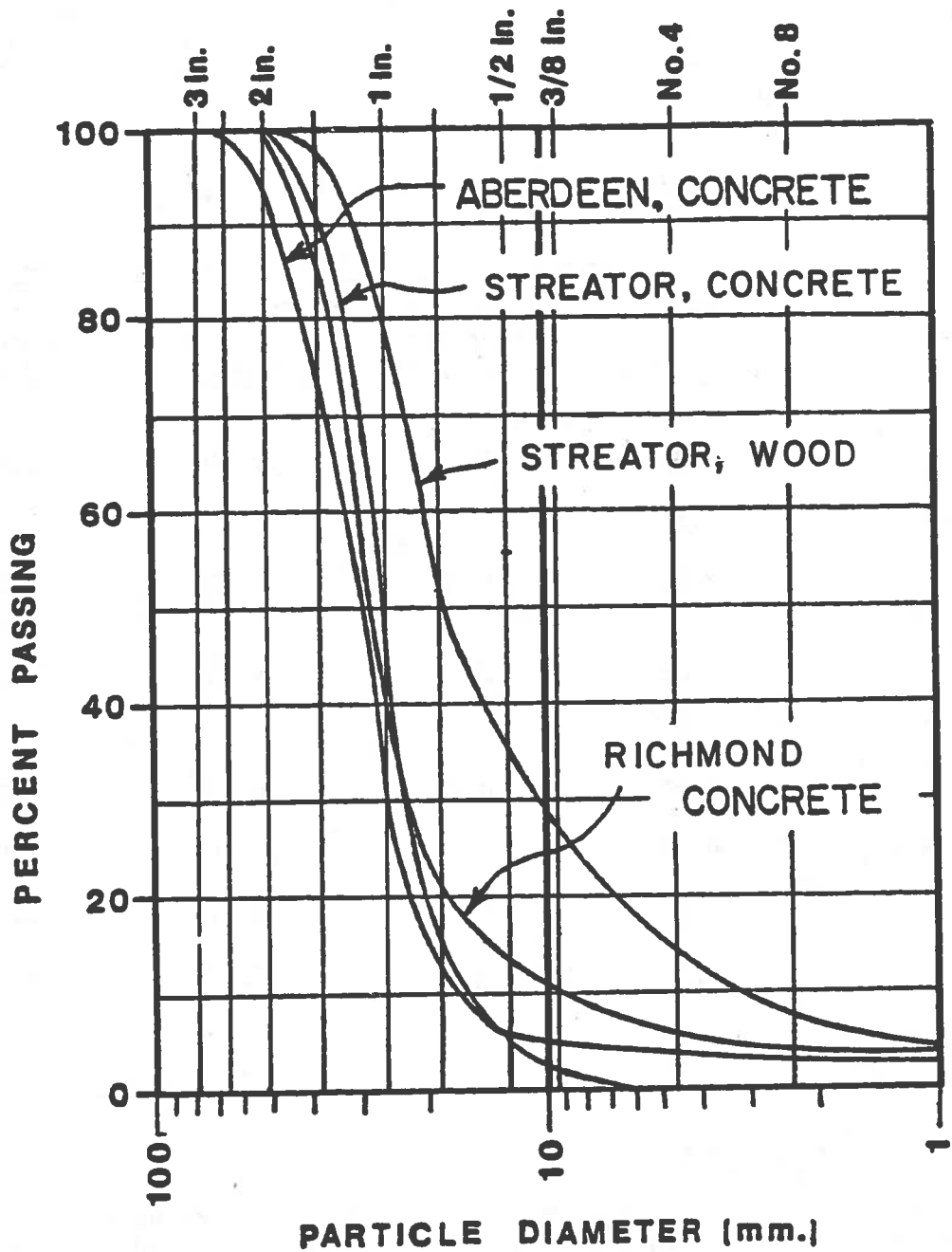


FIGURE 42. COMPOSITE GRADATION CURVES FOR UNDER-TIE BALLASTS FROM REVENUE SITES

the in-situ ballast physical states will be used to provide basic information needed for the correlation of track performance between the revenue sites and FAST.

One month prior to the site visit to Streator, a track gang came through the concrete tie section and performed a track surfacing operation, unaware of the scheduled ballast testing. Thus, the pre-maintenance test series measurements could not be obtained for this site. The amount of track disturbance and amount of raise given to the Streator concrete tie section due to this unscheduled maintenance is unknown.

TABLE 5. SUMMARY OF BALLAST INDEX TEST RESULTS FROM FIELD SITES

| <u>Test</u>                             | <u>Streator<br/>Wood<br/>Under-Tie</u> | <u>Streator<br/>Concrete<br/>Under-Tie</u> | <u>Richmond<br/>Concrete<br/>Under-Tie</u> | <u>Aberdeen<br/>Concrete<br/>Under-Tie</u> |
|---|--|--|--|--|
| Specific Gravity                        |  |  |  |  |
| Bulk                                    | 2.34                                   | 2.78                                       | 2.70                                       | 2.87                                       |
| Apparent                                | 2.50                                   | 2.81                                       | 2.68                                       | 2.90                                       |
| Absorption (%)                          | 2.25                                   | 0.36                                       | 0.33                                       | 0.32                                       |
| Los Angeles                             |  |  |  |  |
| Abrasion (%)                            | 29.22                                  | 39.94                                      | 19.25                                      | 17.79                                      |
| Magnesium Sulfate                       |  |  |  |  |
| Soundness, 5                            |  |  |  |  |
| Cycles (%)                              | 0.37                                   | 0.05                                       | 0.73                                       | 0.00                                       |
| Flakiness Index (%)                     | 9.00                                   | 16.00                                      | 11.00                                      | 17.00                                      |
| Sphericity                              | 0.67                                   | 0.63                                       | 0.61                                       | 0.62                                       |
| Roundness                               | 0.28                                   | 0.25                                       | 0.22                                       | 0.26                                       |
| Scratch Hardness,<br>(%) Soft by Weight | NA                                     | 0.00                                       | 0.00                                       | 0.00                                       |

#### 7.2.1 Ballast Density Tests

The ballast density test determines the in-situ density of the ballast materials. This test, described more thoroughly in References 11 and 12, uses a water replacement technique to determine the volume of a membrane-lined, hand-excavated hole in the ballast. The volume of the hole along with the weight and moisture content of the excavated material is used to calculate the



in-situ dry density,  $\gamma_{df}$ . The field density measurements are used along with a laboratory reference density test [12] to determine the relative compaction state in the field. The maximum density that can be achieved using the reference density apparatus is referred to as the ultimate reference dry density,  $\gamma_{ult}$ . The ratio of the field density to the ultimate reference density is the relative compaction,  $R_c$ , expressed in percent. The smooth steel walls of the mold used to determine reference density in the laboratory result in systematically lower ultimate reference densities than the field measurements, although the actual densities may be similar. Relative compaction is more useful for studying changes in ballast density due to traffic histories and maintenance effects than the actual density values, because it tends to compensate for differences in gradation and particle specific gravity.

The results from the ballast field density tests and the laboratory ultimate reference density tests are shown in Figure 43. For reasons previously explained, the lab ultimate reference densities were all lower than the field measurements. The pre- and post-maintenance densities for the Aberdeen site were very close. The amount of track raise at Aberdeen was only 0.1 in., which could result in less disturbance to the material under the tie than a large raise. The relative compaction of the ballast under the tie at Aberdeen was therefore not affected by the maintenance operation. In contrast to this, the Richmond site exhibited the largest changes in both pre- and post-maintenance densities and relative compaction under the ties. The Richmond site also had the largest raise, about 2 in., which would significantly disturb the ballast structure. A large change in relative compaction was also observed for the Streator wood tie section, which was raised about 1.5 in.

The pre- and post-maintenance densities and lab ultimate densities for the crib locations are shown in Figure 44. The crib densities and relative compactions, both pre- and post-maintenance, were lower than the under-tie values for all of the field sites. The ultimate lab reference densities for the crib ballasts were also lower than the ultimate reference densities for the under-tie material. This may be due to differences in the crib and under-tie gradations. It was previously shown that the crib materials were consistently coarser than the under-tie materials. Also, the crib materials were less fouled and would be expected to have higher void ratios and lower dry densities, since fewer fine particles would be present to fill the interstices between the larger ballast particles.

The changes in relative compaction of the crib ballasts as a result of maintenance are shown in Figure 44. The largest change in crib relative compaction due to the maintenance operation occurred at Aberdeen. Even though the lift height was small for the Aberdeen site, the crib area would be disturbed by the insertion of the tamping tools, independent of the amount of raise. However, the Richmond site contained crib ballast which was very fouled. Thus it would not be expected to densify as much as the clean crib ballasts as a result of traffic vibrations. This may be the reason that the relative compaction change due to maintenance at Richmond was negligible. The ballast in the cribs at the Streator wood tie section was also quite fouled and showed changes in relative compaction about half as large as the changes measured at Aberdeen.

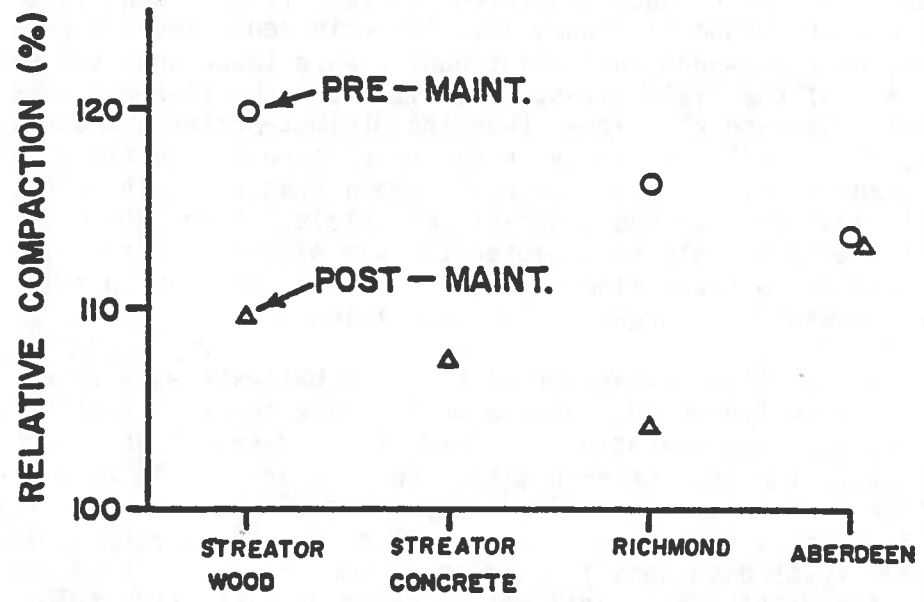
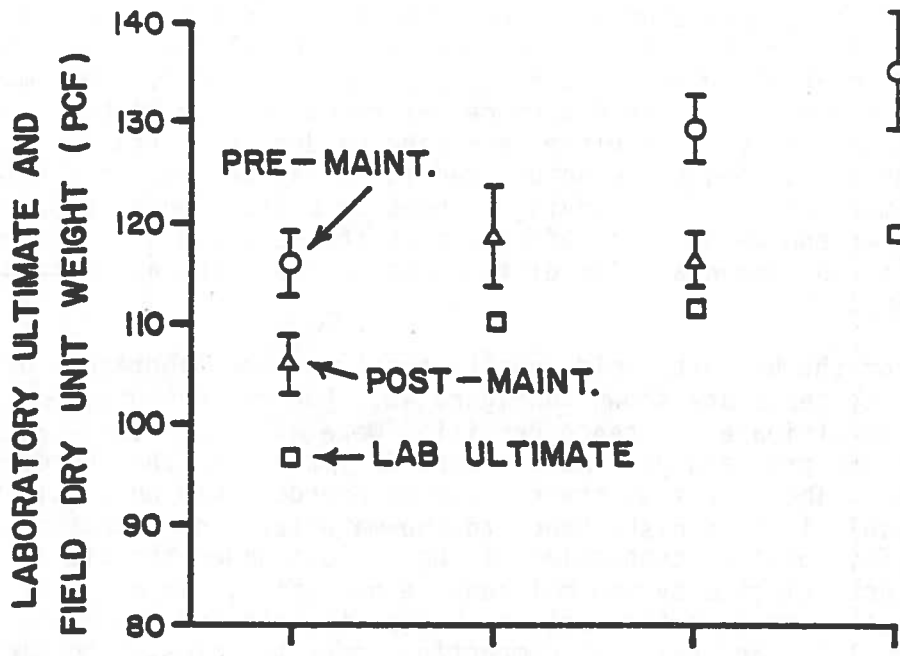


FIGURE 43. BALLAST DENSITIES - UNDER TIE AT RAIL SEAT

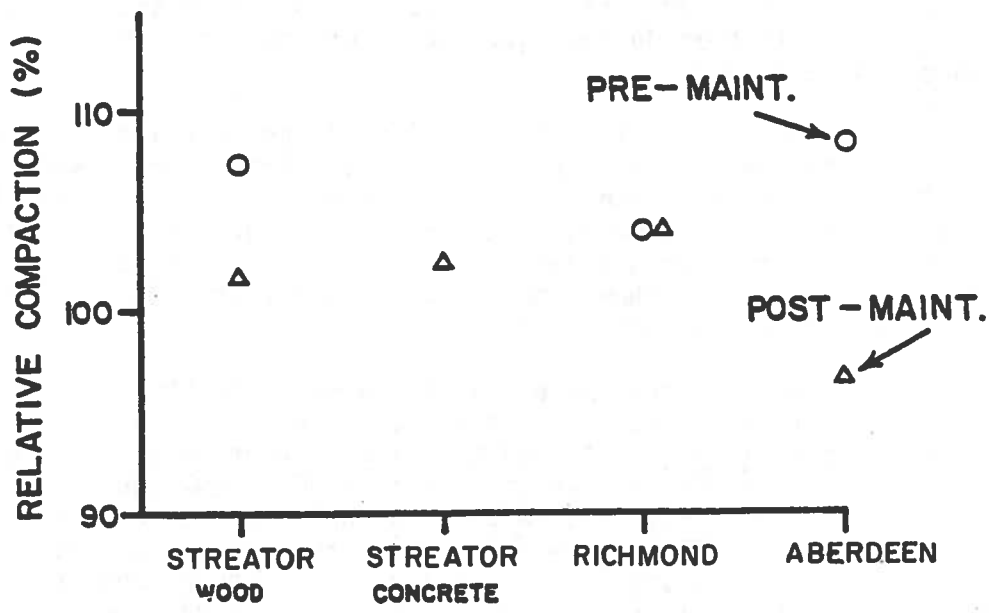
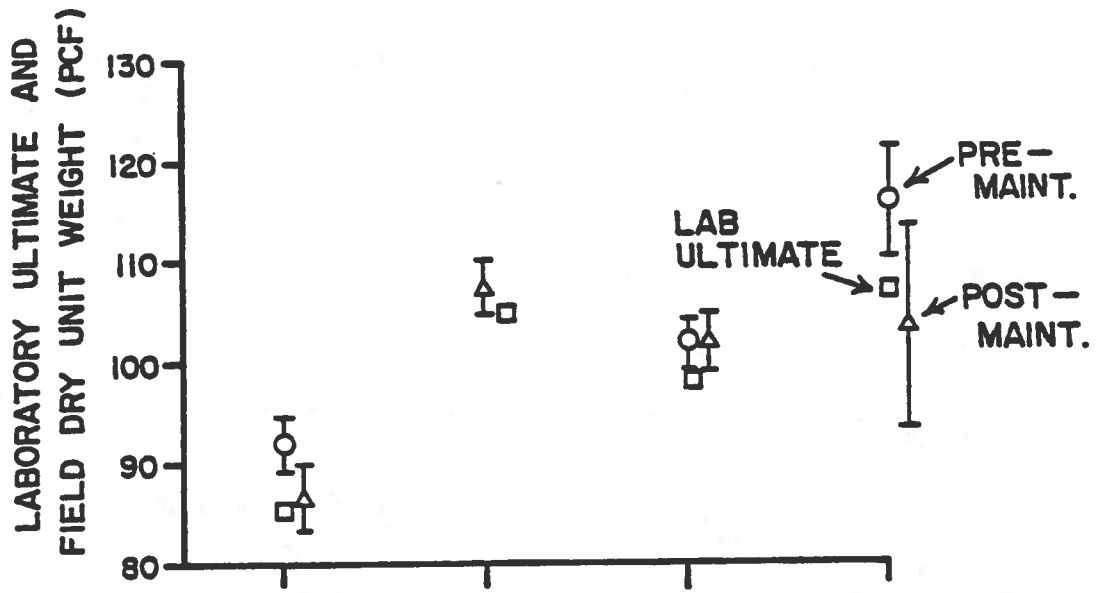


FIGURE 44. BALLAST DENSITIES - CRIB NEAR RAIL SEAT

### 7.2.2 Plate Load Tests

The plate load tests were conducted in the cribs near the rail seats and under the ties, near the rail seats and tie centers. Descriptions of the plate load test procedure and apparatus can be found in Refs. 12, 13 and 14. The test consists of imposing a vertical load on 5-in. diameter steel plate which is seated on the ballast using gypsum gauging plaster. The plate contact pressure per unit deflection is the ballast bearing index,  $B_k$ . This is a measure of vertical ballast stiffness. The  $B_k$  values are calculated as follows:

$$B_k = \frac{P}{A \cdot \delta} ,$$

where  $P$  = applied vertical load,  
 $A$  = plate area, and  
 $\delta$  = vertical deformation.

A deformation level of 0.1 in. was chosen as the reference, although relative comparisons could be made at any deformation value.

The ballast bearing indices,  $B_k$ , at 0.1-in. deformation as measured under the ties at the rail seats are shown in Figure 45 for the revenue sites and FAST. The pre-maintenance values at Richmond were the highest, possibly because of the high degree of fouling. The largest decrease in plate bearing index due to maintenance was also at the Richmond site. This site had the largest raise, about 2 in., which would significantly disturb the ballast structure, particularly when the ballast is fouled. This is consistent with the observation that the Richmond site also showed the largest decrease in relative compaction at the under-tie location. The Aberdeen site showed the smallest change in plate bearing index at the under-tie location as a result of the small raise, only 0.1 in.

The post-maintenance values of plate bearing index were very similar for all of the sites, with the exception of Aberdeen. The maintenance raises for the Streater and Richmond revenue sites were on the order of 1.5 to 2 in. The raises at the FAST site were also about 2 in. For all of the sites where significant trackbed disturbance under the ties resulted from raising and tamping, the plate load tests showed no significant difference in ballast stiffness, independent of ballast type.

Values of the plate bearing index were also measured under the center of the tie. The results of these measurements for the revenue sites are shown in Figure 46. Again, the Richmond site had the highest average  $B_k$  value before the maintenance. The Aberdeen values at this location showed no change resulting from maintenance, but do show that the  $B_k$  values under the center of the ties prior to maintenance were only 1/3 of the value measured under the tie at the rail seat. The plate load tests for all of the revenue sites showed that the ballast stiffnesses were always greater under the tie at the rail seat than under the tie center, prior to maintenance. After the maintenance operations, the ballast stiffnesses under the tie were about the same at both locations, although still slightly greater near the rail seat areas.

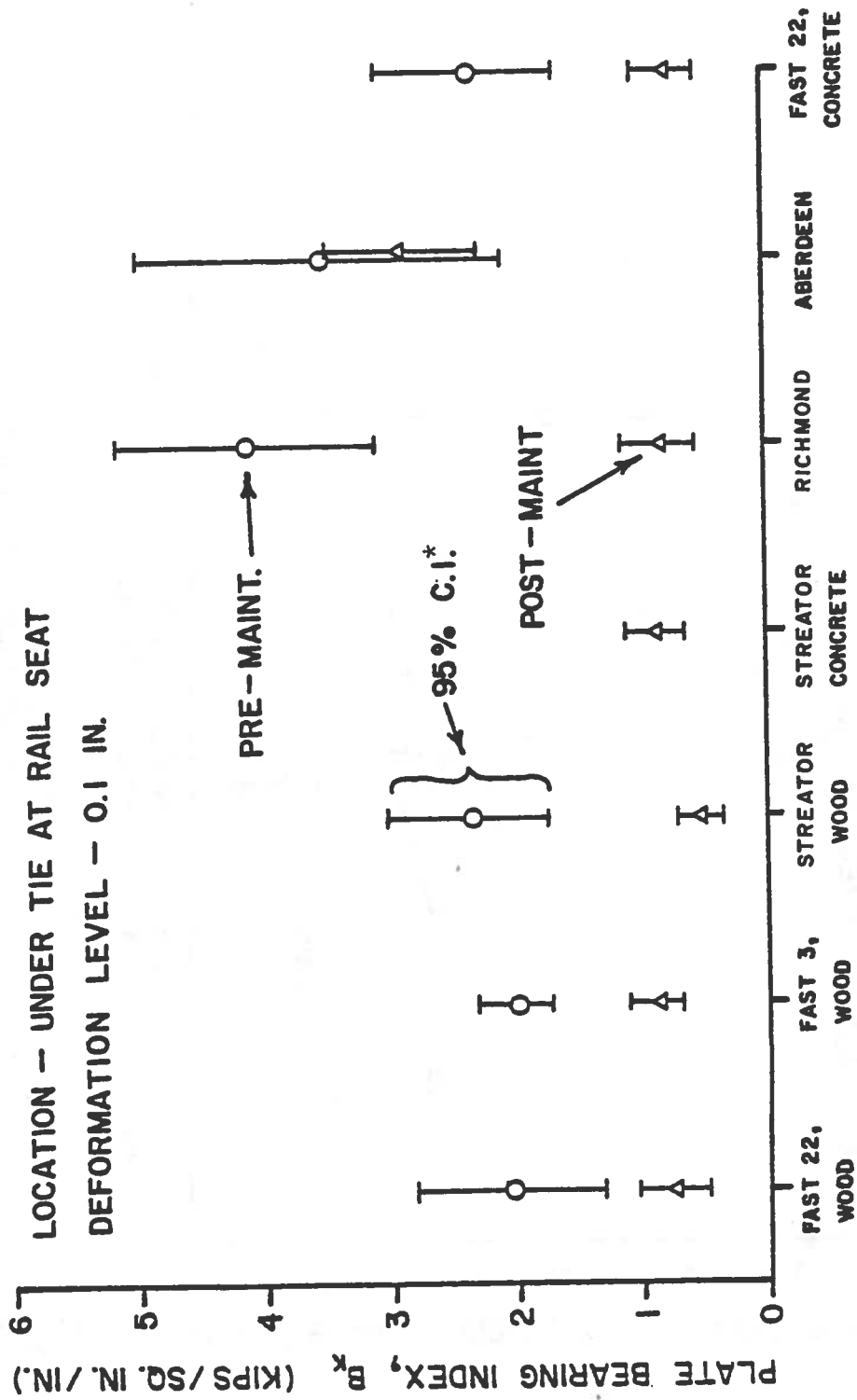


FIGURE 45. PLATE BEARING INDEX - UNDER TIE AT RAIL SEAT

\*Confidence Interval

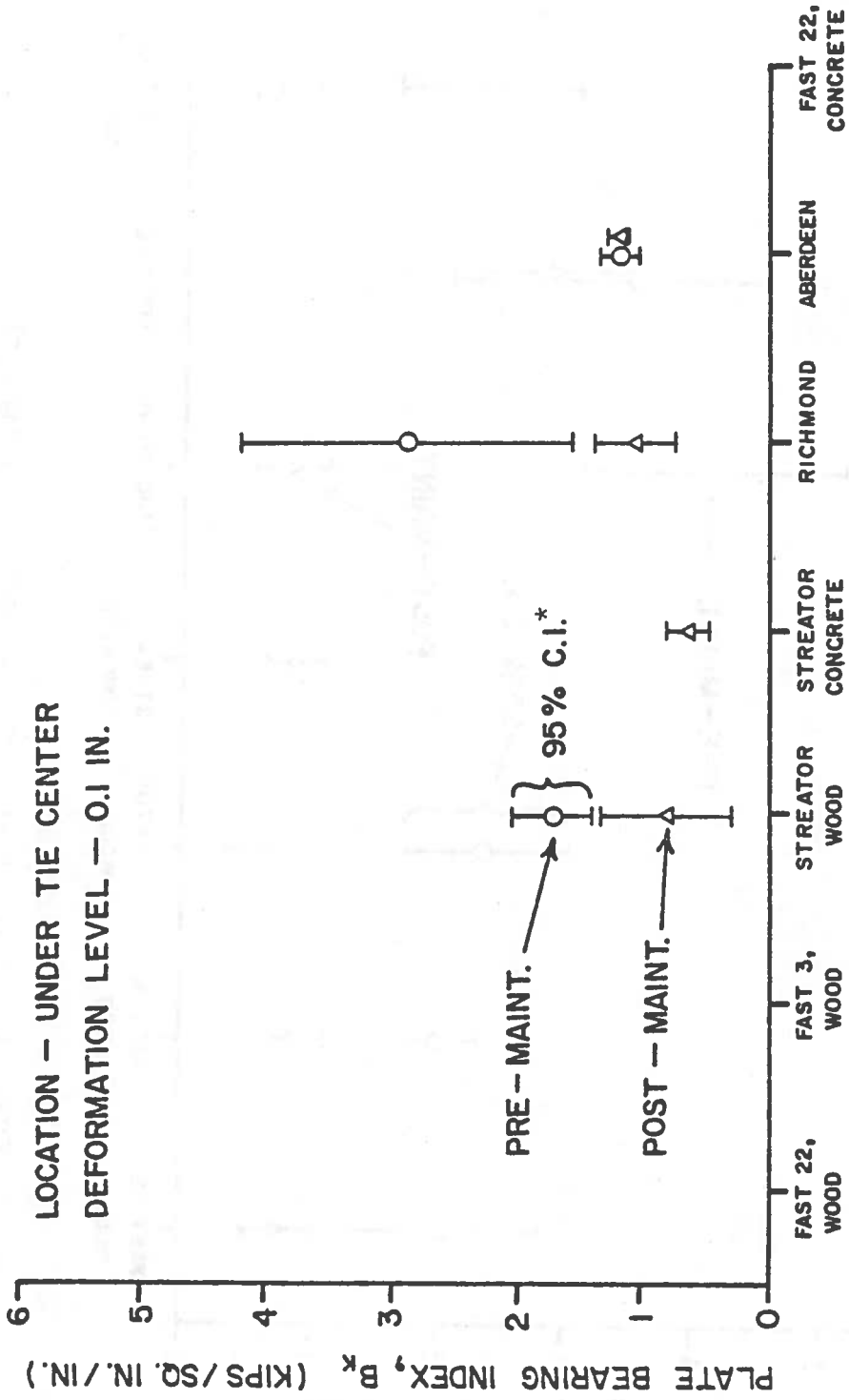


FIGURE 46. PLATE BEARING INDEX - UNDER CENTER OF TIE

\* Confidence Interval

### 7.2.3 Lateral Tie Push Tests

The lateral tie push test is a common field measurement of track conditions used by the railroad industry. The lateral tie push test measures the resistance of a single tie to lateral displacement under unloaded rail conditions. For the test, the tie is separated from the rail and rail fasteners and then pushed from one end after removing the shoulder ballast. The resistance of the tie to lateral loads is an indirect measure of the ballast physical state and degree of compaction. A common variation on the single tie push test involves the use of a track panel containing a number of ties. A compilation of past research and test results of lateral track resistance tests can be found in Ref. 15.

The lateral tie push test results for the test sites are shown in Figure 47. The lateral displacement level at which the results were taken was 2 mm.

The lateral tie resistance for the Aberdeen site again showed the smallest change from maintenance. The Streator concrete tie section post-maintenance results were quite high relative to the FAST, Streator wood, and Richmond sections. Unfortunately, pre-maintenance values for the Streator concrete tie section were not available for comparison. With the exceptions of the Aberdeen and Streator concrete results, as noted, the post-maintenance tie push resistances were all very similar. The low values were due to maintenance disturbance and reduction of crib confinement. Visual observations of the ballast in the cribs at the Richmond site showed unusually depleted cribs after maintenance, with a ballast depth of only a few inches above the bottom of the tie.

### 7.3 Subgrade Description

The subgrade conditions at the revenue field sites were explored using both standard penetration tests (SPT) and Dutch cone penetration tests (CPT). The SPT was selected to aid in the subsurface investigation for two purposes. First, it was an efficient means to obtain samples for visual identification. Second, it provided values of blow count which are commonly used as a rough index of soil properties. The SPT's were done in accordance with ASTM procedure D1586. The CPT was used because it was rapid, was not expected to disturb the roadbed significantly, and was the simplest test thought to have potential for soil property correlations. The CPT's were done in accordance with ASTM procedure D3441, using a mechanical Begemann-type tip with friction sleeve. For all test borings, a truck-mounted drilling rig equipped with rail wheels was used, and borings were taken along the track centerline. A detailed description of the SPT and CPT results from the revenue sites is given in Ref. 16.

#### 7.3.1 Standard Penetration Tests

The standard penetration resistances for the field sites are shown in Figure 48 as a function of depth. The consistencies of the subgrade soils for the Streator sites could be described as stiff for depths from about 5 to 13 ft. Below these depths, the material was very soft.

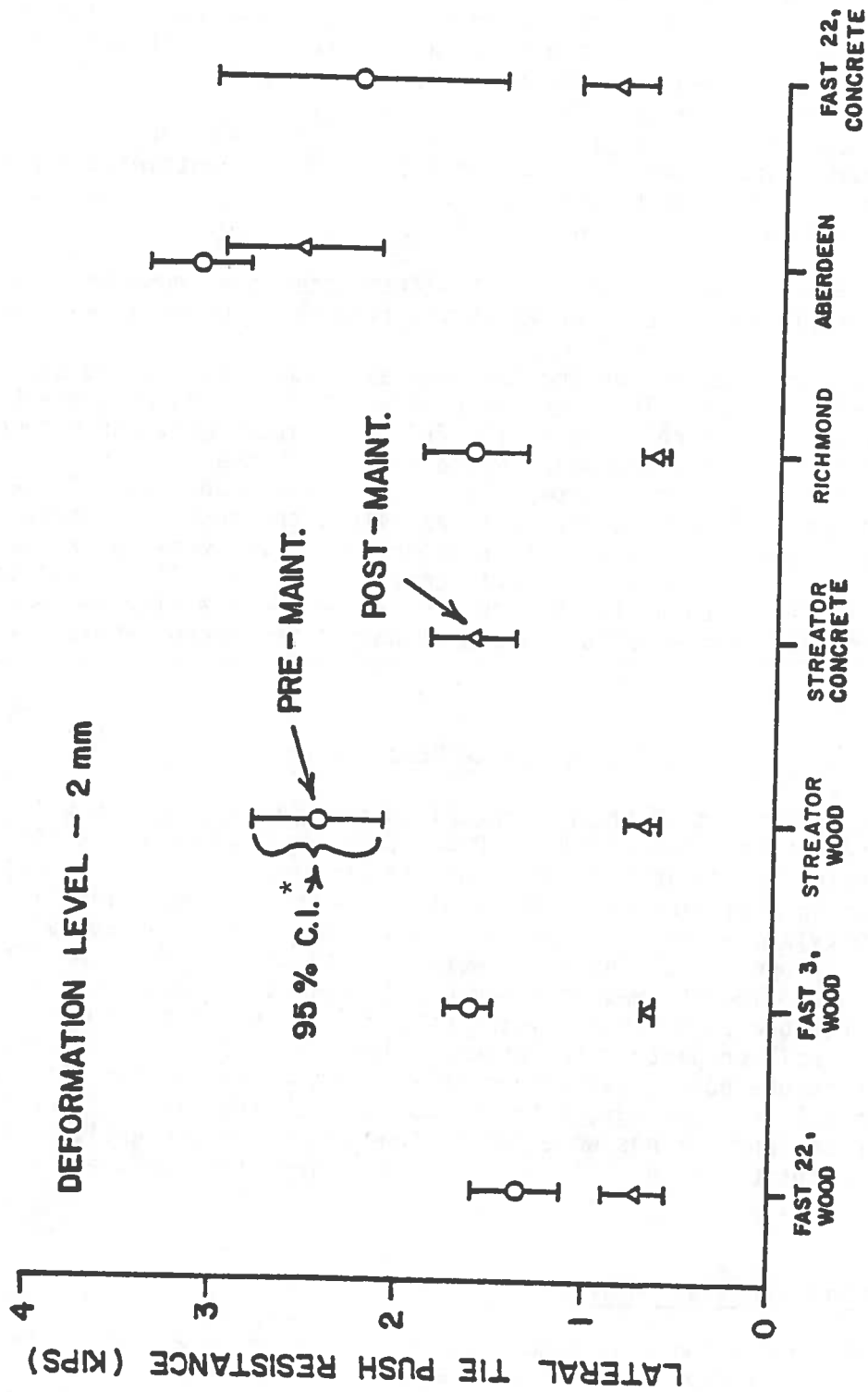


FIGURE 47. LATERAL TIE PUSH RESISTANCE

\*Confidence Interval



## STANDARD PENETRATION RESISTANCE, N (blows / ft)

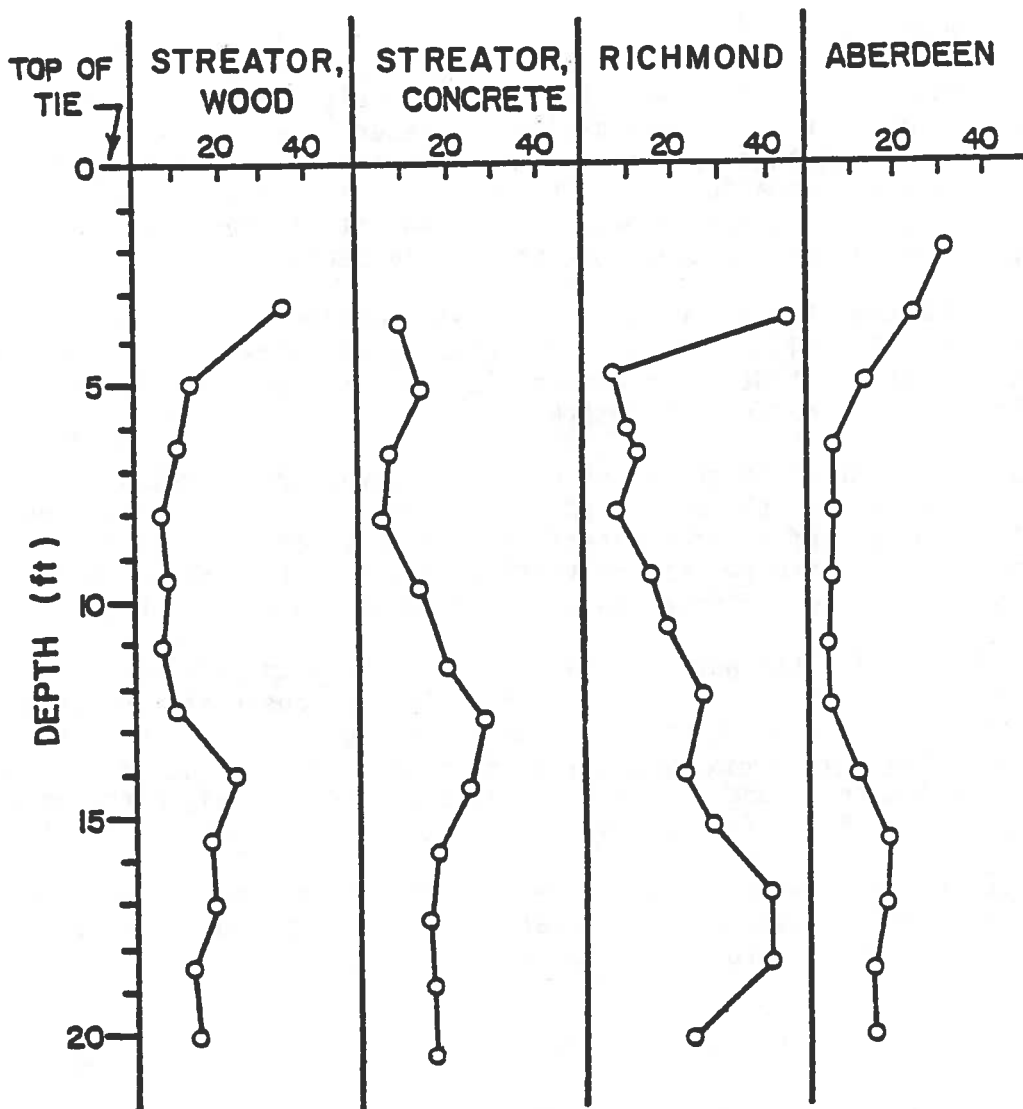


FIGURE 48. STANDARD PENETRATION RESISTANCE VERSUS DEPTH FOR FIELD SITES

The granular material located at depths of 3 to 5 ft at the Richmond site had relative states ranging from dense to medium. From depths of 5 to 16 ft, the consistency of the subgrade increased from stiff to very stiff. Below 16 ft to the end of the exploration depth, the soils were hard.

The materials at the Aberdeen site were primarily granular, with some zones containing varying amounts of silt. From 2 to 7 ft, the relative states of the soil decreased from medium-dense to loose. A uniformly loose zone was located from depths of 7 to 13 ft. The sandy material below 13 ft and extending to the end of the boring depth could be classified as medium.

### 7.3.2 Cone Penetration Tests

The cone penetration resistances for the four field sites are shown in Figure 49 as a function of depth. The values given represent the average cone resistances from 8 to 11 tests per site. Cone penetration through the upper few feet of the track foundations was not possible due to the very dense nature of the ballast and granular materials. Thus it was necessary to auger through these materials before cone soundings could begin.

The CPT values for the Streator wood and concrete sections were again similar, although shifted vertically due to the subsurface stratifications. The trends shown for the SPT tests at Streator can be clearly correlated to the changes in cone resistance measured at these site.

The cone resistances at the Richmond site also followed the trends identified by the SPT. The cone resistances tended to increase with depth. The cone tests identified a zone of stiffer materials at a depth of about 15 ft, followed by a reduction in tip resistance that was not detected using the SPT. However, both the SPT and CPT detected a hard zone at a depth of about 18 ft.

The depth at which SPT tests were initiated at the Aberdeen site was approximately 2.5 ft below the top of the cross ties. As previously stated, cone penetration through the upper 5 ft of the Aberdeen foundation was not possible because of the dense nature of the upper zone of soil. The CPT identified a more gradually increasing resistance to penetration than did the SPT, although the general subsurface profiles explored by each method showed similar results.

At present, there are no well-defined general correlations between cone resistances,  $q_c$ , and soil consistencies or relative states, although considerable effort is being made to develop these relationships [17].

### 7.3.3 Water Content and Atterberg Limits

The variations in natural water content and the Atterberg liquid and plastic limits for the four field sites evaluated are shown in Figure 50. The moisture content in the upper few feet of the formations were very low, even though all the ballast sections were fouled.

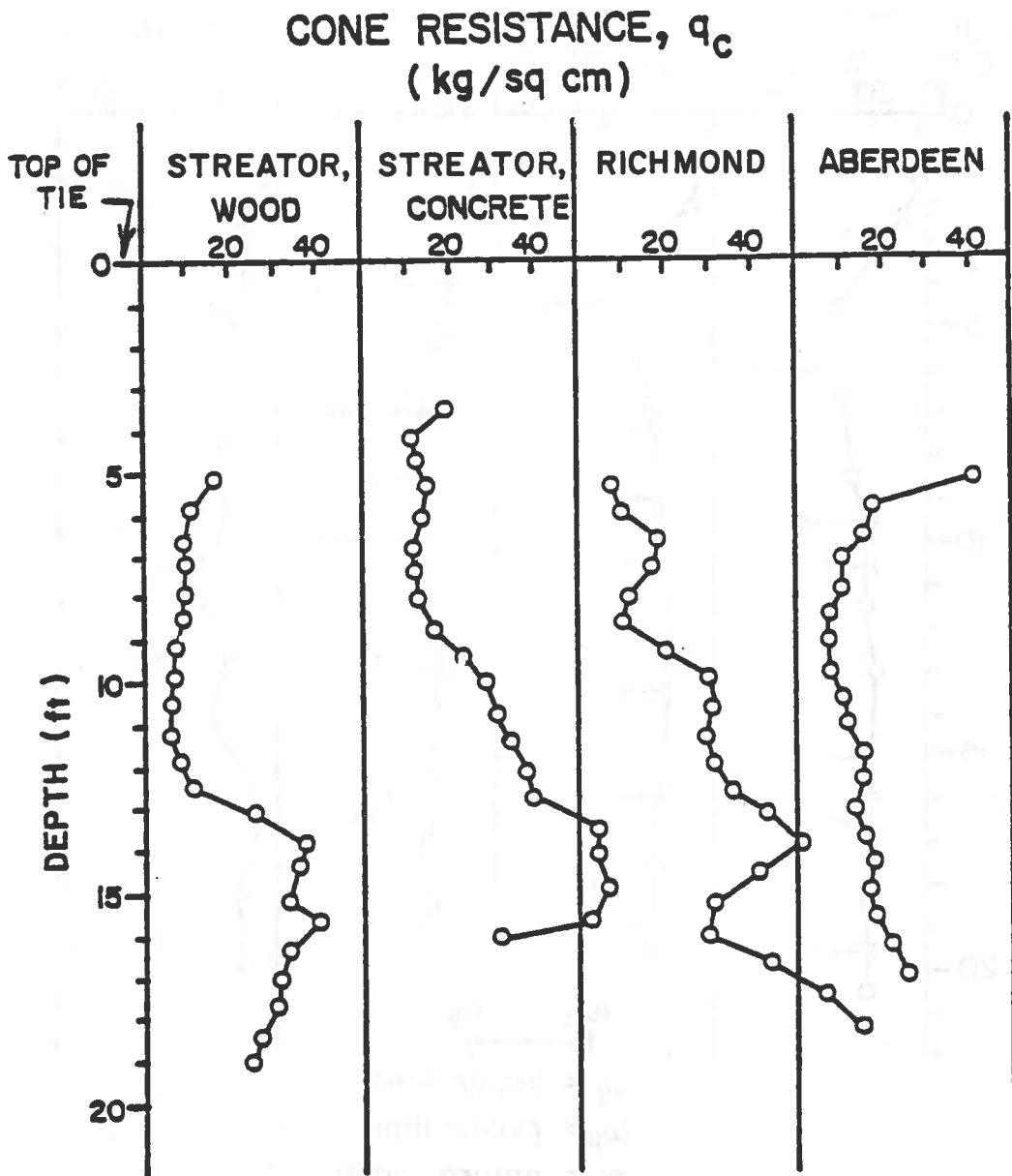


FIGURE 49. CONE RESISTANCE VERSUS DEPTH FOR FIELD SITES

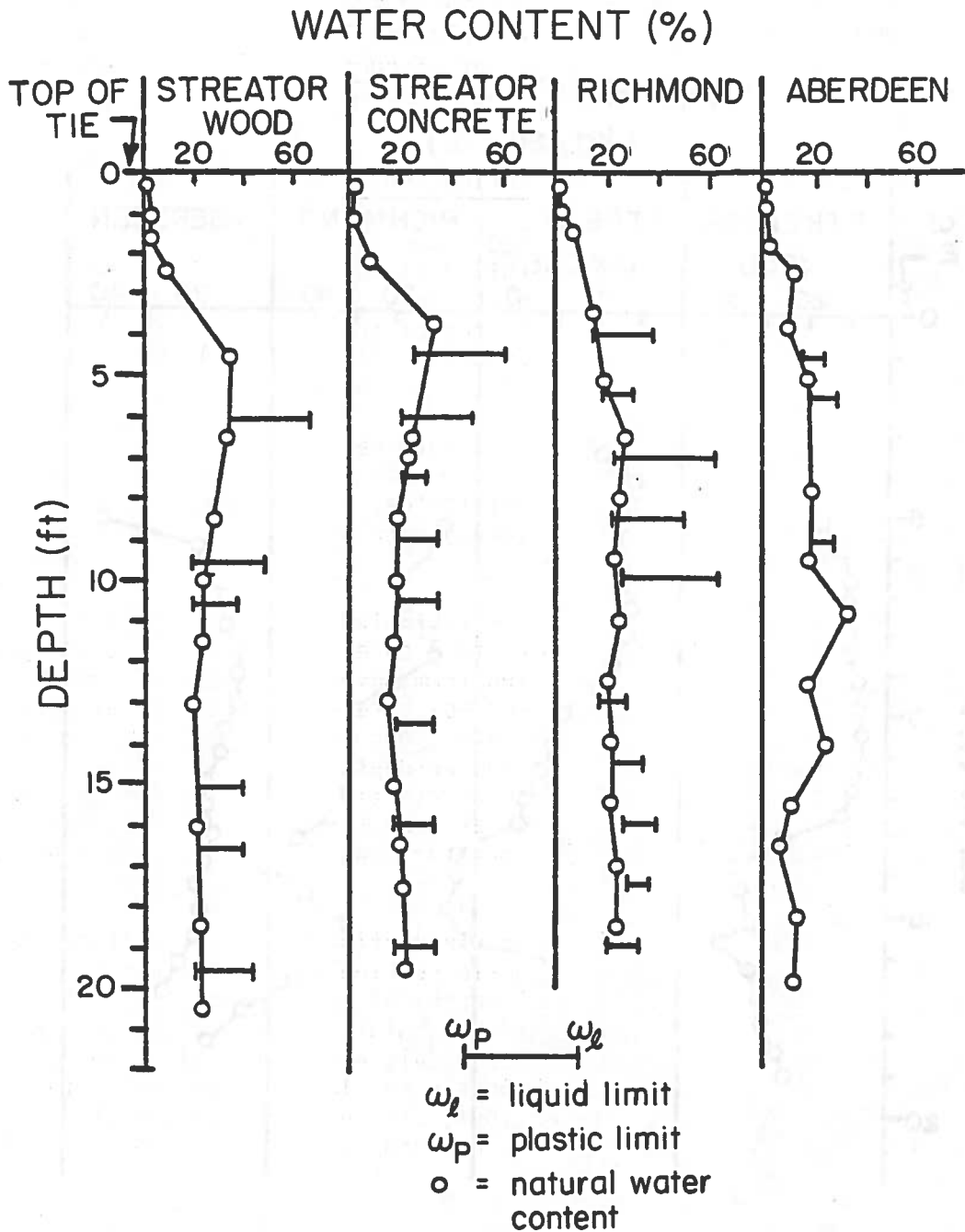


FIGURE 50. WATER CONTENT AND ATTERBERG LIMITS VERSUS DEPTH FOR FIELD SITES

Moisture content and Atterberg limits alone are not sufficient to define specific engineering properties, since soil behavior is a function of moisture content, soil type, and density or void ratio. However, some general trends at the field sites could be identified. The first was the similarity between the adjacent track sections at Streator, as previously noted. Also, the natural moisture content for all of the soils containing significant amounts of plastic fines were at or very close to the plastic limits. This would indicate a low potential for the development of continued excessive subgrade deformations.

#### 7.4 Moisture Instrumentation and Weather Data

Six electronic moisture sensors, patterned after the prototypes developed by Selig and Wobschall [18] [19], were installed at each field site to monitor the variations in moisture that occurred at the top of subgrade. The depths of installation for the sensors below the top of the ties were 18, 25, 20 and 29 in. for the Streator wood, Streator concrete, Richmond, and Aberdeen sites, respectively.

The field measurements with the embedded sensors were taken at weekly intervals by persons residing near each field site using a remote readout device. Weather data in the form of monthly climatological reports from the National Oceanic and Atmospheric Administration (NOAA) were used to supplement the moisture sensor readings.

The reduced data from the moisture sensors implanted at the Streator wood and concrete tie sections, along with the rainfall data for those sites, are shown in Figure 51. These data cover the period from November 1979 to December 1981. This figure shows that the subgrade moisture content at the Streator concrete tie section was consistently greater than that in the Streator wood tie section. This could be due to the greater depth of burial (25 vs. 18 in. below top of tie) of the sensors in the concrete tie section. Reference to Figure 50 shows that the moisture content at a depth of about 2 ft in the Streator concrete section initially was greater than the moisture content at 1.5 ft in the wood tie section.

The moisture content in the Streator wood tie section appeared to fluctuate over a larger range than in the concrete tie section. This could also have been caused by the differences in burial depths of the sensors. During the first year of the measurements, the trends in moisture content between the wood and concrete sections were almost identical, except for an offset of about 4 percent. The readings in the wood tie section became more variable from about February 1981 until December 1981, although they were still consistently lower than the subgrade moisture contents in the concrete tie section.

The subgrade moisture contents and rainfall for the Richmond and Aberdeen sites are shown in Figure 52. The moisture content in the trackbed at a depth of 20 in. at the Richmond site remained constant at 8.1 percent for the duration of the monitoring period, despite the significant amounts of rainfall shown. There were virtually no variations in the moisture contents monitored

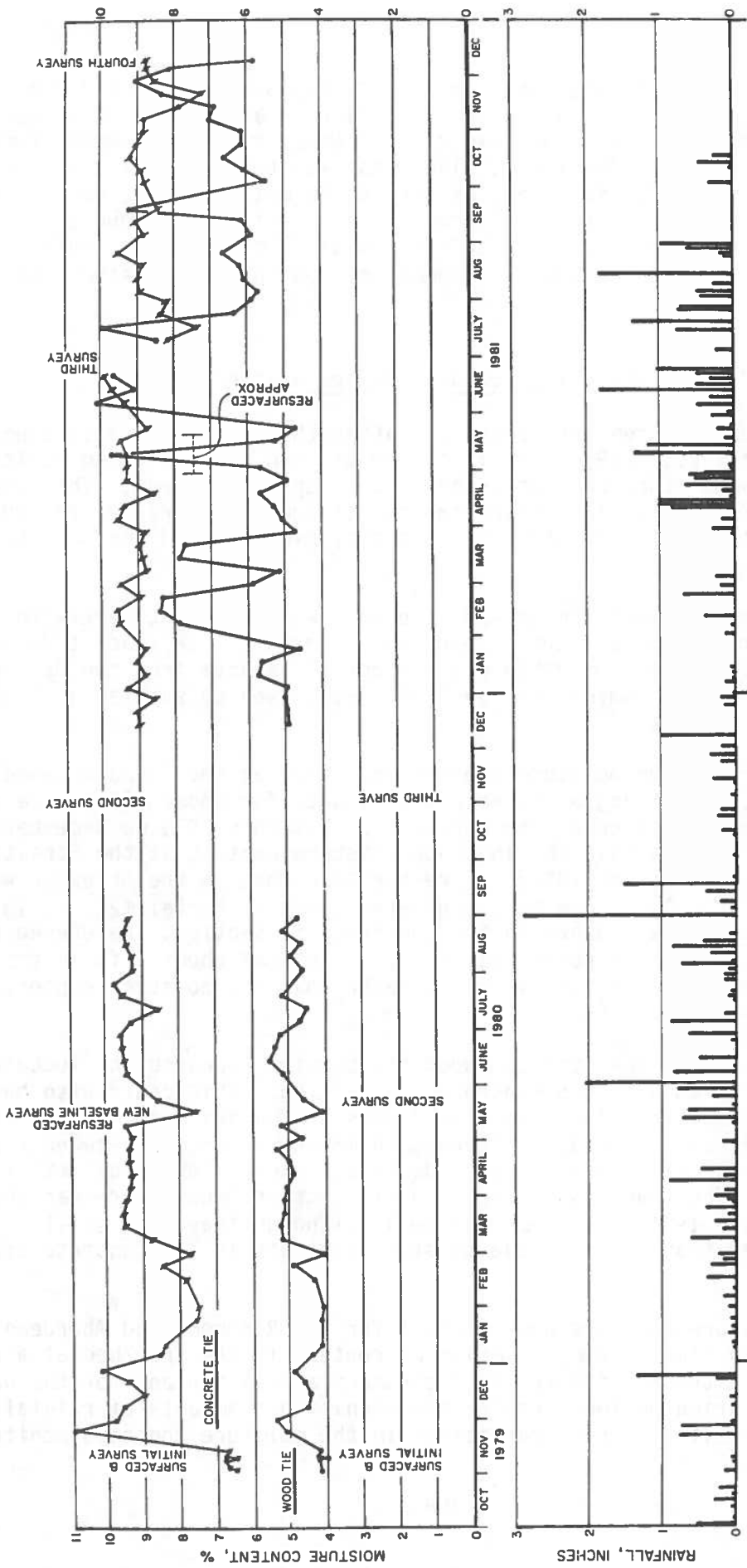


FIGURE 51. MOISTURE CONTENT AND RAINFALL DATA FROM STREATOR

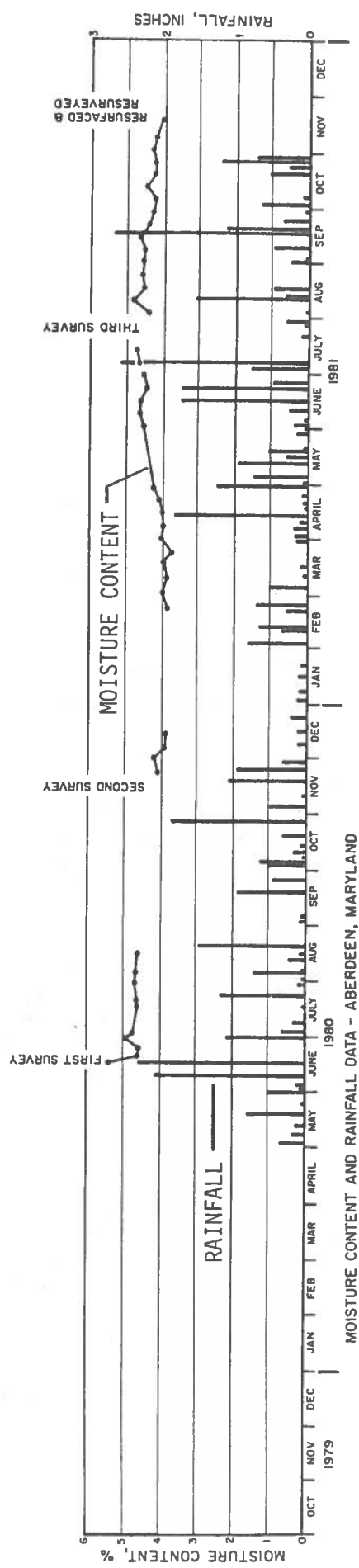
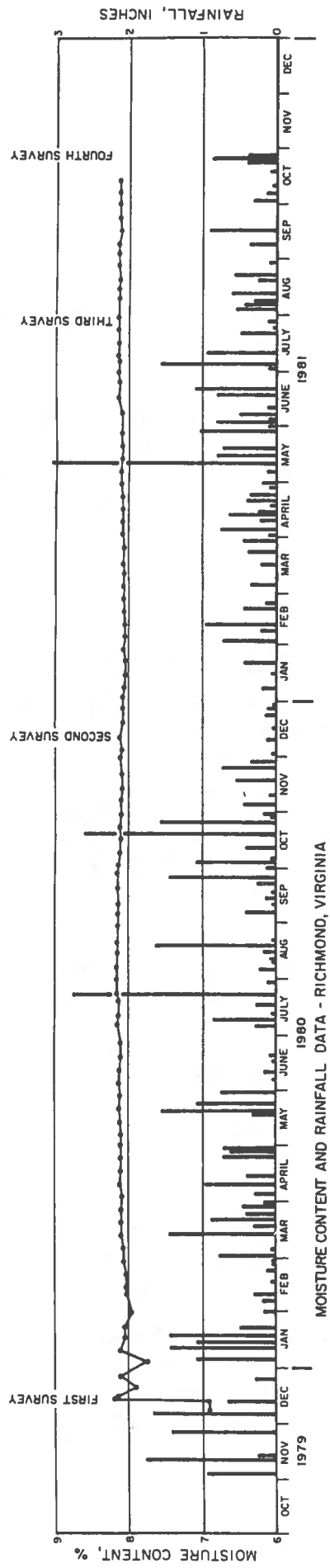


FIGURE 52. MOISTURE CONTENT AND RAINFALL DATA FROM ABERDEEN AND RICHMOND

over this 2-year period. A possible explanation of this is that the very compact, heavily fouled ballast conditions effectively served as a seal for the upper subgrade zone, permitting no downward migration of the water entering the ballast.

The moisture content at a depth of 29 in. at the Aberdeen site also showed only slight variations from the period of June 1980 to December 1981. The average moisture content was about 4.5 percent and independent of rainfall with a range of only about  $\pm 0.5$  percent. This may be attributed to both the depth of burial and the degree of fouling evident in the trackbed.

The cumulative amounts of precipitation recorded at the field sites were also recorded. The seasonal trends for the field sites were in very close agreement. A conclusion drawn from the cumulative rainfall data was that there appeared to be no significant differences in the amounts of precipitation, on a seasonal and long-term basis, between any of the sites. The rates of precipitation accumulation over periods from January to October were the same for each of the sites. The decreases in precipitation accumulation rates from October to January were also similar.

### 7.5 Laboratory Stress-Strain and Strength Testing

Ballast and subgrade samples recovered from the field sites were tested to determine elastic properties and deformation behavior. The results of these tests were used in the prediction of the sites' vertical track moduli and permanent settlement. Resilient moduli values for the ballast materials were determined based upon repeated load triaxial tests. These tests were performed using constant-amplitude and variable-amplitude repeated load conditions, as well as loadings incorporating shear stress reversal. The resilient moduli measurements along with the resulting inelastic behaviors are discussed in detail in Volume II.

A new laboratory testing technique was developed that was intended to simulate field behavior of the ballast. This ballast box apparatus, shown in Figure 53, was used to investigate both the permanent deformation behavior of the ballast and to measure the residual, horizontal stresses that build up due to repeated loadings. The results of these tests indicated that large residual, horizontal compressive stresses build up in ballast within the first few cycles of loading. These residual stresses can have a large effect on the resilient modulus of the ballast.

The residual, horizontal stresses also appear to play an important role in tie migration and may explain the mechanism of tie skewing. For example, during a related study near the test zone at Aberdeen, sixty consecutive ties were replaced with new ties to study tie cracking. On six-week intervals or more, alternate cribs were opened at both railseats to allow for inspection for flexural cracks. They were then refilled with ballast immediately after inspection. After the third inspection (the same alternate cribs were opened each time), the ties had migrated toward each other about two inches in the direction of the opened cribs. This would indicate that the unopened cribs had built up sufficient residual stress prior to each inspection to cause the



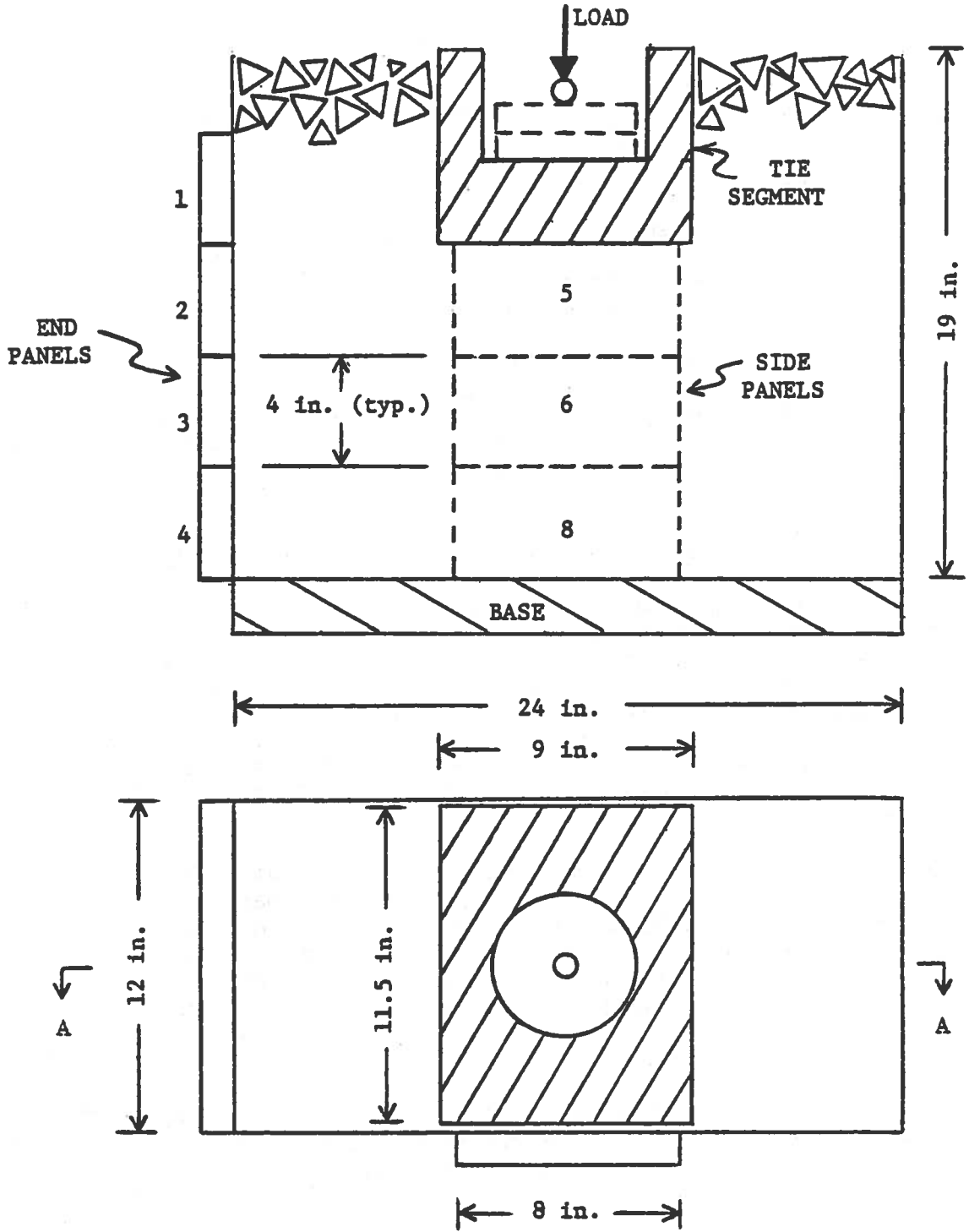


FIGURE 53. BALLAST BOX TEST APPARATUS

ties to move toward the uncompacted cribs after inspection, until equilibrium was achieved.

Similar tie movements were observed at Streator-concrete after the damaged ties were replaced, with some ties being up to six inches from their original positions, along with some skewing. A variety of other causes may, however, have contributed to this case, including unintentional movement caused by the tamper.

Another phenomenon which may be affected by the build-up of residual, horizontal compressive stresses is the relationship between ballast shoulder width and track roughness. Studies at FAST showed the surprising result that wider ballast shoulders help maintain smoother track surface [20]. This may indicate that the residual stresses in the ballast layer are inherently stabilizing and that wider shoulders help sustain higher residual stresses.

There are also indications that the loss in lateral tie resistance after maintenance, shown previously in Figure 47, may be affected by the loss of confinement provided by the crib ballast. Detailed descriptions of the ballast box test results and the implications on the predicted track settlements are given in Volume II.

## 8.0 COMPONENT PERFORMANCE

The long-term response of the ties and fasteners to the combined effects of traffic and environment were evaluated by visual inspections. "Top inspections," which are fairly easy to perform and do not disturb the test sections have been performed routinely by the railroads and other interested groups since these sites were built. To maintain continuity, Mr. John Weber, Consultant and a recognized expert in concrete ties, performed most of these inspections in this project. The corresponding summaries of these top inspections are primarily intended to aid in qualifying the relative condition of the components at each site. A rigorous correlation with FAST components was not possible because of the relatively short time interval, short test zones, and small populations of components available and the random and mostly unknown degree of maintenance which was performed at each revenue site. Component tests at FAST, as well as extensive inspections on the Northeast Corridor, have shown that performance indices are often defined by only one or two percent failures. Test sections on the order of one-quarter-mile long would be more appropriate for these failure levels. In addition, some indices require higher degrees of curvature than were available for the tests.

On the other hand, open crib inspections, when combined with newly developed techniques to identify very small flexural cracks under the rail seats, are fundamental to this correlation study, particularly because of the corresponding measurement of dynamic loads.

### 8.1 Rail Seat Flexural Cracks

Visual inspection for cracks has been a standard procedure for determining the condition of concrete ties. Flexural cracks in the rail seat region as well as in the tie center are generally an indication of tie loading greater than design loads. Other types of cracks may be related to factors such as manufacturing defects, maintenance equipment (procedures) or dragging equipment impacts. Of particular interest in this discussion are the transverse rail seat cracks which generally range from 1 to 6 in. long extending from the bottom surface of the tie as shown in Figure 54. In more advanced cases, ties can have cracks extending up to the top surface after branching out toward the fastener shoulders on either side of the rail seat.

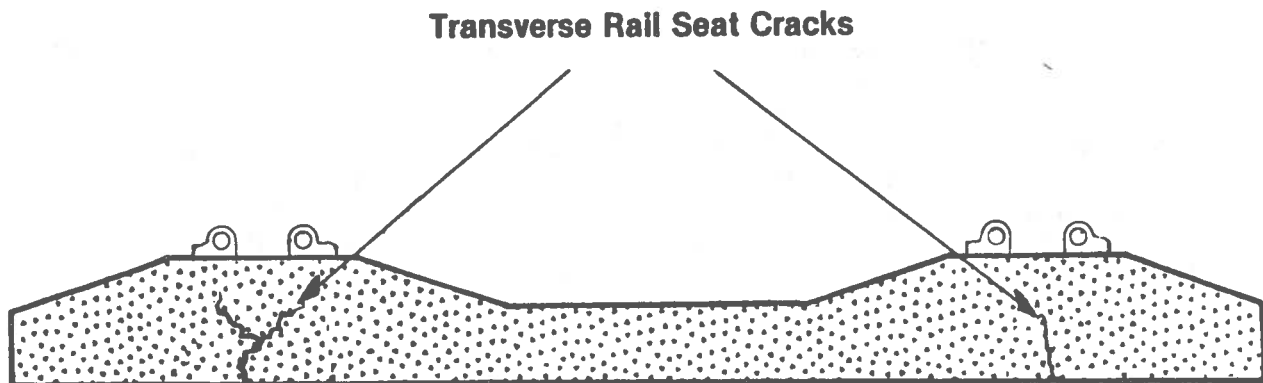


FIGURE 54. CONCRETE TIE TRANSVERSE RAIL SEAT CRACKS

In June 1980 while data were being acquired at the Aberdeen test site, an improved technique was used for the first time to aid in visually inspecting for cracks in the concrete ties. After experimenting with a variety of liquids with different vapor pressures, three were adopted for use, depending on the temperatures of the ambient air and the tie surface being inspected. At the colder temperatures, up to about 50 to 60 degrees F, Freon TF in aerosol cans was used. For moderate to warm conditions, ethyl alcohol was used; and at higher temperatures, isopropyl alcohol or even water provided the best evaporation rate.

The technique for enhancing the crack visibility first required cleaning the area using a rag wet with the inspecting liquid. Then after the surface is clean and dry an initial "unaided" check can be performed, or the enhancing liquid can be applied by spraying (via squeeze bottle or aerosol can) the entire region to be inspected. This is typically no larger than a 6 in. by 8 in. area at one time. It is important to determine an optimum amount of fluid to be applied such that the fluid has an opportunity to soak into any cracks that may exist. Excess fluid can be wiped off the surface with a clean, dry rag. If the proper fluid has been used, it will quickly evaporate off the surface of the concrete leaving the crack enhanced by the dark line generated by the fluid migrating back to the surface. Too slow an evaporation rate seems to draw out the fluid in the crack at almost the same rate as the surface material, while too rapid a rate will make it difficult to spot the crack. If any cracks are observed, the process can be repeated many times if necessary to verify their locations and lengths.

As discussed earlier, once a crack travels up beyond the neutral axis of the tie it will tend to branch out. It is often very difficult to trace exactly the crack in the "branch," but occasionally the crack can be located on the upper corner of the tie and followed back toward the base of the branch. The upper crack may have been generated independently from a reverse bending load, however, and should not necessarily be assumed as "growing" from the lower branch.

Variations of this inspection technique include the use of a minute amount of dye in the fluid to leave a more permanent trace of the crack. The success of this is in part affected by the quality of the surface of the concrete. If minute surface cracks and pits are too numerous, then the flexural crack may be partially obscured.

Certainly, cracks were made visible using this technique which would not previously have been detected. The original visual inspection at Aberdeen showed that over 70 percent of the rail seats were cracked after only 35 MGT of total traffic. Using this technique at the other sites allowed for a consistent set of statistics which revealed considerably more cracked ties than was previously anticipated considering that the results from FAST had shown no rail seat cracks after 450 MGT. A summary of the most recent inspections at each site is shown in Table 6. Note that at Aberdeen, the percentage of cracked rail seats increased to over 90 percent after an additional year of traffic increased the total tonnage to 60 MGT.

TABLE 6. SUMMARY OF CRACKED TIES

| LOCATION           | NO. INSPECTED | NO. CRACKED | % CRACKED | MGT | TRAFFIC LOADS                   |
|--------------------|---------------|-------------|-----------|-----|---------------------------------|
| FAST               | ~ 600         | -0-         | -0-       | 425 | Heavy-No Flats                  |
| Streator (ATSF)    | 80            | 11          | 14        | 125 | Medium-Moderate Flats           |
| Richmond (Chessie) | 80            | 44          | 55        | 220 | Heavy-Mod. To Severe Flats      |
| Aberdeen (AMTRAK)  | 60            | 56          | 93        | 60  | Light, Medium- High Speed Flats |
| Roanoke (N & W)    | 48            | 48          | 100       | 260 | Heavy, Severe Flats             |

While no crack on any tie inspected had progressed to the point where the tie was no longer functional, the history of concrete tie performance in this country indicates that these types of cracks may considerably shorten the 50-year life expectancy of the tie. As can be seen by the brief description of the traffic loads in Table 6, and the more detailed description in Section 5.1, severe flats and wheel irregularities on high-speed passenger trains correlate well with the occurrence of cracked ties. At FAST, where wheels are maintained in very good condition, no flexural cracks were observed in any of 600 ties inspected even though the nominal wheel loads are higher at FAST than at any other location.

## 8.2 Top-of-Tie Inspections and Fastener Performance

The following paragraphs summarize the tie surface and fastener inspections for each of the field sites.

Streator. The test section at Streator (Leeds) provided a unique opportunity to evaluate the consequences of a derailment-like incident on concrete ties while also negating several of the original plans for this site. Table 7 summarizes the top of tie and fastener conditions prior to the damage caused by the dragging side frame. Although a variety of minor surface cracks and spalls are noted, the track was generally in excellent condition. The note at the bottom of the table indicates that the non-sloping ends of the CC244C ties suffered considerably more chipping problems than the sloped ends of the RT-7S. These chips and spalls appear to be primarily cosmetic and are not likely to develop into a structural problem.

Table 8 is a partial description of the track condition a year after maintenance for the derailment damage was completed. However, some general observations may be more enlightening than are the statistics. Santa Fe chose to leave in all damaged ties which could still provide proper fastener support and most damage noted in Table 8 reflects this. All damaged ties were moderately to severely spalled on the east, field side of the north rail seat. As W. Autrey summarized in his address to the AREA [21], the CS-5 fastener in particular suffered the most damage due to the vulnerable position and relatively small cross section of the cast-in-stirrup shaped shoulder. Therefore, proportionately more of the ties with CS-5 fasteners were replaced.

After a year of weathering, a few ties which sustained impacts from the side frame showed additional degradation. Most of this appeared to be a freeze-thaw type of spalling beneath the original spalled areas. One or two ties were developing cracks that were initiated near the original spalls.

Several consequences of the maintenance performed were also noted. The track crew ignored the differences in types of ties and fastener systems within the test section as well as the variety available for replacement. There was no attempt made to match tie types when replacements were made, which left the site looking rather haphazard (much to the chagrin of the engineering department!). However, of more importance to this study, the subtle variations of fastener hardware within one generic type (Pandrol) were mixed between older and newer ties, resulting in possible overstressed clips or reduced toe loads

TABLE 7. SUMMARY OF THE TIE SURFACE AND FASTENER INSPECTION AT STREATOR, 11/2/79

TOTAL NO. OF TIES INSPECTED = 400

|                                 | South Rail |            |            | North Rail |         |
|---------------------------------|------------|------------|------------|------------|---------|
| Longitudinal Tie Surface Cracks | 40         |            |            | 51         |         |
| Surface Spalls or Chips         | Tie End    | Rail Seat  | Tie Center | Rail Seat  | Tie End |
|                                 | 103        | 94         | 7          | 96         | 69      |
| Pads - Dislocated               | 0          |            |            | 2          |         |
| Damaged                         | 0          |            |            | 2          |         |
| Fastener Clips                  | Field Side | Gauge Side | Field Side | Gauge Side |         |
| Dislocated                      | 0          | 0          | 0          | 1          |         |
| Shoulders Worn by Clips         | 8          | 6          | 10         | 6          |         |
| Insulators                      |            |            |            |            |         |
| Cracked                         | 1          | 7          | 1          | 1          |         |
| Broken                          | 0          | 13         | 0          | 11         |         |
| Upside Down                     | 0          | 0          | 1          | 0          |         |
| Plastic Part Broken             | 1          | 2          | 0          | 1          |         |

Note:

- 64 CC244C ties have damaged ends near north rail.
- 5 RT-7S ties have damaged ends near north rail.
- 10 RT-7S ties have damaged ends near south rail.
- 93 CC244C ties have damaged ends near south rail.

TABLE 8. SUMMARY OF TIE SURFACE AND FASTENER INSPECTION AT STREATOR, 4/22/81

TOTAL NO. OF TIES INSPECTED = 210

|                                 | North Rail | South Rail |
|---------------------------------|------------|------------|
| Longitudinal Tie Surface Cracks | 1          | 0          |
| Surface Spalls or Chips         | 107        |            |
| Pads - Dislocated               | 3          | 1          |
| Fastener Clips                  |            |            |
| Broken                          | 1          | 0          |
| Dislocated                      | 3          | 3          |
| Shoulders Worn by Clips         | 12         | 1          |
| Insulators                      |            |            |
| Broken                          | 32         | 4          |
| Dislocated                      | 13         | 4          |
| Plastic Part Broken             | 6          | 0          |

Note:

A good portion of the damage was due to a derailment.



and premature insulator failures. This emphasizes the difficulty for even "production" track such as that on the NEC to keep from inadvertently mixing hardware that long-term changes in hardware design will ultimately allow.

Tie skewing appeared at Streator only as a result of tie replacements. As discussed in Section 7.5, there is a tendency for a tie to migrate toward a recently opened crib, such that the replacement of a tie will generally cause the ties on either side to move toward it. Any differential movement will result in skewing. The final site inspection showed up to six-inch tie movements in the vicinity of several replaced ties. Note however, that some tie movement will occur during the surfacing operation, and this was not measured separately to distinguish it from in-service movement.

Richmond. Table 9 summarizes the top inspection performed at Richmond. Although this track had accumulated 150 MGT, it was generally in good to excellent condition. The CS-5 fasteners exhibited significantly more dislocated pads in the 0-1 inch range than the Pandrol, while no pads were considered damaged under the CS-5's compared to about seven percent under the Pandrol clips.

The most noticeable problem on this curved site is the rail wear. Chessie has had some difficulty with the performance of this rail resulting in more extensive gauge face wear and some corrugation. The corrugation appeared strongest, although barely perceptible, within the concrete tie section compared to the adjacent wood-tie section of the same 3 degree curve.

A more thorough physical inspection of tie tops and fasteners was performed by Chessie and reported to FRA.[22]

Aberdeen. The top inspections at Aberdeen summarized in Table 10 were performed on the 300 ties arbitrarily selected as the "test zone" for the survey-to-benchmark measurements. Within this zone were adjacent "buffer" rail segments attached with field welds into strings of continuous welded rail (CWR) on each rail. Amtrak installs safety straps across these welds and the bolts typically interfere with at least one of the fastener clips on the supporting ties. Normal field practice was to install the clip backwards if the bolt shank caused interference. These backwards clips have reduced toe loads and are more likely to fall out.

Frequent maintenance precludes any conclusions about trends in fastener performance which may otherwise be determined from these inspections. There is currently insufficient knowledge to explain the random occurrence of a single clip missing or broken or a dislocated insulator. Anomalies in the running surface correlate well with a high probability of one or more missing clips and recent walking inspections indicate an average of 0.8 percent missing clips in that region of the NEC.

Roanoke. There was no formal top inspection performed at Roanoke. However, a walking inspection of the site provided several observations.

The constant, downhill direction of traffic appears to cause pads to migrate with traffic, at least relative to tie motion. Average pad dislocation was on the order of 0.5 to 1.0 in.

The composite (two piece) Pandrol insulators tended to work downhill on the north side and uphill on the south side of each rail (downhill is east). Perhaps by coincidence, this orientation is consistent with the direction the clip moves when being installed. Many of the metal "ears" on the composite insulators had begun to move past their respective corners of the fastener shoulders.

Tie condition on the top surface was about average. A few ties had chips and spalls which were apparently caused by freeze-thaw action. Of the ties which had no ballast covering the top, center area (mostly CC244C's) many had readily visible flexural cracks. Some had two or three parallel cracks within the center region. Roughly 10 percent of the ties had center cracks based on the limited number of ties with exposed tops.

One CC244C tie was in an advanced stage of disintegration. The top layers of concrete had spalled away exposing the upper pre-stress wires in the center portion of the tie, although there was no loss of fastener integrity yet. There was no obvious cause for this tie failure such as signs of impact from dragging equipment or advanced center bending cracks. This tie was located however, in the general vicinity of the "rough spot" discussed in Section 3.5.

## 9.0 CORRELATIONS

The following section covers several areas where separate sources of information are compared to show either newly identified relationships such as the cracking of concrete ties versus the measured dynamic traffic loads, or predicted versus measured performance of the track structure such as vertical track settlement.

### 9.1 Tie Loads vs. Tie Cracking

As discussed in Section 8, a selection of concrete ties were inspected at all sites for cracks under the rail seats. For this correlation, however, the initial inspection at Streator and Richmond are excluded because the visual enhancement techniques were not used and would therefore bias the results. Additional data are included from another program [5] which was performed about one-half mile from the Aberdeen site on the same track. These data provide important information about the performance of newly installed ties with low accumulated tonnage.

The percentage of cracked rail seats versus accumulated tonnage are tabulated in Table 11 and plotted in Figure 55. Also tabulated and plotted are the percentages of rail seat bending moments above the cracking strength of the concrete ties, which were obtained in the dynamic measurements.

An empirical equation can be established to correlate the percentage of cracked rail seat regions and the percentage of rail seat bending moments above the cracking strength of the ties. Let

C = percentage of cracked rail seats;

N = total number of axles passing over ties;

B = percentage of rail seat bending moments above the cracking strength of concrete.

The increase in the percentage of cracked rail seats should be proportional to the increase in the percentage of the number of axles producing rail seat bending moments above the cracking strength of concrete. Hence:

$$dC \propto d(NB)/NB$$

Furthermore, the increase in the percentage of cracked rail seats should be proportional to the percentage of uncracked rail seats i.e.,

$$dC \propto (100-C)$$

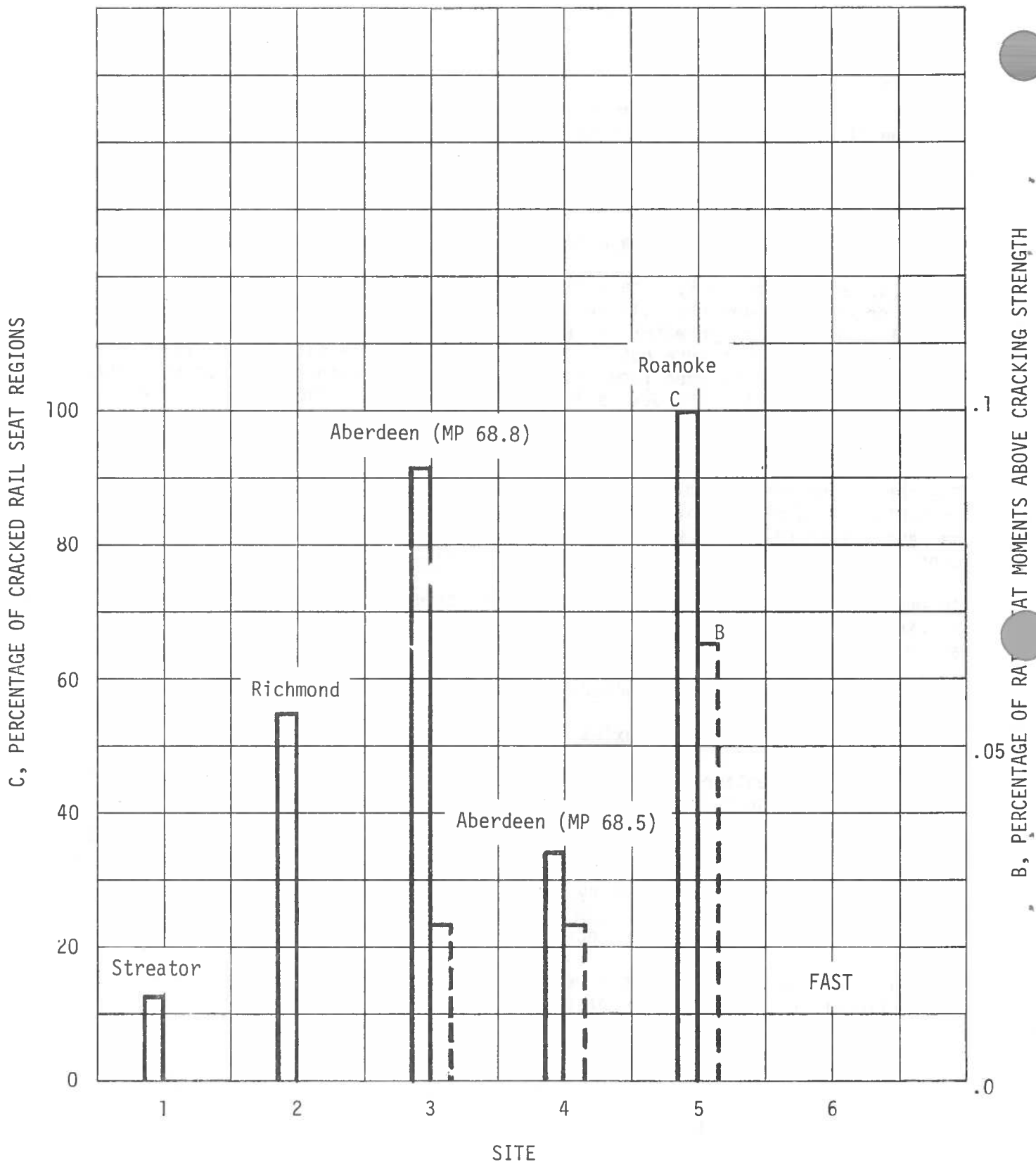


FIGURE 55. RESULTS OF FINAL INSPECTIONS FOR CONCRETE TIE CRACKS

Therefore,

$$\begin{aligned}dC &= K_1 d(NB) (100-C)/NB \\ \int dC/(100-C) &= K_1 \int d(NB)/NB \\ -\ln(100-C) &= K_1 \ln(NB) + K_2\end{aligned}\tag{Eq. 9.1}$$

where  $K_1$  and  $K_2$  are constants. A log-log plot of  $(100-C)$  versus  $(NB)$  at Aberdeen is shown in Figure 56.

In computing the percentage of cracked rail seat regions, we should be able to use any arbitrary crack length to define a crack as long as the same criterion is used consistently, i.e.,

$$-\ln(100-C) = K_{1n} \ln(NB) + K_{2n}\tag{Eq. 9.2}$$

where the subscript  $n$  denotes crack length criterion. The criterion used in Figure 56 is about one inch, the lower limit of detection. Plots with other criteria such as 4 or 6 inches should be straight lines parallel to the line in Figure 56. However, there are insufficient data to validate this.

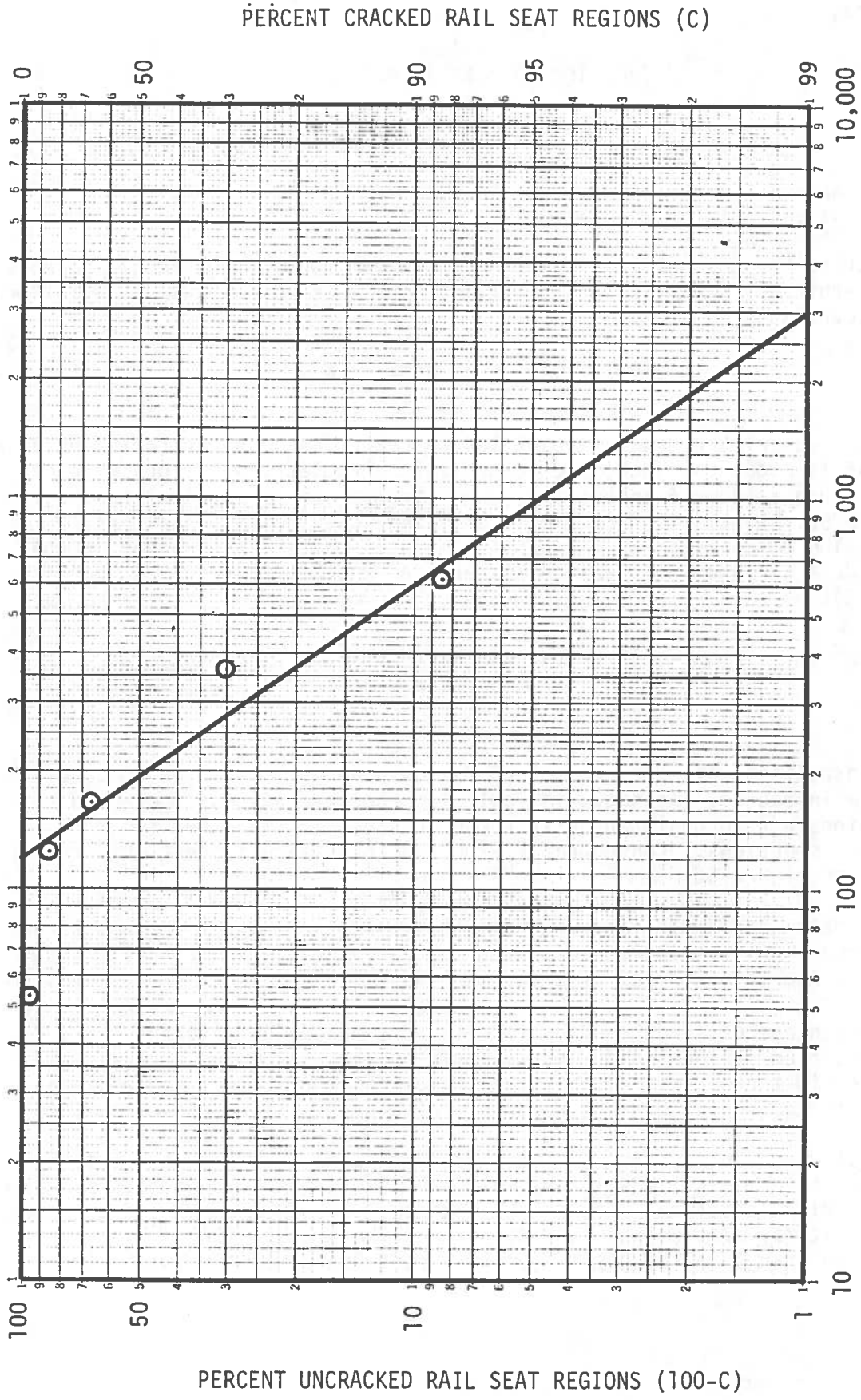
The computation of the total number of axles ( $N$ ) is based on the tonnage data ( $T$ ) and the mean static vertical wheel load ( $V$ ) from load data (Table 11):

$$N_{(\text{axles})} = T_{(\text{MGT})} \times 10^6 / V_{(\text{kips/wheel})} \times \frac{2 \text{ kips/ton}}{2 \text{ wheels/axle}}$$

In two inspections at Aberdeen (MP 68.8), only about 50% of the 30 concrete ties were inspected. As shown in Table 11, the percentages of cracked rail seat regions are inconsistent with those obtained in the other two more complete inspections. Consequently, the two incomplete inspections are not included in Figure 56.

The test data (Table 11) show that at Roanoke the rail seat regions were 100% cracked when  $(NB)$  was 6300. According to Figure 56, 99% of the rail seat regions at Aberdeen will be cracked when  $(NB)$  is 3000, which corresponds to 280 MGT. Table 11 also shows that at Streator and Richmond an extremely small percentage of large bending moments were measured. Although values were identified for inclusion in the table, there is limited statistical confidence in these data. Much larger populations of axle loads would be required to accurately characterize these low probability bending moments.

Conceptually, given the kind of load and crack data acquired at Aberdeen, the trends indicate the ability to estimate the tonnage at which all ties will be cracked. With additional data on the incidence of long cracks and ultimate strength, it may also be possible to predict the useful life of the ties, assuming no change in the population of impact loads seen by the ties.



NUMBER OF AXLES (NB)

FIGURE 56. NUMBER OF AXLES PRODUCING RAIL SEAT MOMENTS ABOVE CRACKING STRENGTH AT ABERDEEN

PERCENT UNCRACKED RAIL SEAT REGIONS (100-C)

PERCENT CRACKED RAIL SEAT REGIONS (C)

TABLE 11. RESULTS AND COMPUTATIONS FOR CONCRETE TIE CRACKS

| Site              | Date     | Percentage of Cracked Rail Seats C (%) | Percentage of Rail Seat Moments Above Cracking Strength B (%) | Tonnage T (MGT) | Mean Static Vertical Wheel Load V (KIPS) | Percentage of Uncracked Rail Seats 100-C (%) | Number of Axles Producing Rail Seat Moments Above Cracking Strength NB |
|-------------------|----------|--|---|-----------------|--|--|--|
| Streator          | 11/6/80  | 12.5                                   | 0.005   | 125             | 17                                       | 87.5   | 363  |
| Richmond          | 10/23/81 | 55.0                                   | 0.006   | 217             | 18                                       | 45.0   | 723  |
| Aberdeen (MP68.8) | 6/17/80  | 70.0                                   | 0.0235  | 34              | 22                                       | 30.0   | 363  |
|                   | 12/9/80  | 67.6*                                  | 0.0235  | 47              | 22                                       | 32.4   | 502  |
|                   | 4/2/81   | 96.8*                                  | 0.0235  | 53              | 22                                       | 3.2  | 566  |
|                   | 6/18/81  | 91.5                                   | 0.0235  | 57              | 22                                       | 8.5  | 609  |
| Aberdeen (MP68.5) | 12/8/80  | 4.2                                    | 0.0235  | 5.0             | 22                                       | 95.8   | 53   |
|                   | 4/2/81   | 15.0                                   | 0.0235  | 11.7            | 22                                       | 85.0   | 125  |
|                   | 6/18/81  | 34.2                                   | 0.0235  | 15.6            | 22                                       | 65.8   | 167  |
| Roanoke           | 5/81     | 100.0                                  | 0.0655  | 260             | 27                                       | 0.0  | 6307   |
| FAST              | 12/79    | 0.0                                    | 0   | 425             | 33                                       | 100.0  | 0  |

\* Only about 50% of 30 concrete ties were inspected.

Assume that a series of dynamic measurements at several sites was made for a sufficient time to produce the family of tie bending moments depicted in Figure 57a. Correlation of these load populations with crack lengths might produce a distribution of equal probability curves such as shown in Figure 57b. Or looking at it another way, population "e" could produce the family of curves in Figure 57b at successive accumulations of tonnage. In fact, the horizontal line along the minimum level of detection is the threshold from which the actual data plotted in Figure 56 were referenced.

## 9.2 Predicted vs. Measured Track Vertical Load-Deflection Response

Using procedures discussed in detail in Volume II, track vertical load-deflection response was predicted for Streator (Leeds) concrete and wood tie sites, Richmond, Aberdeen, and FAST, Section 22. The approach used was to combine the results of laboratory tests and physical states measured in the field to provide appropriate parametric values for running the computer model, GEOTRACK. Figure 58 summarizes the dimensions and material properties used to make the prediction. The specific load-deflection increment used for the prediction was the 6-to-30-kip interval previously shown in Table 3.

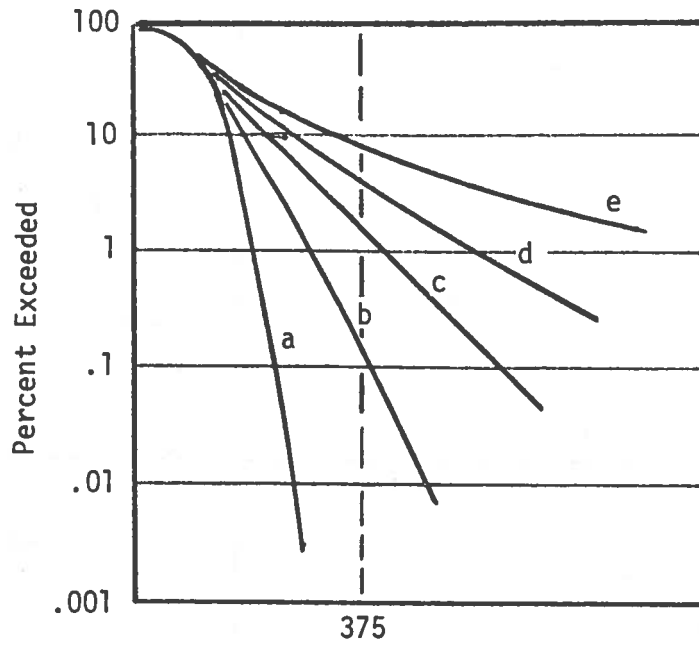
Figure 59 shows the results of the comparison of measured and predicted track deflection for the 6-to-30-kip load increment. The corresponding calculated values for track moduli, both predicted and measured, are shown in Figure 60. The success of the prediction is excellent for Aberdeen and Richmond and reasonable for Streator wood and concrete sections. However, both of the Streator site predictions underestimate the deflections, resulting in corresponding overestimation of the moduli. This is, however, a remarkable achievement considering the complexities of modeling soils behavior.

The measured and predicted values of track modulus are dependent on several factors, one of which is the support condition of the tie. These support conditions are a function of track settlement and maintenance effects. The support conditions would affect concrete and wood ties in a different fashion.

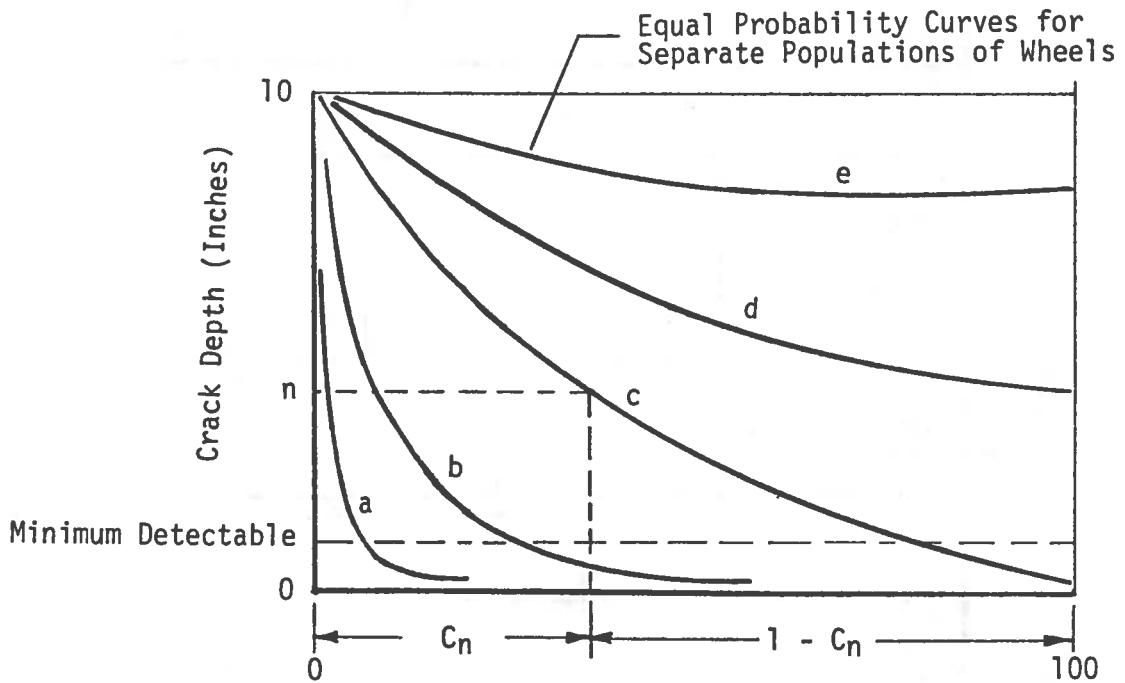
The GEOTRACK model used uniform properties throughout each layer, including the support and contact under all ties. The field plate load tests [2] showed that the ballast stiffness was not uniform under the ties, but was greater near the rail seat areas than under the tie centers. Furthermore, after the maintenance, the ballast physical state was more uniform than before maintenance. However, even uniform physical state or modulus does not result in uniform support conditions along the tie.

After the maintenance operation in which a high raise was given to the track, the ballast physical properties would be more uniform. However, the tamping and raise during the maintenance is done only near the rail seats, which could cause a gap near the center of the ties. This causes the actual load bearing areas to be near the rail seats because of the lack of contact near the centers. This increased load bearing near the rail seats would cause higher rail deflections directly under the applied load than would result from a continuously supported condition. The GEOTRACK model uses continuous contact between





(a) Tie Bending Moment (In-Kip)



(b) Percent Cracked Ties

FIGURE 57. CONCEPT FOR ESTIMATION OF TONNAGE AT WHICH ALL TIES WILL BE CRACKED

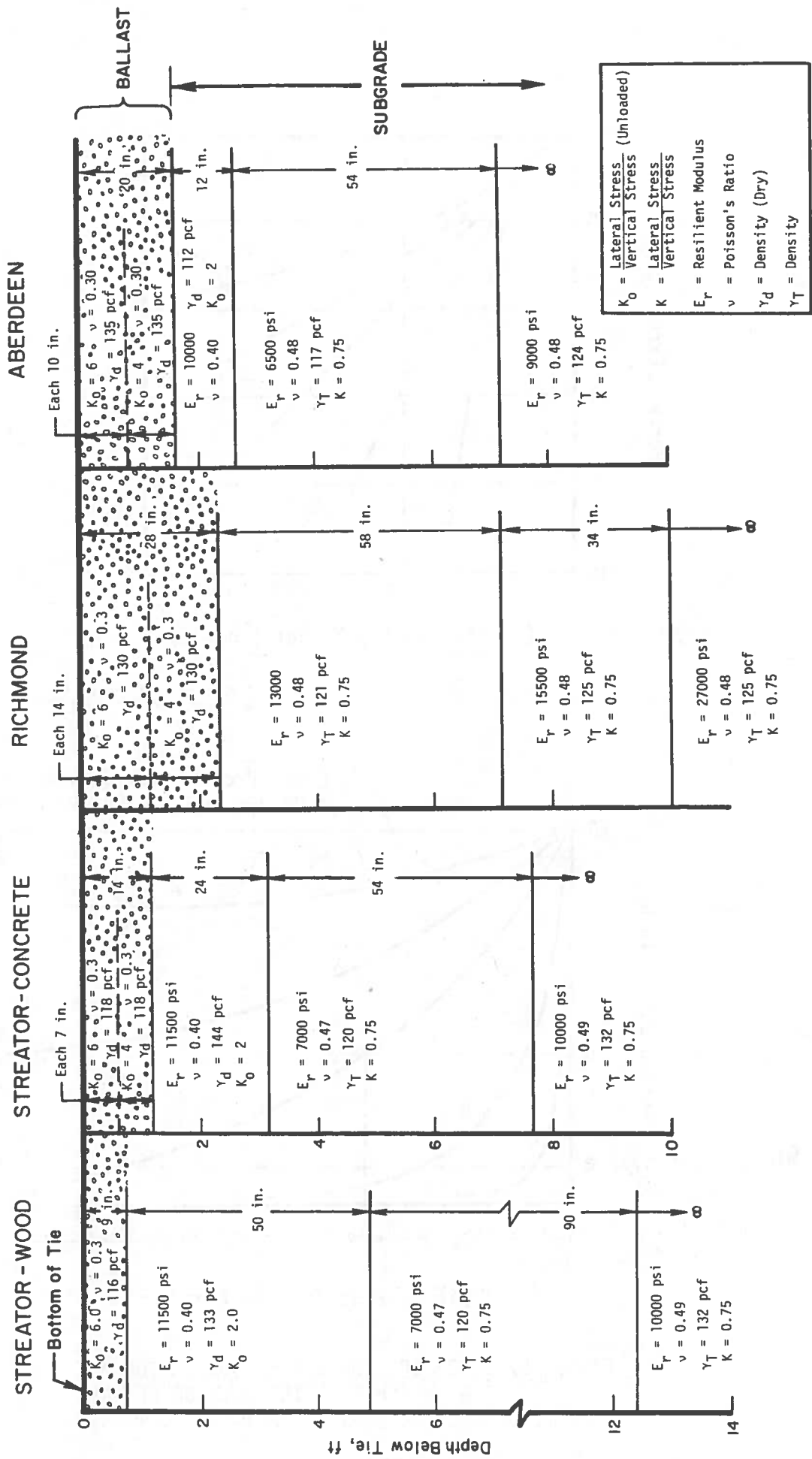


FIGURE 58. BALLAST AND SUBGRADE PROPERTIES USED FOR ANALYTICAL PREDICTIONS

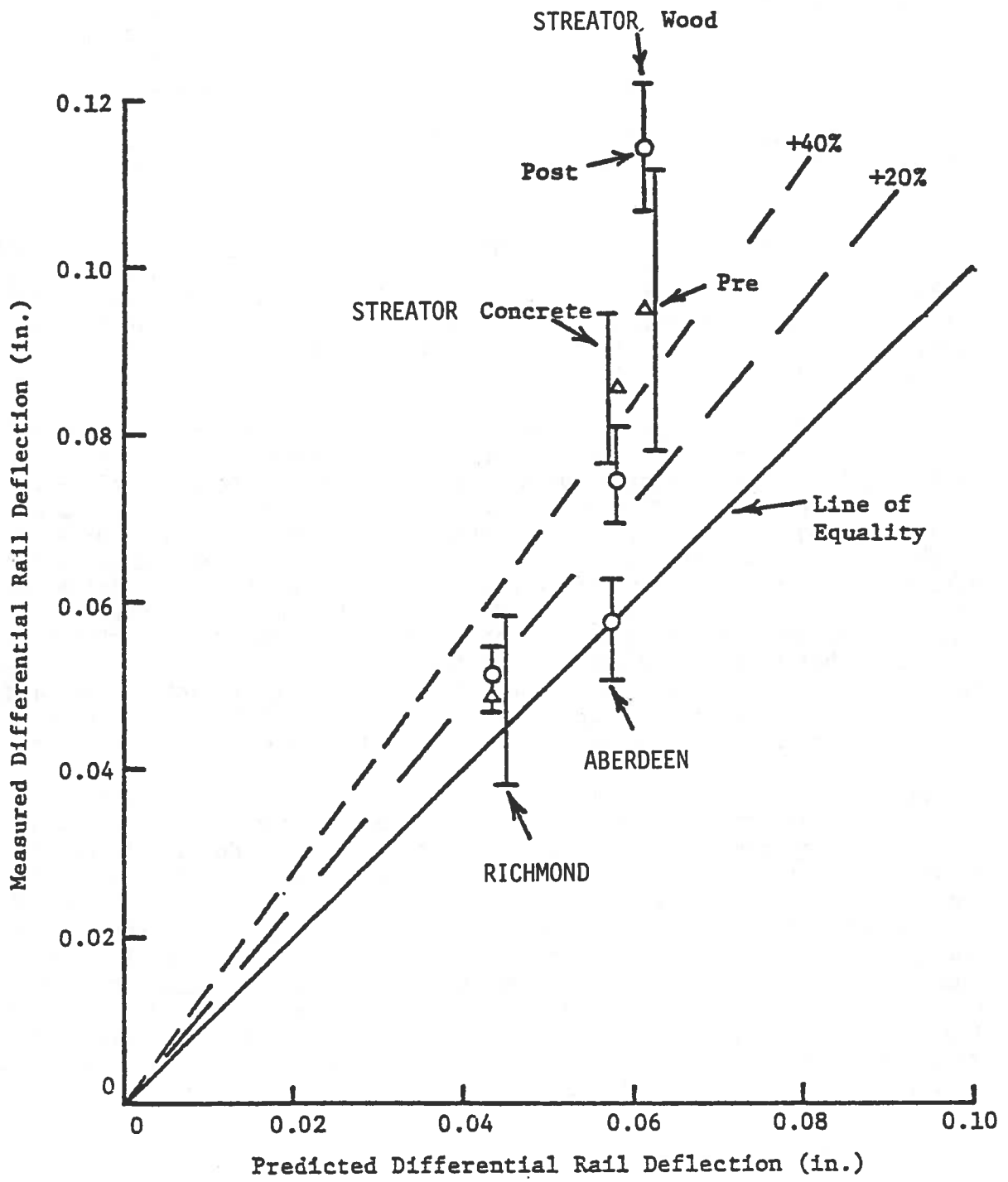


FIGURE 59. MEASURED VERSUS PREDICTED DIFFERENTIAL RAIL DEFLECTIONS FOR 6- TO 30-KIP LOAD RANGE

the tie directly under the applied vertical load and the ballast surface, leading to a lower rail deflection and higher track modulus than measured in the field after maintenance.

As traffic accumulates over the track, the ballast beneath the rail seats is recompacted and becomes stiffer, but the tie contact becomes continuous (at least above some initial load level). The more uniform support across the tie leads to a lower rail deflection and hence a higher track modulus. In the case of a small maintenance raise, the initial ballast physical states may be less uniform under the tie than after a large raise; however, the contact along the tie may be more continuous. This would result in a higher track modulus after a small raise than after a large raise, or at least not much change in the pre- and post-maintenance values.

In the case of centerbound track, a greater portion of the rail loads would be carried by the central portion of the ties. In this situation, as the applied loads increase, the wood ties would have a greater bending deflection prior to achieving contact with the ballast surface beneath the rails than the concrete ties, because the bending stiffness of concrete ties is about 4.5 to 6 times greater than that of wood ties.

The interactions between the variable ballast physical states, tie support conditions, and structural factors such as tie stiffness and rail size make generalizations about track modulus uncertain. This is particularly true since the degree and type of maintenance disturbance and traffic history of a site can change the ballast physical states in varying amounts. The scatter of the field measurements were such that there were no clear trends distinguishing the pre-maintenance track moduli values from the post-maintenance values. The predictions of track modulus using the GEOTRACK program are somewhat limited by the uniform layer property and full contact representations, and the inability to represent the maintenance factors for the field sites. For these reasons, variations between the measured and predicted track moduli values for the sites can be expected because of the variation in ballast properties and support conditions which were affected by the maintenance operations.

The possible effects of centerbinding and uniformity of support conditions beneath the tie bottom are not fully understood. However, these effects may not be a significant contributing factor to the track modulus values. Differences between the bending stiffnesses of the wood and concrete ties would also not result in large differences in track moduli. Since only 10% to 20% of the total track deformation occurs because of ballast compression (not including the above mentioned tie/ballast interface effects), the subgrade deflections appear to be much more important. Parametric studies indicate the subgrade contribution to track modulus should be about the same for wood and concrete ties. The FAST dynamic measurements of resilient subgrade deflection also showed no significant difference between the deflections in wood and concrete sections.

### 9.3 Correlation of Track Modulus With Ballast Depth

The track modulus values shown previously in Figure 60 were also evaluated to determine causes for the differences in absolute magnitude between the four sites. Part of the differences in absolute magnitude of the average field track modulus measurements can be explained in terms of the differences in the track substructures. The parametric study using the GEOTRACK model indicated that track modulus increased as ballast depth increased. The ballast profiles and the simplified layer characterizations used in the GEOTRACK analyses shown in Figure 58 show that the Streater wood section had only about 9 in. of ballast beneath the tie, whereas the Streater concrete section contained about 14 in. The Aberdeen site had 20 in. of ballast, and the ballast depth at Richmond was estimated to be 28 in. below the tie. This trend of increasing track modulus with increasing ballast depth for the field sites is clearly confirmed by the field measurements in Figure 61.

The track modulus is also influenced by the subgrade characteristics. As mentioned earlier, the GEOTRACK model indicates that the compression of the ballast layer accounts for about 10 to 20% of the total vertical elastic deflection of the track structure. The remainder of the total deflection is due to the compression of the subgrade materials. Furthermore, 25 to 40% of the subgrade elastic deformation indicated by GEOTRACK occurs below a depth of about 10 ft., even though the stresses below this depth are low [23]. This is in contrast to the inelastic (permanent) deformation which occurs mostly in the ballast and is responsible for track settlement.

### 9.4 Predicted vs. Measured Track Settlement

An important goal established at the beginning of this program was to attempt a prediction of vertical track settlement and compare that prediction to actual settlement at each of four revenue sites (excepting Roanoke) and at FAST, Section 22. The procedures for these predictions are discussed in detail in Volume II.

The goal was to follow the settlement process from the initial condition of freshly surfaced track to an advanced, traffic-consolidated state. As discussed in Volume II, permanent deformations or settlement resulting from maintenance (surfacing) are almost entirely restricted to the ballast layer. (This is assuming an old, established roadbed.)

The stress states were estimated using GEOTRACK. The layer profiles and divisions and subgrade moduli for the revenue sites were the same as used for the track modulus predictions shown previously in Figure 58. The layer divisions used for the FAST predictions consisted of two 7.5 in. ballast layers underlain by the silty sand subgrade material.

The resilient strain-shear stress ballast formulation, as described in Volume II, was used to characterize the ballast at all of the sites, and multiple-axle loading configurations were used to accommodate the synergistic influence of adjacent wheel loads. Because it was not practical to directly utilize the detailed descriptions of dynamic wheel loads discussed in Section 5 and shown

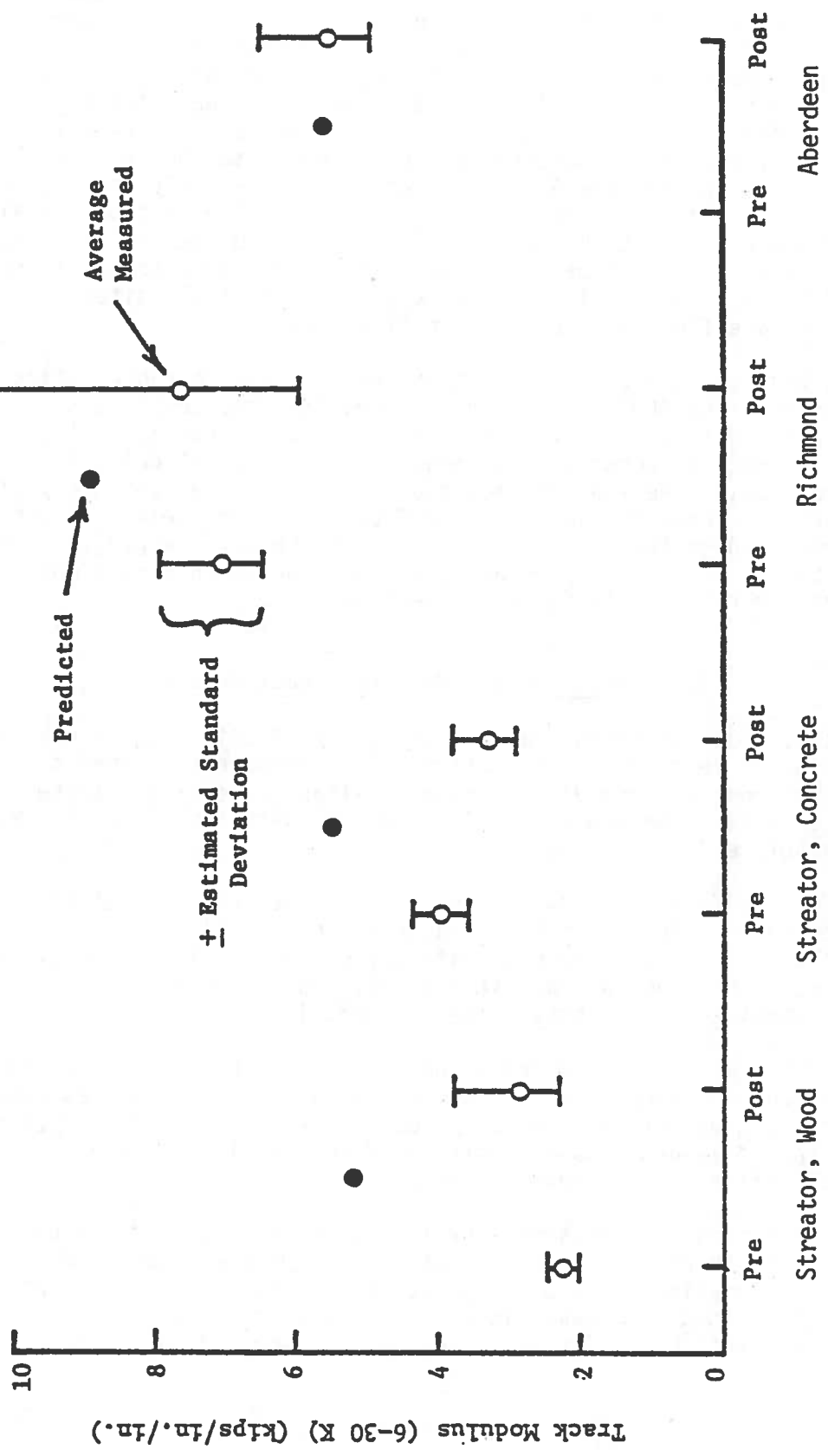


FIGURE 60. MEASURED AND PREDICTED TRACK MODULI FOR REVENUE FIELD SITES, 6- TO 30-KIP LOAD RANGE

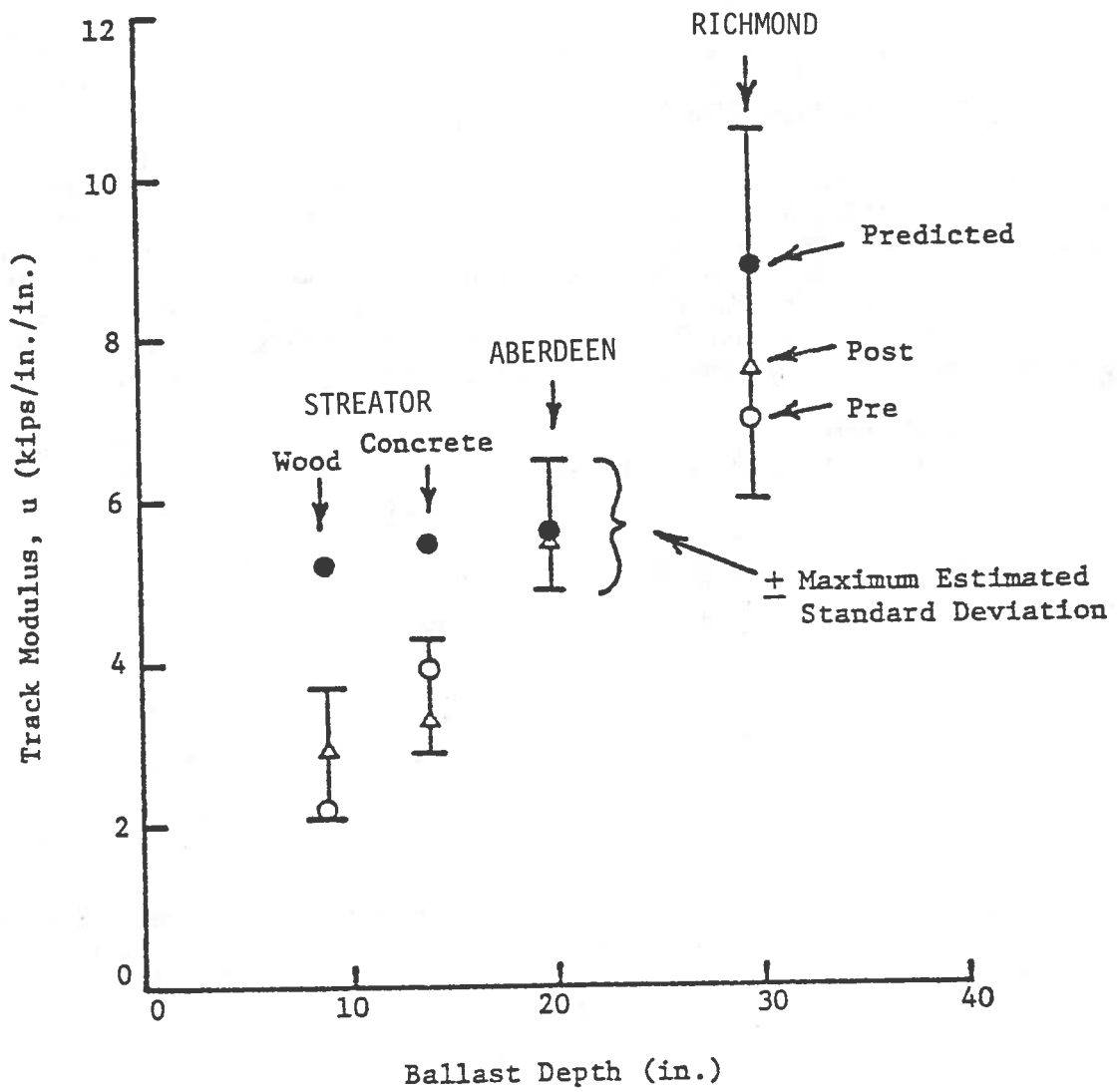


FIGURE 61. BALLAST DEPTH VERSUS TRACK MODULUS FOR REVENUE FIELD SITES

in Figure 19, representative loads at the 50, 10, 1, and 0.1 percent load exceeded levels were selected to characterize the traffic at each site. These were shown previously in Table 2. The number of associated load cycles at each load level were determined for each MGT of traffic by estimating the average number of axles per MGT. Ballast and subgrade dynamic data have previously shown [24] that the effective load cycle for the ballast includes both axles on one truck. At greater depths, the stress distributions overlap sufficiently that all four axles at adjacent ends of two cars represent one load cycle. This effect was included in the prediction process.

Variations in the assumed stress paths along with the consideration of shear stress reversals discussed briefly in Section 7 and thoroughly in Volume II provided four separate stress paths for consideration in the prediction process. Once the stress paths had been established for the various combinations of dynamic wheel loadings, the next operation was to determine the strains that would be expected to develop due to repeated applications of the prescribed stresses. This was done using the laboratory results from the various test series described in Section 7 and Volume II.

The permanent deformations that accumulate in ballast due to repeated application of vertical stresses were shown to be related, in general, to the permanent strain or deformation that occurred in the first cycle of load. Thus, the first step in predicting the track deformations was to determine the strains that are expected to develop from the first load cycle. Since the stress paths for the ballast layers involve shear stress reversals, the accurate determination of these first cycle strains is difficult.

For each of the field site predictions, the first cycle strains were estimated from the curves shown in Figure 62 for four stress ratios. These are:

| <u>Ratio</u>   | <u>Stress Path</u> | <u>Strain Curve</u>         |
|----------------|--------------------|-----------------------------|
| $q_{max}/q_f$  | CB                 | One-Way Uncompacted         |
| $q_{max}/q_f$  | DE                 | One-Way Uncompacted         |
| $\Delta q/q_f$ | CB                 | Uncompacted Stress Reversal |
| $\Delta q/q_f$ | DE                 | Uncompacted Stress Reversal |

The rates of strain accumulation with repeated load cycles were determined with further laboratory tests along with pertinent ballast constants as discussed in Volume II. These soil constants along with the first cycle strains were used in the equation

$$\epsilon_N = \epsilon_1 (1 + C \log N) \quad (\text{Eq. 9.3})$$

where  $\epsilon_N$  is the permanent axial strain at the  $N^{\text{th}}$  cycle

$\epsilon_1$  is the permanent axial strain developed due to the first



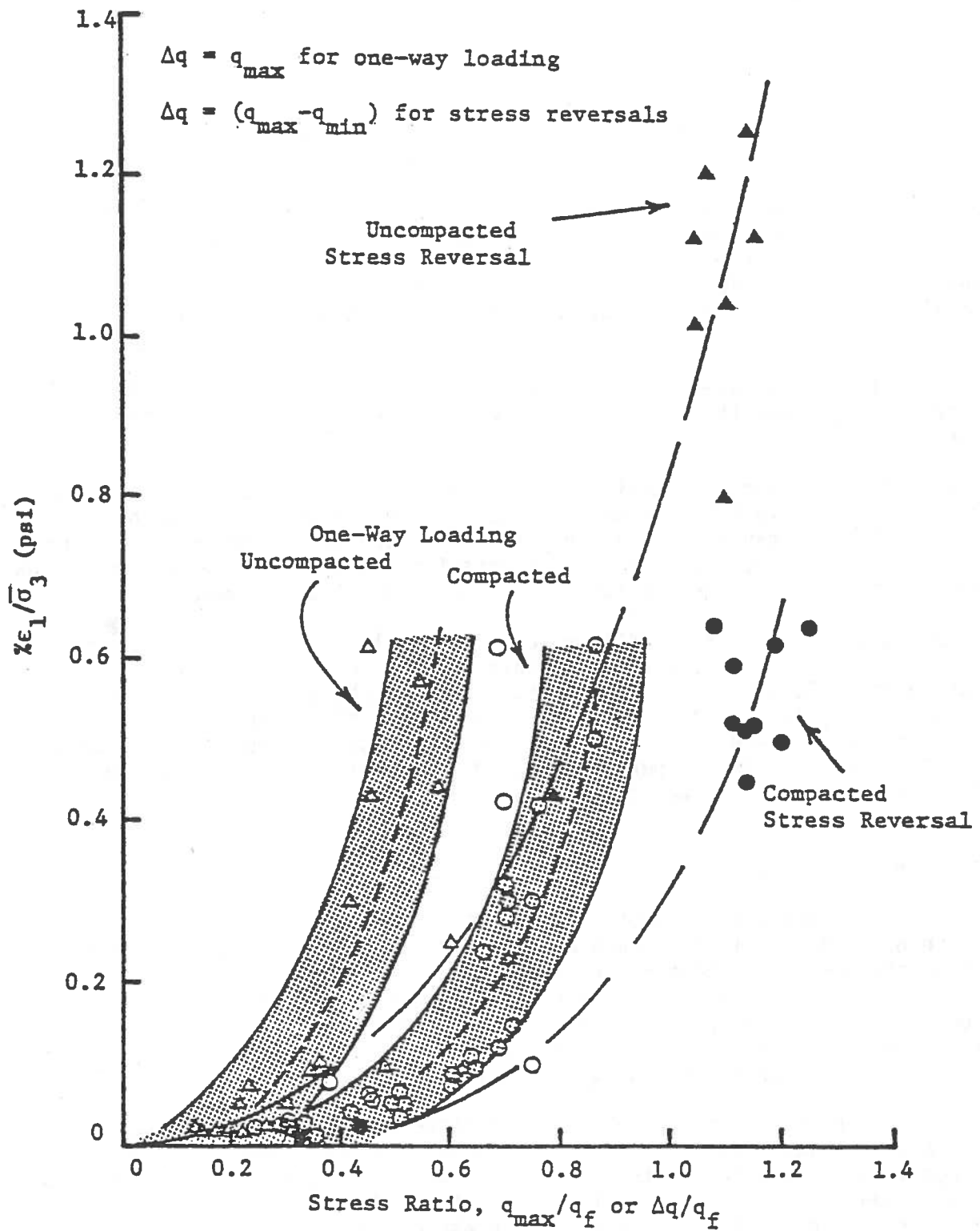


FIGURE 62. NORMALIZED FIRST CYCLE STRAINS AS A FUNCTION OF STRESS RATIOS

cycle of load,  $N = 1$  which is also the intercept of the  $\epsilon_N$  vs.  $\log N$  relationship

$C$  is the soil constant, and

$N$  is the number of applied load cycles, to determine the permanent strain after  $N$  cycles of a constant cyclic load.

Because wheel loads are not constant, a valid superposition of the representative loads was necessary. Therefore, a series of staged triaxial tests were performed on ballast materials to justify the use of a cumulative damage rule (see Volume II). Briefly, this rule states that the sequence of loading is not important so long as the total number of cycles at each load level remains fixed.

The resulting calculated strains in each layer must then be multiplied by the corresponding layer thickness to get the total settlement contributed by that layer.

As discussed earlier, for settlement predictions related to maintenance, only the disturbed ballast layers were included. The depths influenced by the revenue site maintenance operations were estimated to be from 6 to 8 inches below the ties. The representative points for these ballast depths were thus taken as the midpoint depths for these disturbed ballast zones.

Since the survey data from FAST indicated only slight differences between the wood and concrete track settlement, only predictions for the concrete tie section of FAST, Section 22, were made. However, these were subdivided into two sets. The first set was for the 0 to 93 MGT (after rebuild) period and considered the entire 15-in. ballast depth. The second was for FAST, Section 22, after the maintenance operations at 93 MGT. For this set, a 7.5-in.-deep disturbed ballast layer was assumed.

### Streator Settlement

The predicted track settlements for the Streator wood tie section are shown in Figure 63. The predictions made using stress path DE gave the largest deformation and were close to the uncorrected survey measurements. The settlement rates appeared to level off for the second field measurement interval and was about parallel to the predictions. However, the predictions all underestimated the track vertical settlement, particularly when any adjustments were made to correct for the initial settlement.

The measurements and predictions for the Streator concrete tie track section are shown in Figure 64. The field survey measurements showed a very large change in track settlement from the 10 to 24 MGT measurements, which was much larger than the initial change from the 0 to 10 MGT readings. This occurred over the winter months and may have been associated with frozen ballast. The two final survey measurements appear to indicate that the track settlement rate was leveling off, as was expected and predicted, but additional data are required to substantiate this conclusion. The predicted values are all much

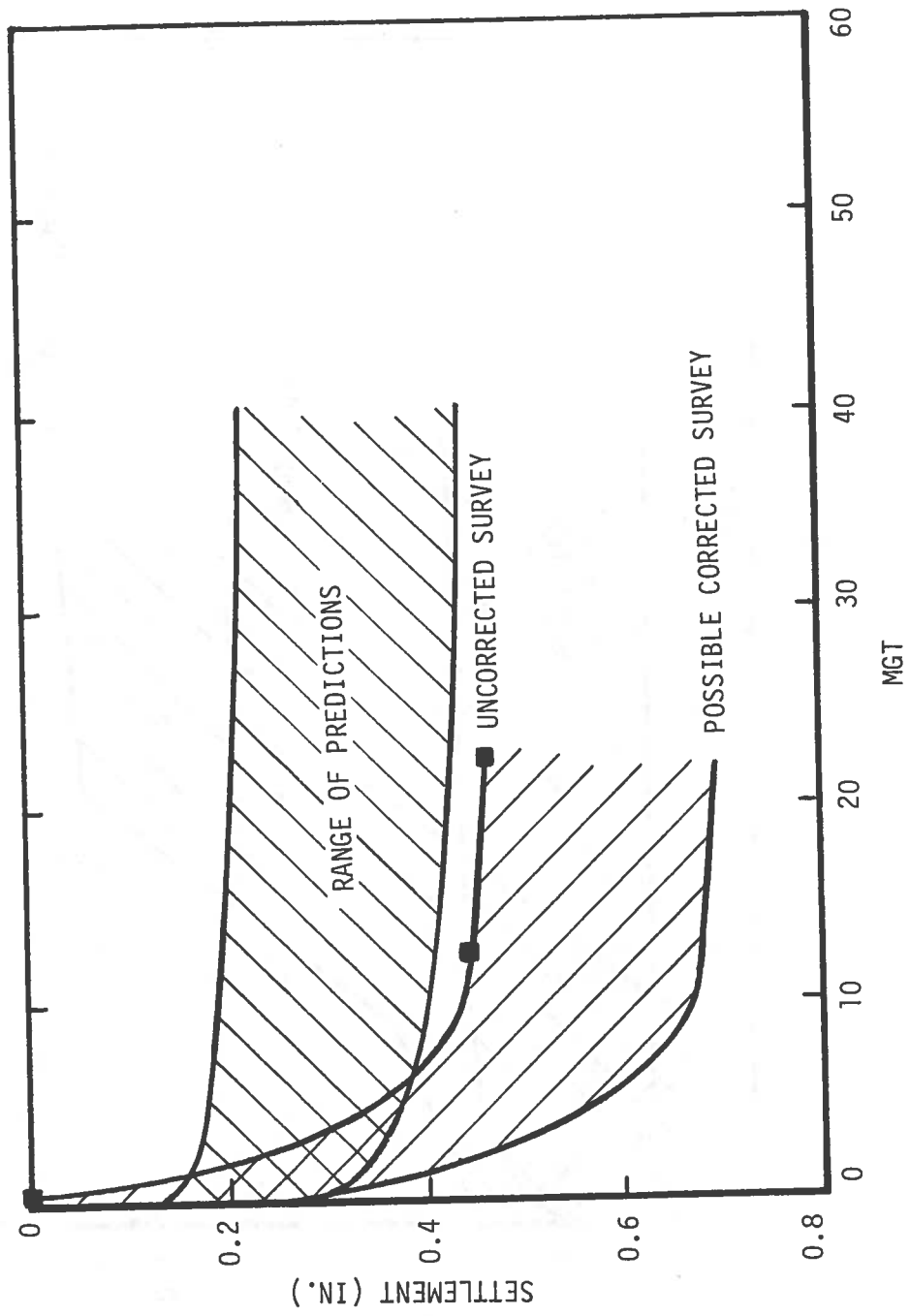


FIGURE 63. MEASUREMENTS AND PREDICTIONS OF TRACK SETTLEMENT FOR STREATOR WOOD TIE SECTION

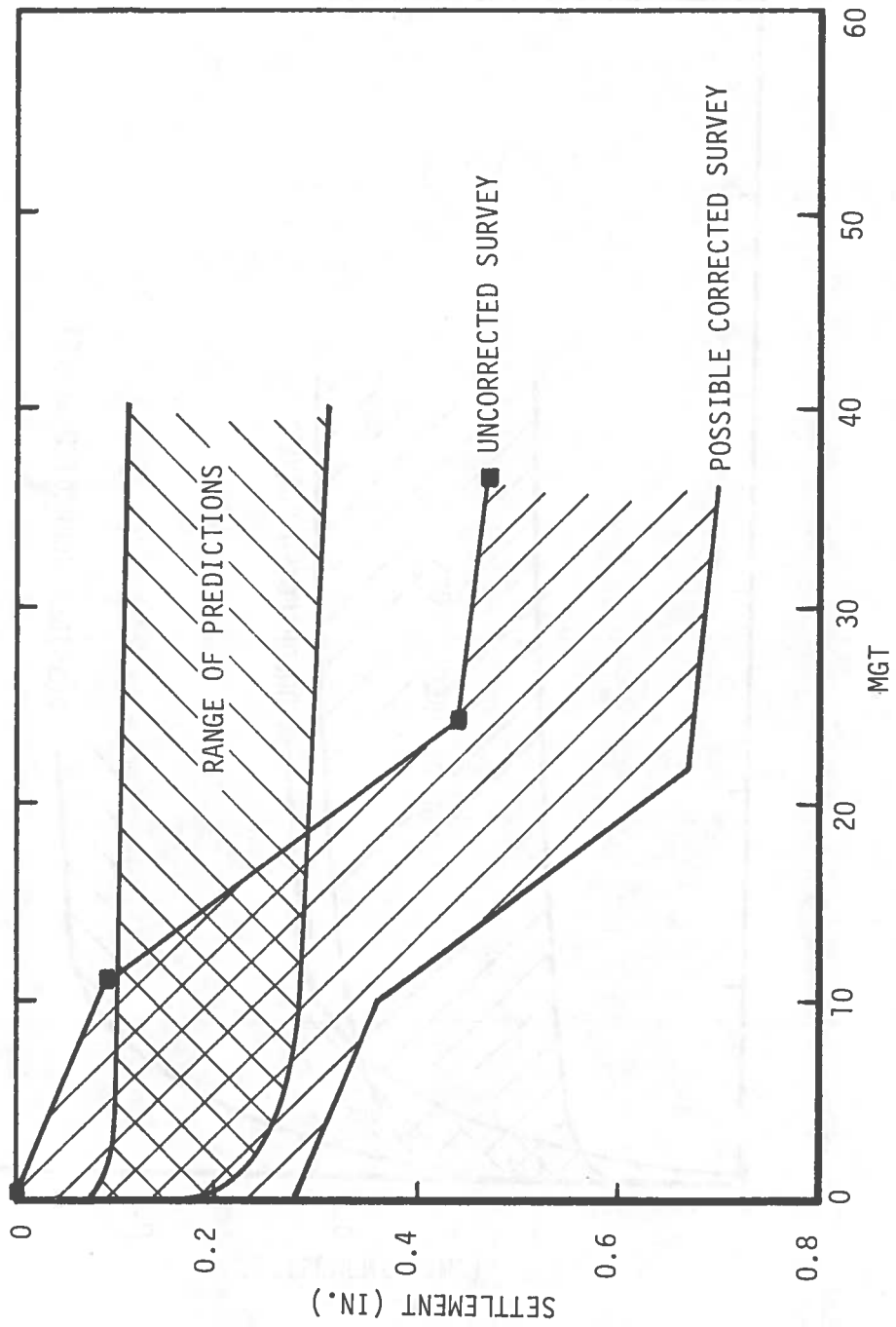


FIGURE 64. MEASUREMENTS AND PREDICTIONS OF TRACK SETTLEMENT FOR STREATOR CONCRETE TIE SECTION

lower than the measured values after 20 MGT and show a slower rate of increase with MGT.

### Richmond Settlement

Figure 65 shows the measured survey track settlement and the predicted track settlement for the Richmond site. The field measurements indicated a continuous settlement of the track, with no indication that the deformations were leveling off with increased MGT. The predictions always showed a lower settlement rate after about 10 MGT traffic. All predictions for the Richmond site overestimated both the initial settlement and the cumulative settlement.

### Aberdeen Settlement

The results from the strain coil measurements and corrected survey measurements, along with the predictions of track settlement for the Aberdeen site, are shown in Figure 66. As previously indicated, the track settlement at Aberdeen apparently was due primarily to the upper ballast permanent deformations. The linear format of Figure 66 shows that following a high initial deformation rate in the first 3 MGT, the ballast deformations continued to increase at a lower constant rate, showing no tendency to level off with increased traffic accumulation. Again, further survey data or strain coil measurements would have been useful to help interpret longer term trends past the 30 MGT level. Although the measured values lie within the range of predicted values, the shapes of the predicted curves after about 5 MGT were quite different from the observed settlements. These data are discussed further in a subsequent section.

### FAST Settlement

Two sets of predictions were made for FAST, Section 22. Both sets were done for the concrete tie section track parameters. The first set of predictions considered the 0 to 93 MGT period directly after the 1979 rebuild. For these predictions, the full 15-in. depth of newly placed ballast was considered. The second set of predictions assumed that only the top half of the ballast was disturbed because of the maintenance operation that took place after 93 MGT traffic.

The measured and predicted vertical track settlement at FAST are shown in Figure 67. The 0 to 93 MGT track settlements and ballast deformations both showed an irregular increase from about the 30 to 50 MGT interval, followed by a reduced settlement rate up to the time of the surfacing operations. The shapes of both measured and predicted ballast deformations were similar. However, the predictions for 0 to 93 MGT were all greater than the measured ballast deformations obtained from the strain coils. This could be due to the compaction sequences used during the rebuild operation, which would have resulted in lower ballast strain under subsequent traffic loading.

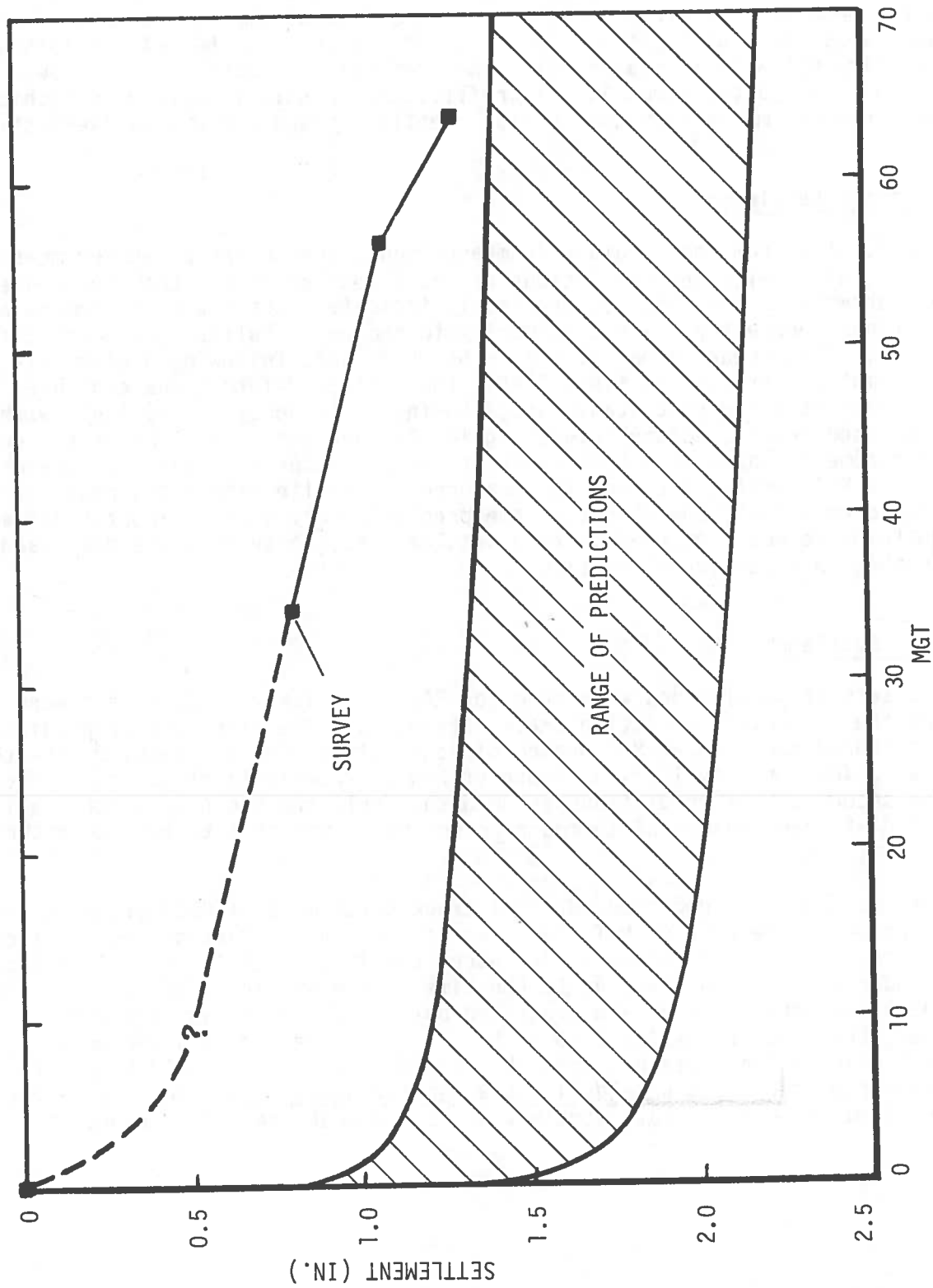


FIGURE 65. MEASUREMENTS AND PREDICTIONS OF TRACK SETTLEMENT FOR RICHMOND

lower than the measured values after 20 MGT and show a slower rate of increase with MGT.

#### Richmond Settlement

Figure 65 shows the measured survey track settlement and the predicted track settlement for the Richmond site. The field measurements indicated a continuous settlement of the track, with no indication that the deformations were leveling off with increased MGT. The predictions always showed a lower settlement rate after about 10 MGT traffic. All predictions for the Richmond site overestimated both the initial settlement and the cumulative settlement.

#### Aberdeen Settlement

The results from the strain coil measurements and corrected survey measurements, along with the predictions of track settlement for the Aberdeen site, are shown in Figure 66. As previously indicated, the track settlement at Aberdeen apparently was due primarily to the upper ballast permanent deformations. The linear format of Figure 66 shows that following a high initial deformation rate in the first 3 MGT, the ballast deformations continued to increase at a lower constant rate, showing no tendency to level off with increased traffic accumulation. Again, further survey data or strain coil measurements would have been useful to help interpret longer term trends past the 30 MGT level. Although the measured values lie within the range of predicted values, the shapes of the predicted curves after about 5 MGT were quite different from the observed settlements. These data are discussed further in a subsequent section.

#### FAST Settlement

Two sets of predictions were made for FAST, Section 22. Both sets were done for the concrete tie section track parameters. The first set of predictions considered the 0 to 93 MGT period directly after the 1979 rebuild. For these predictions, the full 15-in. depth of newly placed ballast was considered. The second set of predictions assumed that only the top half of the ballast was disturbed because of the maintenance operation that took place after 93 MGT traffic.

The measured and predicted vertical track settlement at FAST are shown in Figure 67. The 0 to 93 MGT track settlements and ballast deformations both showed an irregular increase from about the 30 to 50 MGT interval, followed by a reduced settlement rate up to the time of the surfacing operations. The shapes of both measured and predicted ballast deformations were similar. However, the predictions for 0 to 93 MGT were all greater than the measured ballast deformations obtained from the strain coils. This could be due to the compaction sequences used during the rebuild operation, which would have resulted in lower ballast strain under subsequent traffic loading.

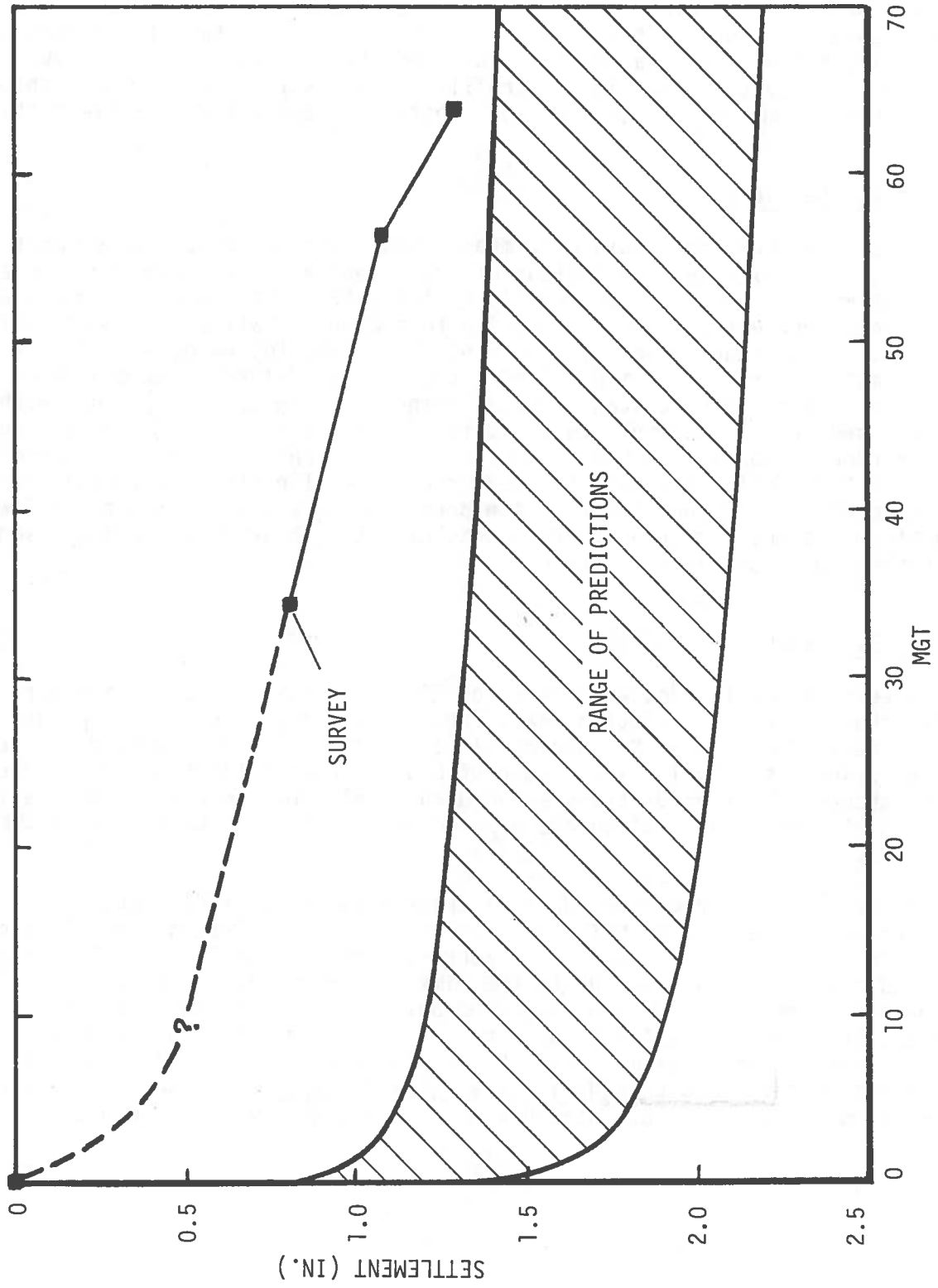


FIGURE 65. MEASUREMENTS AND PREDICTIONS OF TRACK SETTLEMENT FOR RICHMOND



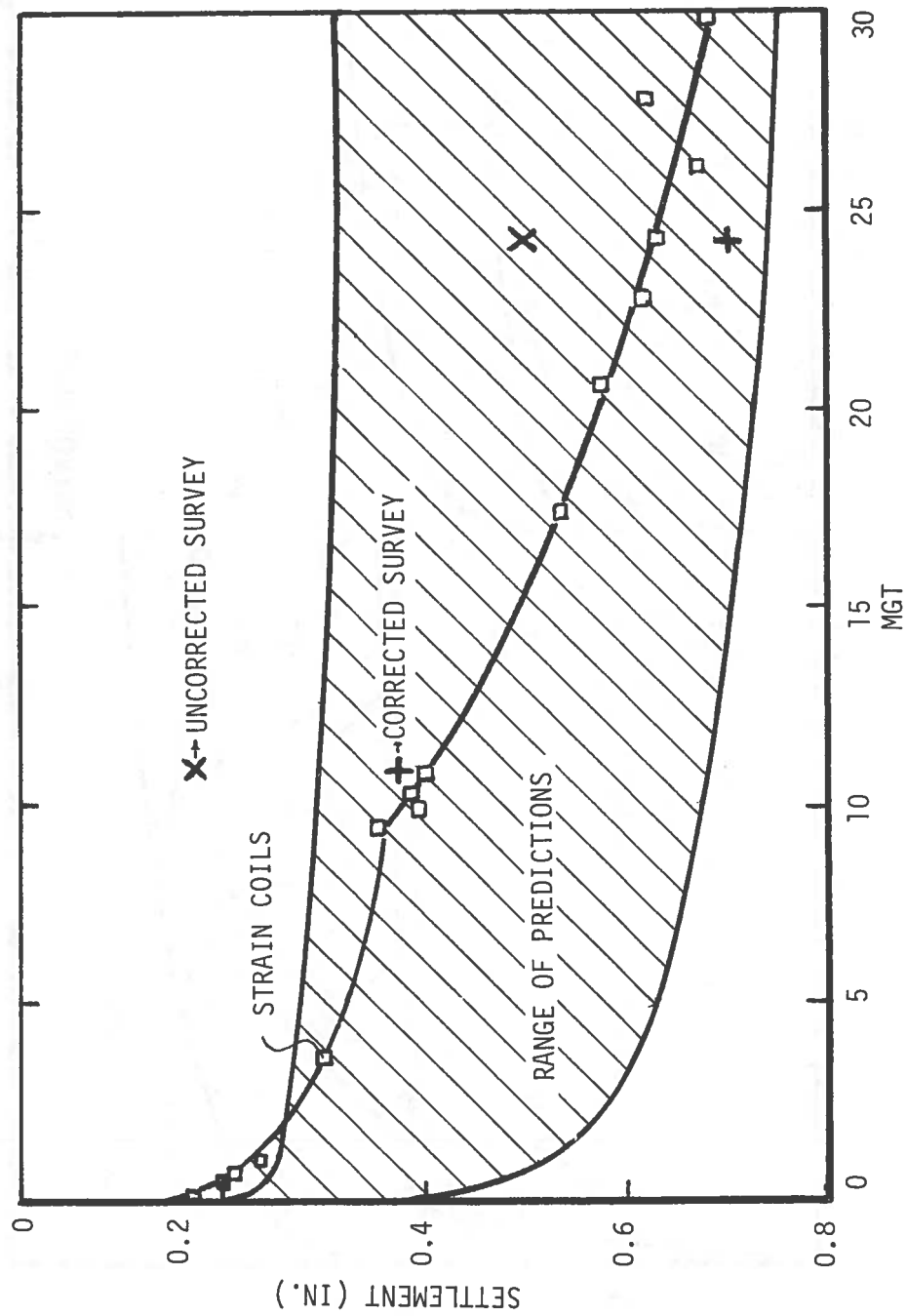


FIGURE 66. MEASUREMENTS AND PREDICTIONS OF TRACK SETTLEMENT FOR ABERDEEN

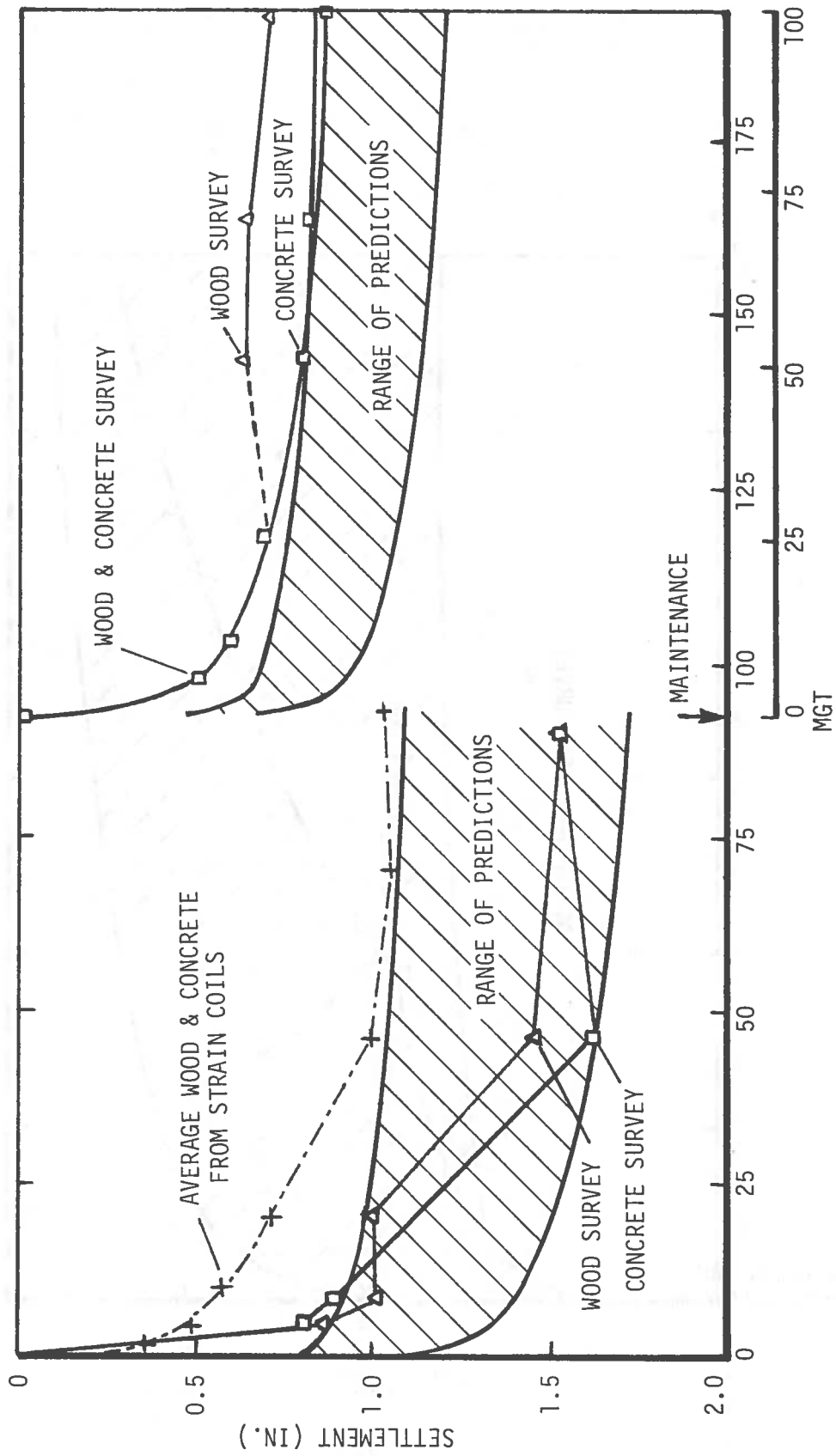


FIGURE 67. MEASUREMENTS AND PREDICTIONS OF TRACK SETTLEMENT FOR FAST SECTION 22 AFTER REBUILD

The difference between the 0 to 93 MGT survey measurements and the ballast deformations from the strain coil readings appeared consistent with the measured subgrade deformations, even though the subgrade deformation data are questioned. This could have resulted from compensating errors.

Instrumentation measurements of the ballast and subgrade cumulative deformations were not available after the 93 MGT maintenance at FAST. However, the survey measurements and predictions after the surfacing are shown in Figure 67. Both the shapes of the initial and longer term predicted settlement were similar to the survey measurements. The magnitudes were also in general agreement for the CB stress paths.

The measured track settlement from 0 to 93 MGT after rebuild for the stain coils and from the surveys after the maintenance showed a similar amount of initial track settlement. However, these data, as well as the predictions, showed larger deformations from traffic after rebuild than were observed after subsequent maintenance. This was primarily due to the differences in the initial ballast physical state in the lower portion of the ballast layers, even though there was some initial compaction of the ballast during the rebuild. This appears to confirm the previous assumptions that only the upper 6 to 8 in. of the ballast layer should be considered as disturbed by maintenance. Overall, the agreements between measured and predicted track settlements were good.

#### Discussion of Settlement Predictions

There are a variety of factors which influence the accuracy of the predictions. Generally, these factors can be divided into two broad areas: those associated with the complexities of the loading environment, and those associated with the necessary abstraction of measuring soil performance in practical, laboratory tests.

The best example of the first area is the comparison of the load environment at FAST with those at the revenue sites. The FAST loads, as discussed in Section 5, are very consistent. There are no extraordinarily large loads as seen at most revenue sites. There are only minimal track vibrations because these vibrations are usually induced by the same wheel tread irregularities causing the large loads. As a result (perhaps by coincidence) the FAST settlement predictions are very good. They not only predict about the right settlements, but also the shape of the settlement curves are very close. Other factors may influence the loading environment or cause ballast degradation such as the seasonal effects (or other unique influences) that resulted in non-uniform settlement at Streator during the winter-early spring interval between surveys. Pursuing these anomalous effects was beyond the scope of this project

The second area of measuring soil performance was based on the invariant transformations of the three-dimensional stress tensors, elements of which are assumed and/or measured in the field, into axisymmetric, constant-confining-pressure triaxial test conditions. The roadbed stresses were then approximated by the assumed equivalent stress paths labeled CB and DE in the settlement prediction plots since paths similar to the one defined by the actual

section indicate most of the "heave" occurred toward the end of the test zone away from the concrete section. Cross-checking of maintenance data did not reveal any spot maintenance in that area.

With the availability of the strain coil data from Aberdeen, a similar attempt was made to identify a logarithmic settlement rate. These data were also taken frequently at the early part of the monitoring period with progressively longer intervals after the first six months. The surprising results of plotting these data on a logarithmic scale are shown in Figure 69. For some reason there is a very distinct break in the settlement rate at about 10 MGT. This happened to occur, like Streator, in the late fall/early winter period, so a seasonal effect may be present.

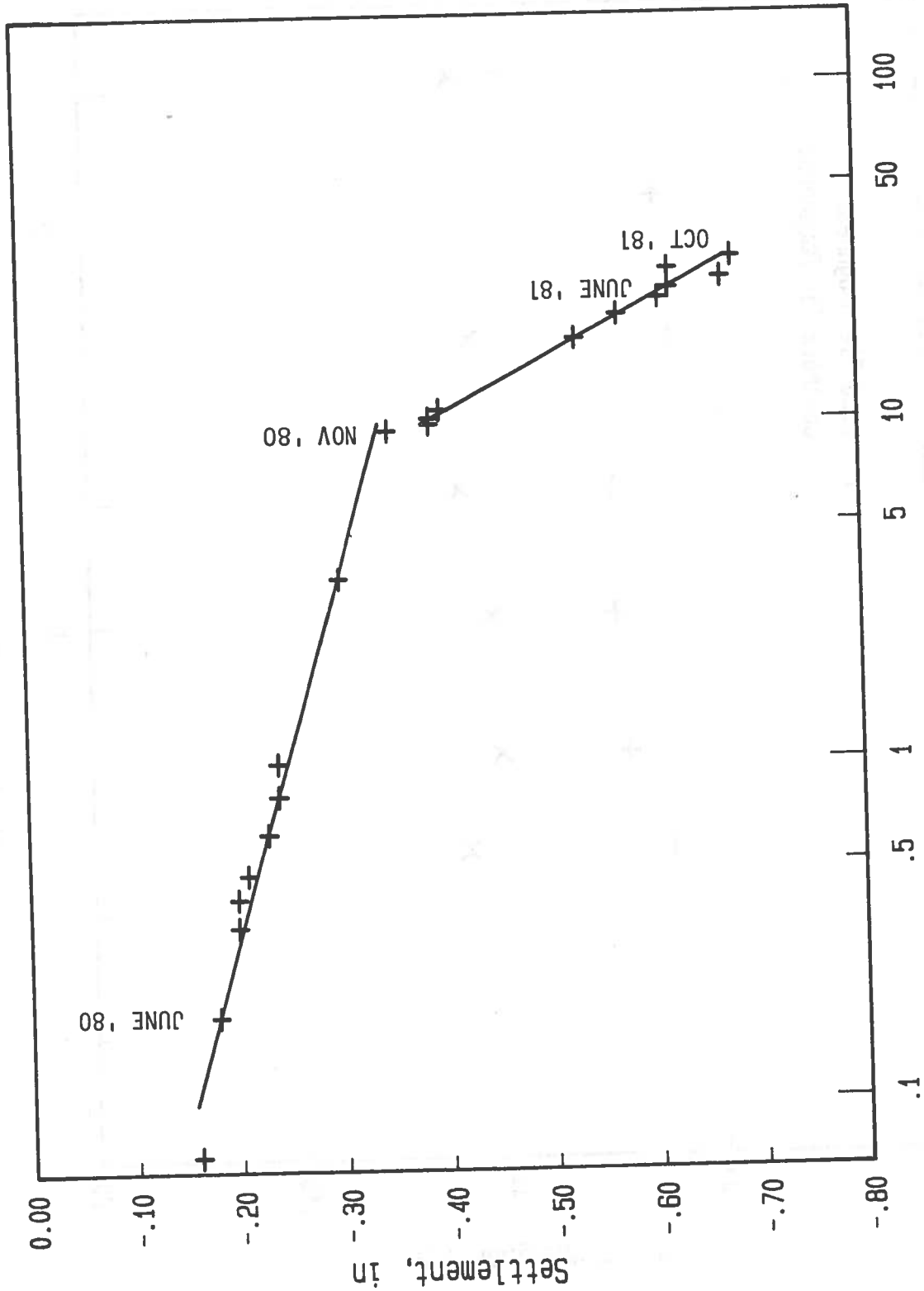
The log curve fit happens to be nearly perfect for each of the two curve segments and, as indicated, most data points fall directly on the curves. Currently, the only explanation for this shift in rates is the increase in impact loading resulting from the track structure hardening from extended consolidation from traffic with a possible "trigger" caused by either frozen ballast or cold temperature set on the tie pads. Neither effect can be substantiated at this time.

#### 9.5 Track Roughness vs. Absolute Settlement

Differential settlement, or roughness, is one of the principle criteria which determines the need for track maintenance. In general, one would expect differential settlement to increase with some proportionality to the increase in absolute settlement which results from cumulative traffic tonnage. As discussed in Section 6, however, the survey data did not show any qualitative indication of this relationship. In an effort to establish the relationship within the limits of the available data, a variety of analyses were performed.

As discussed in Section 6, the surveys were performed at 10-ft intervals over 600 ft of track, thus providing up to 122 elevation readings (both rails) per survey. Unfortunately, in the context of roughness, 10-ft intervals do not reveal the same types of roughness that would normally be identified by track geometry cars. Nevertheless, to approximate this effective roughness, the survey data were "string-lined" by a computer program with lengths of string-lines between 20 and 60 feet long. The string-lined data were then evaluated for roughness by computing the standard deviation of all readings. Because of the commonly used 62-ft chord, the roughly comparable 60-ft chord data were then evaluated for a trend of increased roughness with settlement.

FAST Section-22 data were used because of the number of surveys performed and because of the opportunity to compare wood and concrete tie construction under ideal conditions. Figure 70 is a plot of the roughness values for both test sections against MGT. Because settlement was shown to be related to Log MGT in the previous discussion, this should show any comparable trends for roughness. Both the wood tie and the concrete tie results are inconclusive. For the concrete tie data, if the "wild point" at 53 MGT is included, then there is a slight dependency on settlement, while excluding the 53 MGT value would leave a constant value for roughness. A similar effect can be seen for the wood tie data, if the 100 MGT point is considered.



Millions of Gross Tons

FIGURE 69. LOGRITHMIC SETTLEMENT AT ABERDEEN - BALLAST STRAIN COIL DATA

between the long-term maintenance following potential indicators: ballast fouling, and ballast

between settlement and roughness surfaced track and extending up examined contained uniform lies. The lack of correlation tive roughness is driven largely lies, such as rail defects or

is proportional to the log of and has been well known in labora-erified in track because of poor-ity of loads at FAST allowed this

Concrete Tie Track

ences in the development of and concrete tie track built on ades at FAST, although differences the varied length and condition rated condition of the ballast constructed concrete tie test

t offered by concrete tie track is onsistently.

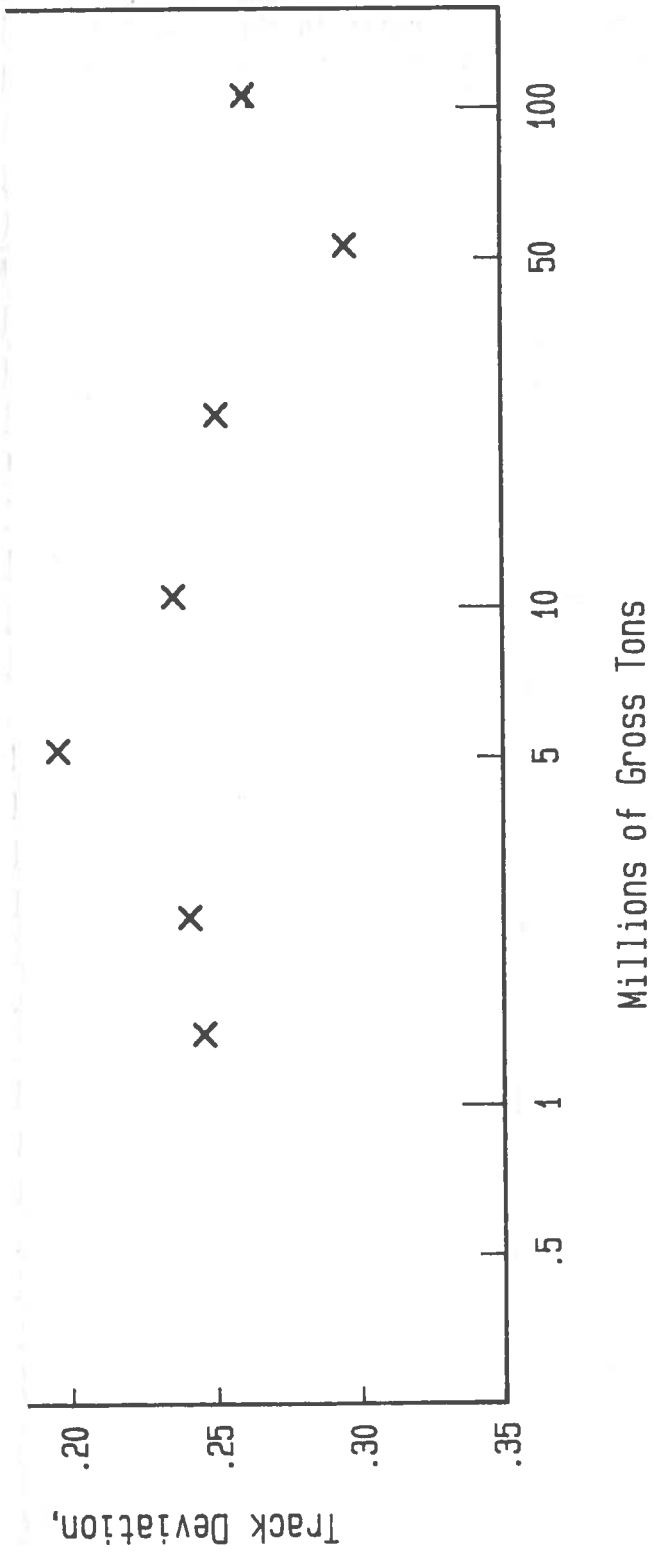


FIGURE 71. TRACK ROUGHNESS FOR 95th PERCENTILE DEVIATION

## REFERENCES

- [1] Dean, F.E., Harrison, H.D., Prause, R.H., Selig, E.T., McMahon, D., Measurement and Correlation Analysis Plan for Concrete Tie and Fastener Performance Evaluation, U.S. Department of Transportation, Federal Railroad Administration, 1979, Report No. FRA/ORD-79-51, (PB 80-183-882).
- [2] Stewart, H.E., and Selig, E.T., Correlation of Concrete Tie Track Performance in Revenue Service and at the Facility for Accelerated Service Testing, Volume II, Predictions and Evaluations of Track Settlement, U.S. Department of Transportation, Federal Railroad Administration, 1984, Report No. DOT/FRA/84/02.2.
- [3] Dean, F.E., Harrison, H.D., Stewart, H.E., McMahon, D., Correlation of Concrete Tie Track Performance in Revenue Service and at the Facility for Accelerated Service Testing, Volume III, Field Measurements and Data Analysis, Progress Report, July 1982.
- [4] Prause, R.H., Kennedy, J.C., Arnlund, R.C., An Evaluation of Performance Requirements for Cross Ties and Fasteners, U.S. Department of Transportation, Federal Railroad Administration, 1978, Report No. FRA/ORD-78/37.
- [5] Dean, F.E., Harrison, H.D., Prause, R.H., Tuten, J.M., Investigation of the Effects of Tie Pad Stiffness of the Impact Loading of Concrete Ties in the Northeast Corridor, U.S. Department of Transportation, Federal Railroad Administration, 1982, Report No. FRA/ORD-82/18.
- [6] Ahlbeck, D.R., "An Investigation of Impact Loads Due to Wheel Flats and Rail Joints," Paper No. 80-WA/RT-1, American Society of Mechanical Engineers Winter Annual Meeting, November 1980.
- [7] Dean, F.E., Investigation of Rail Fastener Performance Requirements, U.S. Department of Transportation, Federal Railroad Administration, 1982, Report No. FRA/ORD-82/10.
- [8] Prause, R.H., Harrison, H.D., Kennedy, J.C., Arnlund, R.C., An Analytical and Experimental Evaluation of Concrete Crosstie and Fastener Loads, U.S. Department of Transportation, Federal Railroad Administration, 1977, Report No. FRA/ORD-77/71.
- [9] Dean, F.E., and Harrison, H.D., Laboratory Study to Determine the Effects of Tie Pad Stiffness on the Attenuation of Impact Strain in Concrete Railway Ties, U.S. Department of Transportation, Federal Railroad Administration, 1982, Report No. FRA/ORD-82/19.
- [10] Gaskin, P.N., and Raymond, G.P., "Contributions to Selection of Railroad Ballast," Journal of the Transportation Engineering Division, American Society of Civil Engineers, Vol. 102, No. TE5, May 1976.
- [11] Yoo, T.S., Chen, H.M., and Selig, E.T., "Railroad Ballast Density Measurement," Geotechnical Testing Journal, American Society for Testing and Materials, Vol. 1, No. 1, pp 41-54, March 1978.

- [12] Selig, E.T., Yoo, T.S., and Panuccio, C.M., Mechanics of Ballast Compaction, Vol. I, Field Methods for Ballast Physical State Measurements, U.S. Department of Transportation, Federal Railroad Administration, 1982, Report No. FRA/ORD-81/16.1.
- [13] Panuccio, C.M., Wayne, R.C., and Selig, E.T., "Investigation of a Plate Index Test for Railroad Ballast," Geotechnical Testing Journal, ASTM, Vol. 1, No. 4, pp 213-222, December 1978.
- [14] Panuccio, C.M., Dorwatt, B.D., and Selig, E.T., "Apparatus and Procedures for Railroad Ballast Plate Index Test," Geotechnical Testing Journal, ASTM, Vol. 1, No. 4, pp 223-227, December 1978.
- [15] Selig, E.T., Yoo, T.S., and Panuccio, C.W., Mechanics of Ballast Compaction, Vol. 5, Summary Report, U. S. Department of Transportation, Federal Railroad Administration, 1984, Report No. FRA/ORD-81/16.5.
- [16] Bukoski, R.F., "Railroad Subgrade Soil Characterization for Track Performance," M.S. Project Report, Department of Civil Engineering, University of Massachusetts at Amherst, No. FRA-81-2, February 1981.
- [17] Schmertmann, J.H., "Guidelines for Cone Penetration Test Performance and Design," U.S. Department of Transportation, Federal Highway Administration, Report No. FHWA-TS-78-209, Washington, D.C., 1978.
- [18] Selig, E.T., Wobschall, D.C., Mansukhani, S., and Motiwala, A., "Capacitance Instrumentation for Measurement of Moisture in Bases, Subgrades and Earth Materials," SUNYAB, Final Report No. 21-2(2) to Highway Research Board, National Cooperative Highway Research Program, Washington, D.C., July 1974.
- [19] Selig, E.T., Wobschall, D.C., Mansukhani, S., and Motiwala, S., "Capacitance Sensor for Soil Moisture Measurement," Transportation Research Board, Record No. 532, Washington, D.C., pp 64-76, 1975.
- [20] Bosserman, B., and Sluz, A., Ballast Shoulder Width Experiment, Facility for Accelerated Service Testing Report, FAST/TTC/TN-81/03, June 1981.
- [21] Autry, W.S., "Incident at Leeds - Emergency on Concrete Tie Track," American Railway Engineering Association Bulletin 683, June-July 1981.
- [22] Reiner, I.A., Concrete Tie In-Track Performance Test, Report No. FRA/ORD-20015-L-8F, September 1981.
- [23] Stewart, H.E. and Selig, E.T., "Predicted and Measured Resilient Response of Track," Accepted for Publication in Journal of the Geotechnical Engineering Division, ASCE, April 1982.
- [24] Selig, E.T., Yoo, T.S., Adegoke, C.W., and Stewart, H.E., "Status Report - Ballast Experiments, Intermediate (175 MGT) Substructure Stress and Strain Data," Interim Report No. FRA/TTC/Dr-10 (IR), 1979.